DEVELOPMENT AND CONTROL OF A MULTIGRASP MYOELECTRIC HAND PROSTHESIS

BY

SKYLER ASHTON DALLEY

Dissertation

Submitted to the Faculty of the

Graduate School of Vanderbilt University

in partial fulfillment of the requirements

for the degree of

DOCTOR OF PHILOSOPHY

in

Mechanical Engineering

August, 2013

Nashville, Tennessee

Approved:

Dr. Michael Goldfarb

Dr. Eric J. Barth

Dr. Peter Konrad

Dr. Nilanjan Sarkar

Dr. Pietro Valdastri

Dr. Robert J. Webster III

Table of Contents

List of Figures

List of Tables

Chapter 1 – Overview

Skyler A. Dalley

Vanderbilt University

Nashville, TN

Introduction

The human body is, in many ways, the ultimate machine. As a component of this complex and highly functional system the hand is of particular interest, as it allows us to physically experience, manipulate, and thereby *interact with* our environment. The hand also plays an important role socially, where its myriad gestures form a basis for many aspects of nonverbal communication. As it is the product of an evolutionary process which spans millions of years, the hand is well adapted to these tasks and constitutes a major aspect of the human identity. The absence or loss of a hand is therefore associated with a loss of function, sensation, and body image [1], and may have significant physical, social, and psychological implications. The corollary loss of communication with the motor and somatosensory cortex is also particularly debilitating, and cannot be restored directly.

As of 2005, limb loss in the United States was estimated to affect nearly 1.6 million people. Approximately one-third of this figure is comprised of individuals who have suffered amputation of the upper extremity [2]. Upper limb loss is primarily caused by trauma and tends to affect a relatively young population as compared to lower limb loss, which is primarily caused by dysvascular disease. Specifically, over 66% of traumatic amputations occur in individuals less than 45 years of age, whereas approximately 64% of dysvascular amputations occur in individuals over 65 years of age [2], where approximately 69% of traumatic amputations involve the upper limb, and 97% of dysvascular amputations involve the lower limb [3]. The extent to which these amputations, and the prosthetic interventions that follow, affect an individual's ability to perform the Activities of Daily Living (ADLs) is of particular interest, as it largely determines an individual's level of independence and quality of self-care. If, as in [4], one considers the Activities of Daily living to be comprised of Mobility (positioning the body in space under ambulatory power), Basic ADL's (daily activities concerned with basic self-care such as feeding, grooming, and toileting), and Instrumental ADL's (daily activities concerned with independent living such as preparing meals, using the telephone, and doing housework), it is apparent that lower extremity amputations will primarily impact mobility, whereas upper extremity amputations will primarily impact the Basic and Instrumental ADLs. This is supported in [5], where it is suggested that upper extremity amputees may have more difficulty with the (basic and instrumental) activities of daily living than lower limb amputees due to the fine motor component involved in the performance of these tasks. Thus, while upper extremity amputees represent a smaller percentage of the amputee population as a whole, they are a relatively young and presumably active demographic whose ability to perform the activities of daily living is likely significantly affected.

Background and Significance[1]

Until recently, externally-powered prosthetic hands have been restricted to single degree-of-freedom (DoF) devices, driven by a single actuator, and commanded by a single electromyogram (EMG) input (two EMG electrodes placed on antagonistic muscle pairs of the residual forearm). Although such prostheses have far fewer DoFs than the native hand, and are therefore a simplistic abstraction, there are some appreciable advantages related to this approach. Primarily, the control of these devices requires little cognitive effort due to the one-to-one mapping between the actuator and EMG input. Also, traditional myoelectric prostheses can provide direct, proportional control of motion. Because they only require a single pair of EMG electrodes, the interface is manageable and is easily incorporated into a socket. Furthermore, the control method is not computationally demanding and can occur with minimal delay. A modern version of a single grasp myoelectric prosthesis is the MyoHand VariPlus Speed (Otto Bock, Germany).

Despite these advantages, it has also been noted that single grasp devices have limited grasping capability (because they cannot conform to objects and there is little contact area) and unnatural appearance of motion (mainly due to their low level of articulation) [6]. This is supported by surveys in which amputees indicate that greater functionality [7] and increased articulation [8] are among their top design priorities. In response to these limitations, and facilitated greatly by recent technological advances (such as improved batteries, actuators, and microelectronics), several multigrasp prosthetic hands have been developed [9-18]. These multigrasp hands are highly articulated (containing 8 to 16 joints), are driven by a plurality of actuators (ranging from 2 to 6), and hold the potential for improved grasping, manipulation, and fidelity of motion. However, as noted in [19], *the full realization of this potential requires the development of an effective multigrasp control interface*. An effective multigrasp interface must enable the user to access the multifunctional capability of the prosthetic hand accurately and dependably. The control approach should be direct and intuitive, offering continuous and proportional control of motion with negligible latency. Such is the goal of the research described herein.

Prevalent approaches to multigrasp control thus far include pattern recognition [19-24] and event-driven finite-state control [25-32]. Pattern recognition for multigrasp hands involves determining user intent (i.e., selecting postures and grasps) based on the observation (of typically a plurality) of EMG inputs, which are observed in a series of moving windows in time (frames). In this approach, a classifier is trained which associates EMG input patterns with intended postures and grasps. During operation, the classifier examines each frame of EMG data and makes a decision (or classification) about which movement is being commanded.

In event-driven finite-state (EDFS) approaches, the controller consists of a series of interconnected states. For each state the control action is uniquely defined. Transitions among the respective states are based on predefined events or conditions which depend on sensory

[1] For an early history of upper extremity prostheses, the reader is referred to Appendix A.

inputs. The overall behavior of an EDFS controller is therefore a function of the structure and interconnectedness of the states, the device behavior within each state, and the events and conditions required to transition among states (all of which are interdependent). This approach was initially developed and applied to myoelectric prosthetic hand control in the 1960's ([25, 26]), followed by the more recent work described in [27-32]. In [27-29], EDFS control approaches were used to modulate grasp within a preselected hand posture based on measured EMG amplitudes. In these works, posture preselection depended on the activation of contact switches located on the prosthesis. Later in [30, 31], a control approach was proposed which also utilized EDFS for grasp modulation, but where EMG pattern recognition, rather than contact switches, was utilized for posture preselection. Alternatively, in [32], an EDFS control approach was described in which an EMG amplitude based algorithm was used to preselect a given posture, but where the grasping process was automated by the controller to differing degrees. Specifically, after posture preselection, an automated grasping action was initiated by the controller or by the user (depending on controller variation). Grasping was then either terminated automatically, based on measured grasp force, or manually via a subsequent EMG command (depending again on controller variation).

A control method is presented in this dissertation which, like the approaches presented in [27-32], also involves event-driven finite-state control, but where posture selection and grasp modulation occur simultaneously. This is possible because the states (postures) in the finite state control structure have been arranged deliberately based on the degree of hand closure and the position of the thumb, allowing for direct and intuitive access to any one of nine possible hand postures (states), in addition to the continuum of configurations between them, using a standard two-site EMG interface. The studies described herein indicate that this method is both reliable and efficient, and may provide enhanced functionality during the activities of daily living.

Document Organization

The dissertation is comprised of six chapters. Chapter 1 provides introductory material to motivate and describe the scope of the work contained herein. Chapters 2 through 5 consist of manuscripts which have either been published (Chapters 2-4), or submitted (Chapter 5), as technical journal papers, and which describe and comprise the main body of work. Specifically, Chapters 2 and 3 describe the initial development and characterization of the Vanderbilt Multigrasp Hand prosthetic hardware, Chapter 4 describes the Multigrasp Myoelectric Controller used to control the prosthetic hardware, and Chapter 5 describes the functional assessment of the system as a whole. A Prologue and an Epilogue is included in each of these chapters to motivate and summarize the individual works. The dissertation closes in Chapter 6, which includes an overall summary and key contributions. Overviews of the manuscripts presented in this document are as follows:

Manuscript 1 (Chapter 2): *Design of a Multifunctional Anthropomorphic Prosthetic Hand with Extrinsic Actuation*, Skyler A. Dalley, Tuomas E. Wiste, Thomas J. Withrow, and Michael Goldfarb

Abstract: This paper presents an anthropomorphic prototype hand prosthesis that is intended for use with a multiple channel myoelectric interface. The hand contains 16 joints, which are differentially driven by a set of five independent actuators. The hand prototype was designed with the minimum number of independent actuators required to provide a set of eight canonical hand postures. This paper describes the design of the prosthesis prototype, demonstrates the hand in the desired eight canonical postures, and experimentally characterizes the force and speed capability of the device. A video is included in the supplemental material that also illustrates the functionality and performance of the hand.

Manuscript 2 (Chapter 3): *Design of a Multigrasp Transradial Prostheses*, Tuomas E. Wiste, Skyler A. Dalley, H. Atakan Varol, and Michael Goldfarb

Abstract: This paper describes the design and performance of a new prosthetic hand capable of multiple grasp configurations, and capable of fingertip forces and speeds comparable to those used by healthy subjects in typical activities of daily living. The hand incorporates four motor units within the palm, which together drive sixteen joints through tendon actuation. Each motor unit consists of a brushless motor that drives one or more tendons through a custom two-way clutch and pulley assembly. After presenting the design of the prosthesis, the paper presents a characterization of the hand's performance. This includes its ability to provide eight grasp postures (but where, due to reduced actuation, digits IV and V move with digit III in the tripod grasp), as well as its ability to provide fingertip forces and finger speeds comparable to those described in the biomechanics literature corresponding to activities of daily living.

Manuscript 3 (Chapter 4): *A Method for the Control of Multigrasp Myoelectric Prosthetic Hands,* Skyler A. Dalley, Huseyin Atakan Varol, and Michael Goldfarb

Abstract: This paper presents the design and preliminary experimental validation of a multigrasp myoelectric controller. The described method enables direct and proportional control of multigrasp prosthetic hand motion among nine characteristic postures using two surface EMG electrodes. To assess the efficacy of the control method, five non-amputee subjects utilized the multigrasp myoelectric controller to command the motion of a virtual prosthesis between random sequences of target hand postures in a series of experimental trials. For comparison, the same subjects also utilized a data glove, worn on their native hand, to command the motion of the virtual prosthesis for similar sequences of target postures during each trial. The time required to transition from posture to posture and the percentage of correctly completed transitions were evaluated to characterize the ability to control the virtual prosthesis using each method. The average overall transition times across all subjects were found to be 1.49 and 0.81 seconds for

the multigrasp myoelectric controller and the native hand, respectively. The average transition completion rates for both were found to be the same (99.2%). Supplemental videos demonstrate the virtual prosthesis experiments, as well as a preliminary hardware implementation.

Manuscript 4 (Chapter 5): *Comparative Functional Assessment of Single and Multigrasp Prosthetic Terminal Devices,* Skyler A. Dalley, Daniel A. Bennett, and Michael Goldfarb

Abstract: This work presents a case study involving the functional assessment of a variety of prosthetic terminal devices. In particular, a transradial amputee subject performed the Southampton Hand Assessment Procedure (SHAP) using five different terminal device types, including a Hosmer-Dorrance Corp. 5XA body-powered split hook, a Motion Control Inc. Electric Terminal Device, an Otto Bock MyoHand VariPlus Speed, a Touch Bionics Inc. i-Limb Revolution multigrasp hand, and the Vanderbilt Multigrasp Hand. While the highest Index of Function (IoF) was obtained with the two split-hook terminal devices (92 out of 100 points), the IoF scores for the other devices differed by no more than eight percent. However, the similarity of these results was not consistent with the functional differences experienced by the participant when using the various devices in the activities of daily living. In order to address the disparity between the quantitative results obtained here and the experience of the subject in daily living, the authors offer considerations for future assessment instruments, which, if implemented, may better characterize some aspects of terminal device functionality of importance to upper extremity amputees.

References

[1] H. K. Bowker and J. W. Michael, Eds., *Atlas of Limb Prosthetics: Surgical, Prosthetic, and Rehabilitation Principles*. St. Louis: American Academy of Orthopedic Surgeons, 1992.

[2] K. Ziegler-Graham, E. Mackenzie, P. Ephraim, T. Travison, and R. Brookmeyer, "Estimating the Prevalence of Limb Loss in the United States: 2005 to 2050," *Archives of Physical Medicine and Rehabilitation,* vol. 89, pp. 422-429, 2008.

[3] NLLIC-Staff, "Amputation Statistics by Cause: Limb Loss in the United States," National Limb Loss Information Center, Fact Sheet, 2008.

[4] S. Katz, "Assessing Self-Maintenance: Activities of Daily Living, Mobility, and Instrumental Activities of Daily Living," *Journal of the American Geriatrics Society,* vol. 31, pp. 721-727, 1983.

[5] S. L. H. Winkler, "Upper Limb Amputation and Prosthetics Epidemiology, Evidence, and Outcomes," in *Care of the Combat Amputee*, M. K. Lenhart, Ed., ed Fort Sam Houston: Office of The Surgeon General, Department of the Army, United States of America and US Army Medical Department and School, 2009, pp. 597-605.

[6] M. Zecca, S. Micera, M. C. Carrozza, and P. Dario, "Control of multifunctional prosthetic hands by processing the electromyographic signal," *Critical Reviews in Biomedical Engineering,* vol. 30, pp. 459-85, 2002.

[7] E. Biddiss, D. Beaton, and T. Chau, "Consumer design priorities for upper limb prosthetics," *Disability & Rehabilitation: Assistive Technology,* vol. 2, pp. 346-357, 2007.

[8] D. J. Atkins, D. C. Y. Heard, and W. H. Donovan, "Epidemiological Overview of Individuals with Upper-Limb Loss and Their Reported Research Priorities," *Journal of Prosthetics and Orthotics,* vol. 8, pp. 2-10, 1996.

[9] J. L. Pons, E. Rocon, R. Ceres, D. Reynaerts, B. Saro, S. Levin, and W. Van Moorleghem, "The MANUS-HAND dextrous robotics upper limb prosthesis: mechanical and manipulation aspects," *Autonomous Robots,* vol. 16, pp. 143-163, Mar 2004.

[10] J. Chu, D. Jung, and Y. Lee, "Design and control of a multifunction myoelectric hand with new adaptive grasping and self-locking mechanisms," in *IEEE International Conference on Robotics and Automation*, 2008, pp. 743-748.

[11] C. Cipriani, M. Controzzi, and M. C. Carrozza, "Progress towards the development of the SmartHand transradial prosthesis," in *IEEE International Conference on Rehabilitation Robotics*, 2009, pp. 682-687.

[12] C. Cipriani, M. Controzzi, and M. C. Carrozza, "Objectives, criteria and methods for the design of the SmartHand transradial prosthesis," *Robotica,* vol. 28, pp. 919-927, 2010.

[13] C. M. Light and P. H. Chappell, "Development of a lightweight and adaptable multiple-axis hand prosthesis," *Medical Engineering & Physics,* vol. 22, pp. 679-684, Dec 2000.

[14] S. Jung and I. Moon, "Grip force modeling of a tendon-driven prosthetic hand," in *International Conference on Control, Automation and Systems*, 2008, pp. 2006-2009.

[15] A. Kargov, C. Pylatiuk, R. Oberle, H. Klosek, T. Werner, W. Roessler, and S. Schulz, "Development of a multifunctional cosmetic prosthetic hand," in *IEEE International Conference on Rehabilitation Robotics*, 2007, pp. 550-553.

[16] C. Pylatiuk, S. Mounier, A. Kargov, S. Schulz, and G. Bretthauer, "Progress in the development of a multifunctional hand prosthesis," in *Proceedings of the IEEE Engineering in Medicine and Biology Society*, 2004, pp. 4260-3.

[17] T. E. Wiste, S. A. Dalley, H. A. Varol, and M. Goldfarb, "Design of a Multigrasp Transradial Prosthesis," *ASME Journal of Medical Devices,* vol. 5, pp. 1-7, 2011.

[18] S. A. Dalley, T. E. Wiste, T. J. Withrow, and M. Goldfarb, "Design of a Multifunctional Anthropomorphic Prosthetic Hand With Extrinsic Actuation," *IEEE/ASME Transactions on Mechatronics,* vol. 14, pp. 699-706, 2009.

[19] F. C. P. Sebelius, B. N. Rosén, and G. N. Lundborg, "Refined myoelectric control in below-elbow amputees using artificial neural networks and a data glove," *The Journal of Hand Surgery,* vol. 30, pp. 780-789, 2005.

[20] M. Vuskovic and D. Sijiang, "Classification of prehensile EMG patterns with simplified fuzzy ARTMAP networks," in *Proceedings of the 2002 International Joint Conference on Neural Networks*, 2002, pp. 2539-2544.

[21] J. Zhao, Z. Xie, L. Jiang, H. Cai, H. Liu, and G. Hirzinger, "EMG control for a five-fingered underactuated prosthetic hand based on wavelet transform and sample entropy," in *IEEE/RSJ International Conference on Intelligent Robots and Systems*, 2006, pp. 3215-3220.

[22] L. H. Smith, L. J. Hargrove, B. A. Lock, and T. A. Kuiken, "Determining the Optimal Window Length for Pattern Recognition-Based Myoelectric Control: Balancing the Competing Effects of Classification Error and Controller Delay," *IEEE Transactions on Neural Systems and Rehabilitation Engineering,* vol. 19, pp. 186-192, 2011.

[23] L. Hargrove, Y. Losier, B. Lock, K. Englehart, and B. Hudgins, "A real-time pattern recognition based myoelectric control usability study implemented in a virtual environment," in *IEEE International Conference of the Engineering in Medicine and Biology Society*, 2007, pp. 4842-4845.

[24] G. Li, A. E. Schultz, and T. A. Kuiken, "Quantifying pattern recognition-based myoelectric control of multifunctional transradial prostheses," *IEEE Transactions on Neural Systems and Rehabilitation Engineering,* vol. 18, pp. 185-192, 2010.

[25] J. C. Baits, R. W. Todd, and J. M. Nightingale, "The feasibility of an adaptive control scheme for artificial prehension," *Proceedings of the Institution of Mechanical Engineers,* vol. 183, pp. 54-59, 1968.

[26] M. Rakic, "The 'Belgrade Hand Prosthesis'," *Proceedings of the Institution of Mechanical Engineers,* vol. 183, pp. 60-67, 1968.

[27] J. M. Nightingale, "Microprocessor control of an artificial arm," *Journal of Microcomputer Applications,* vol. 8, pp. 167-73, 1985.

[28] P. H. Chappell and P. J. Kyberd, "Prehensile control of a hand prosthesis by a microcontroller," *Journal of Biomedical Engineering,* vol. 13, pp. 363-369, 1991.

[29] P. J. Kyberd, O. E. Holland, P. H. Chappell, S. Smith, R. Tregidgo, P. J. Bagwell, and M. Snaith, "MARCUS: a two degree of freedom hand prosthesis with hierarchical grip control," *IEEE Transactions on Rehabilitation Engineering,* vol. 3, pp. 70-76, 1995.

[30] C. M. Light, P. H. Chappell, B. Hudgins, and K. Englehart, "Intelligent multifunction myoelectric control of hand prostheses," *Journal of Medical Engineering & Technology,* vol. 26, pp. 139-146, 2002.

[31] D. P. J. Cotton, A. Cranny, P. H. Chappell, N. M. White, and S. P. Beeby, "Control strategies for a multiple degree of freedom prosthetic hand," *Measurement & Control,* vol. 40, pp. 24-27, Feb 2007.

[32] C. Cipriani, F. Zaccone, S. Micera, and M. C. Carrozza, "On the shared control of an EMG-controlled prosthetic hand: analysis of user-prosthesis interaction," *IEEE Transactions on Robotics,* vol. 24, pp. 170-184, 2008.

Chapter 2 - Design of a Multifunctional Anthropomorphic Prosthetic Hand with Extrinsic Actuation

Skyler A. Dalley, Tuomas E. Wiste, Thomas J. Withrow, and Michael Goldfarb

Vanderbilt University

Nashville, TN

From: IEEE/ASME Transactions on Mechatronics, Volume 14, Issue 6

Status: Published November 3, 2009

Prologue

Initial work began with the design, construction, and control of extrinsic actuation (i.e. actuation external to the hand) for an anthropomorphic prosthetic hand (referred to in the following as the extrinsic hand). A solid model of this prosthetic system can be seen in Fig. 2.i, showing the actuator housing relative to the hand (left), as well as the actuation hardware itself (right). An exploded view of an individual actuation unit is provided in the following manuscript. It is important to note that the actuation units were fully backdriveable in this version of the device.

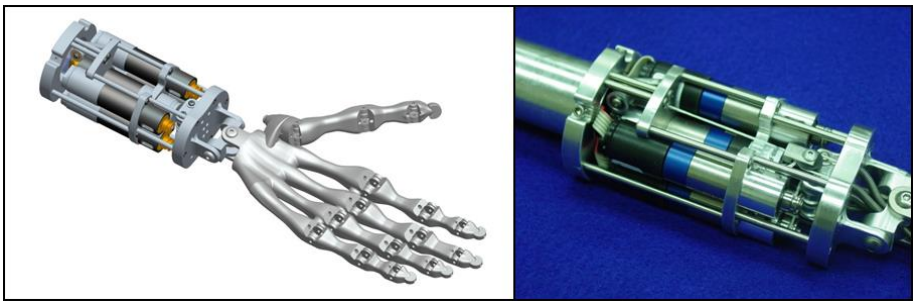

Figure 2.i - Solid model of extrinsically actuated prosthesis (left) and actuation hardware (right).

Analog circuitry was also designed and constructed to power and control the extrinsic hand. This consisted of servoamps (Cirrus Logic PA75) to drive the motors via control signals emanating from Simulink, connectors for data acquisition cards (Humusoft MF624 and PCI QUAD04) to acquire/send signals from/to Simulink, and signal conditioning for the user interface. At this point in the design cycle the user interface consisted of a joystick with embedded force sensitive resistors (Interlink 402 FSR) which allowed for independent control of thumb flexion and opposition, index finger flexion, middle finger flexion, and flexion of the ring and pinky fingers (the latter two digits being coupled by a pulley differential). These systems may be seen in Fig. 2.ii.

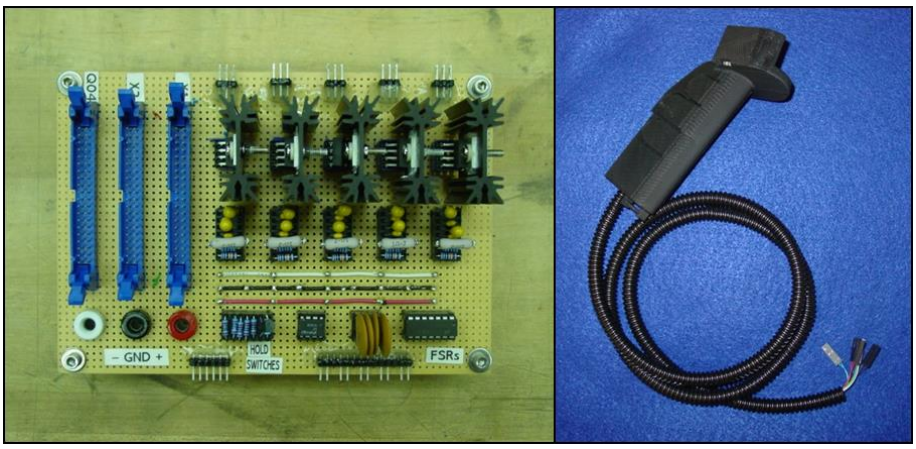

Figure 2.ii - Analog circuitry (left) and joystick with embedded force sensitive resistors (right) for power and control of the extrinsic hand.

The control methodology (implemented in simulink) for this revision was quite straightforward, where force exerted on the joystick FSRs was proportional to the current delivered to the brushed motors. Alternatively, control signals could be autamtically generated from within Simulink, the method by which the hand characterization (described below) was performed. Some notable features were also incorporated. These included thermal protection and virtual damping. Thermal protection for each motor was implemented by selectively saturating commanded current based on a temperature estimate of the motor windings. The temperature estimate was produced by an open-loop, second-order thermal model of the motor windings and housing, and was experimentally found to be conservative. To protect the prosthetic hardware from opening against hard stops at high speeds, selective virtual damping was employed in which the command signal was reduced proportionally to velocity when the hand was both opening and beneath a certain positional threshold.

Abstract

This paper presents an anthropomorphic prototype hand prosthesis that is intended for use with a multiple channel myoelectric interface. The hand contains 16 joints, which are differentially driven by a set of five independent actuators. The hand prototype was designed with the minimum number of independent actuators required to provide a set of eight canonical hand postures. This paper describes the design of the prosthesis prototype, demonstrates the hand in the desired eight canonical postures, and experimentally characterizes the force and speed capability of the device. A video is included in the supplemental material that also illustrates the functionality and performance of the hand.

I. Introduction

A highly constraining factor in the development of upper extremity prostheses has been the limited number of communication channels with which the user can control the prosthesis. Specifically, whether the input is a body-powered cable or a myoelectric signal, upper extremity prostheses have typically been limited to a single control input. In the case of a transradial prosthesis, the single control input is typically used to open and close a single degree-of-freedom (DoF) hand. In the case of a transhumeral prosthesis, the single control input is switched between control of the hand and control of the elbow joint. Recent advances in neural interface technology bring to the horizon the potential to significantly increase the number of (electrical) communication channels available to control an upper extremity prosthesis. The approach described in [1], which utilizes “targeted reinnervation” of peripheral nerves into residual muscle sites, has been shown to provide control input for devices with as many as six degrees of freedom [2]. Given the availability of several additional myoelectric control channels, an upper

extremity prosthesis with several independent actuators can be developed to leverage increased functionality with the availability of additional inputs. However, an increased number of control channels generally requires increased complexity, cost, and mass in the prosthesis, increased complexity (and possibly cost) of the surgical intervention, and increased complexity (and most likely cost) in the electrode interface. Therefore, in the development of an appropriate multifunctional prosthesis, one must balance enhanced performance with the consequent increases in cost and complexity that it may incur.

The prosthetic hand described in this paper and shown in Fig. 2.1 was designed in an effort to strike this balance. Specifically, the prosthesis was designed to provide the principal functions of a hand through eight canonical grasps with the fewest number of independent control inputs. Further, it was assumed (and is the case with myoelectric devices) that no conduit exists to bring sensory information to the user. Because of this the device was designed to be force controlled, such that the information contained in the muscle contraction is in essence preserved in the prosthesis. Finally, the device was designed to provide useful levels of force and appropriate speeds of motion relative to the activities of daily living (ADL's).

Several prosthetic hands have recently been described in engineering research literature [3-10]. These hands contain between one and six independent actuators and between eight and sixteen joints distributed in various ways in the digits (thumb, index, etc.). In each device, the discrepancy between the number of independent actuators and the number of joints is accommodated either by differential drives, which prescribe a given torque distribution between joints, kinematic linkages, which prescribe a given relative motion between joints, variable compliance couplings, which prescribe given relative compliance between joints, or by a combination of these. These devices are summarized in Table 2.1.

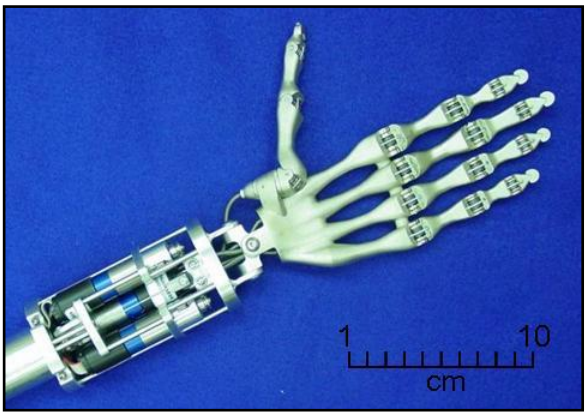

Figure 2.1 - The hand prosthesis prototype, showing the hand and the extrinsic actuation units.

Table 2.1 - Comparison of State of the Art in Research Prosthetics

REF.	# ACTUATORS	# ACTIVE DIGITS	# JOINTS	UNDERACTUATION METHOD
[3]	1	5, all coupled	15	Differential Drive
[4]	2	3, 2 coupled	8 and 9	Kinematic Linkage
[5]	3	5, 3 coupled	13	Kinematic Linkage, Compliant Coupling
[6]	4	3 independent.	10	Moment Isotropy
[7]	4	5, 3 coupled	16	Moment Isotropy, Differential Drive
[8]	5	5, 3 coupled	18	Hydraulic Valve Distribution
[9]	6	5 independent	11	Kinematic Linkage
[10]	6	5 Independent	16	Kinematic Linkage

In addition to these devices, the i-LIMB, a commercially available multi-degree-of-freedom hand prosthesis, has recently been developed by the company Touch Bionics. This device, which is intended for transradial amputees, utilizes two EMG inputs to drive five motors (one in each finger), and uses a kinematic linkage to address the underactuation in each finger. The hand is capable of multiplexing between four postures, which are a pointing posture, a tip grasp, a lateral grasp, and a cylindrical grasp.

This paper describes an anthropomorphic prosthetic hand designed to fully accommodate a set of eight grasp and gesture taxonomies with a minimum number of independent actuators. The prosthetic hand described herein possesses five independent actuators and 16 joints. The discrepancy between the number of joints and number of actuators is accommodated by moment isotropy, wherein each digit achieves static equilibrium when the moment in each joint is essentially equal to the other joints in the same actuation chain. Moment isotropy is realized by a combination of tendons spanning multiple joints and a differential pulley mechanism which distributes forces across tendons. This enables fully conformal, highly stable grasping [7] with significantly fewer independent actuators than joints in the hand. Additionally, the hand was designed with the assumption that near-term myoelectric interfaces will not be capable of providing graded, multi-degree-of-freedom force sensing to the user. Because of this the device was designed to preserve open-loop force information (i.e., to preserve the force command from the muscles providing the myoelectric signals) by virtue of force-control and backdriveability. In this manner the force sensing within the user's own muscle can be mapped to the control of the device. Such an approach provides the possibility to provide to the user some degree of force information, or feedback, with the interface, hardware, and control methods described herein rather than through the use of additional instrumentation.

II. Design Objectives

The essential objective of this work is to develop and characterize an anthropomorphic hand prosthesis for use with a multiple channel myoelectric interface (i.e., with multiple efferent communication channels from the user and no afferent communication) such as that enabled by targeted muscle reinnervation surgical techniques. Because additional channels incur liabilities with respect to cost, complexity, and reliability, the objective is further to obtain the desired functionality with a minimum number of independent actuators through the use of differential drives and underactuated digits. The desired functionality, in terms of varying postures, is to achieve the following set of eight canonical hand postures: a pointing posture (e.g., for punching buttons or keys); lateral and tip grasps between the thumb and forefinger (for grasping small objects); a tripod grasp between the thumb, forefinger, and middle finger (for more stable grasping of small objects); a hook grasp (e.g., for carrying a briefcase); cylinder and spherical whole hand grasps (i.e., for whole-hand grasping of objects); and a platform posture (e.g., for holding a book or plate). These grasps are a superset of the six basic types of prehension as identified by Schelisinger and summarized by Taylor and Schwartz [11] (where the tripod grasp is considered a “palmar” grasp) and represent each branch of the grasp taxonomy described by Cutkosky [12].

The design objectives have also been influenced by the nature of myoelectric interfaces which do not provide multi-axis force feedback. As reported in [2], targeted motor reinnervation is generally accompanied by some degree of sensory reinnervation (and therefore feedback); but does not directly accommodate force sensing and requires additional device complexity to relay the appropriate sensory information. In the proposed approach, sensory information is not provided to the user, per se, but rather is retained by the actuation method. Specifically, the user’s musculature (from which the myoelectric command signals are measured) possesses force sensing capabilities. By incorporating force-controlled, backdriveable actuation, some degree of force sensing can be preserved (i.e., the tendon forces retain some degree of proportionality with the electromyogram (EMG) command). Thus, an additional design objective is to ensure fully backdriveable, force-controlled actuation.

Note that surveys of prosthetic users [8, 13-15] offer the following as important factors in the performance of a prosthetic hand (relative to commercially available prosthetic devices):

1. *Increased functionality*
2. *Natural interaction with the environment*
3. *Reduced weight*
4. *Higher grasping speeds and forces*
5. *Low Noise*
6. *Better cosmetic appearance*

These factors have been incorporated as design criteria in the prosthetic hand in a variety of ways. The first two criteria are accommodated in the anthropomorphic hand by the previously discussed design objectives. Specifically, increased functionality is attained through the achievement of eight canonical grasps and natural interaction is facilitated via implicit force sensing and anthropomorphic design. The eight grasps described here represent a grasp taxonomy which considerably expands upon the (1 DoF) state of the art. Backdriveable, force controlled actuation enables some degree of force sensing by preserving native force sensing in the existing musculature, and allows both the generation and absorption of power. This in turn enables a more natural interaction with high impedance kinematic constraints (i.e. stiff objects in the environment) relative to velocity-controlled, non-backdriveable systems [16].

In addition to utilizing underactuation to reduce weight, the third criterion is addressed by utilizing hollow structural elements in the hand, visible in Figs. 2.4 and 2.5, and a space-frame to house the actuation units in the forearm, visible in Figs. 2.9 and 2.10. The third and fourth criteria, low weight and higher grasping speeds and forces, are generally competing objectives although both, in addition to the fifth criterion (low noise), are served by ensuring an efficient transmission (i.e., minimizing friction in the system). Finally, the sixth criterion is achievable with conscientious design. An anthropomorphic design based on scalable skeletal characteristics of the human hand has been utilized. In doing this it is believed that the cosmetic appearance of the device will be as natural as possible.

The remainder of this paper describes the hand design, demonstrates the ability to provide the aforementioned canonical postures with the prosthesis, and experimentally demonstrates the force and speed characteristics of the hand in operation.

III. Hand Design

The anthropomorphic hand, shown in Fig. 2.2, has 16 joints which are driven by five independent actuators. The tendon-based actuation units for the hand reside in the forearm, similar to the native human anatomy. The actuation units, which are described in the following section, use DC motors coupled with low-ratio gearheads and small diameter pulleys to pull hand tendons. Each joint in the hand includes embedded torsional springs in parallel with the hand tendons as discussed subsequently. The five actuators are allotted to the 16 joints in the hand as described in Table 2.2.

In all cases, the underactuation is governed by moment isotropy (i.e., differential coupling), rather than by kinematic constraints. In other words, the hand will reach a configurational equilibrium when all joint moments are (essentially) equal, excepting tendon friction and nonlinearities in the relationship between tendon force and joint moment as a function of joint angle. Note that this is achieved by a combination of having the tendon span multiple joints and

using a pulley differential to split the force of the actuator output equally into two tendons, as briefly described in Table 2.2.

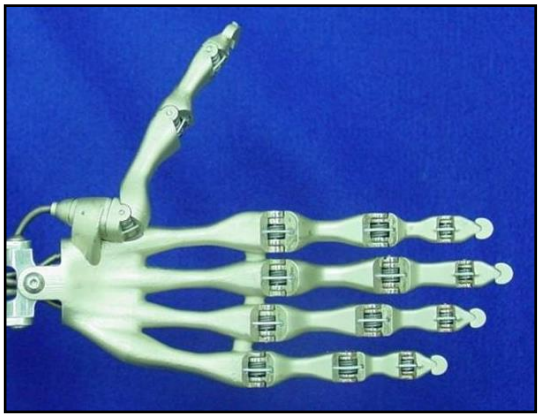

Figure 2.2 - The 16-joint anthropomorphic hand.

Table 2.2 - Distribution of Actuation and Mechanism of Coupling in the Hand.

ACTUATOR	DoF's	COUPLING	MECHANISM OF COUPLING
Index finger Flexion	3	Same Moment Across All Joints	Tendon Spans Multiple Joints
Middle finger Flexion	3	Same Moment Across All Joints	Tendon Spans Multiple Joints
Ring & Little Finger Flexion	6	Same Moment Across All Joints	Two Tendons Coupled by Pulley Tendons Span Multiple Joints
Thumb Flexion	3	Same Moment Across All Joints	Tendon Spans Multiple Joints
Thumb Opposition	1	Direct Drive	Direct Drive

Each joint in the hand incorporates embedded torsional springs, as shown in Fig. 2.3. The use of torsional springs in the joints serves several important purposes. First, and perhaps most obviously, the compliance provides a return force for finger extension. This methodology simplifies tendon actuation of the joints as additional tendons for finger extension are not necessary. Such joint compliance has been employed in several previous hand designs for this purpose [6, 7]. Second, the compliant joints map joint motion to tendon force in free space, thus 1) eliminating the need for position sensing in the hand and 2) eliminating the need to switch between motion control and force control. Specifically, the hand frequently engages in both motion control (e.g., when gesturing or reaching) and force control (e.g., when grasping or squeezing). In the hand, the tendons are always under (open-loop) force control. When the fingers are not in contact with an object, the springs in the fingers map the tendon force to finger position, such that the fingers are in effect under position control. When the fingers come into contact with a rigid object, the force-controlled tendons map directly to force control, and thus the switching between position and force control is natural and seamless.

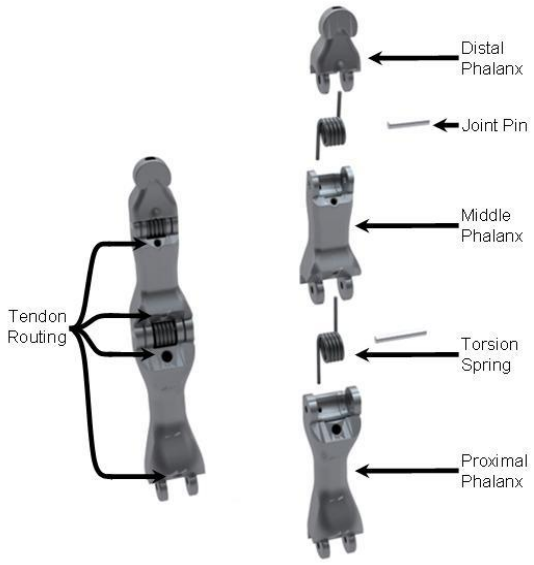

Figure 2.3 - Unexploded and exploded view of a digit showing the phalanges, torsion springs of the joints, and joint pins.

To achieve a high strength to weight ratio, the skeletal/structural components of the hand employ a monocoque structure, as shown in Figs. 2.4 and 2.5. Once drawn in CAD software, the parts were physically realized in high strength, nickel coated thermoplastic using an additive direct manufacturing method. The resulting structure weighs less than 80 g, with springs and connecting pins adding an additional 20 g. This high strength, low weight, and low cost approach to constructing each hand, in conjunction with a parametric code-based approach to CAD modeling, facilitates tailoring the dimensions of each hand to the individual user. The structure of the prosthetic hand is designed to fit well within the user's expected anatomical envelope by mimicking skeletal dimensions with high anthropometric fidelity. The artificial skeleton leaves room for mimicking the soft tissue (skin and muscle) components of the natural hand with a skin of silicone rubber wrapped around other soft materials such as synthetic viscoelastic urethane polymer and viscoelastic polyurethane foam.

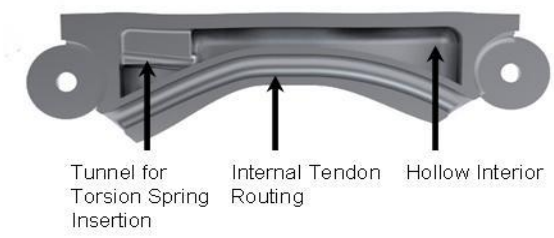

Figure 2.4 -Saggital section of a proximal phalanx, showing the tunnel for torsion spring insertion, internal tendon routing, and the hollow interior.

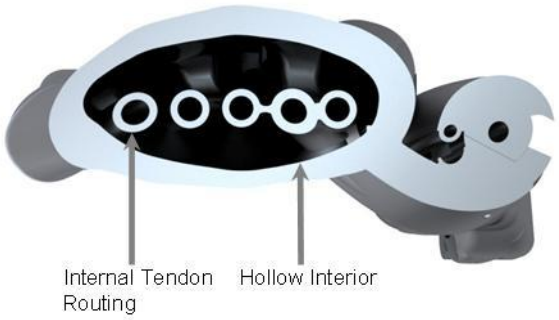

Figure 2.5 - Transverse section of the base of the palm, showing internal tendon routing, and the hollow interior. The base of the thumb is visible on the right.

The hand was designed to achieve a set of eight grasp postures. These postures are the tip, lateral pinch (or "key grasp"), tripod, spherical, cylindrical, and hook grasps, in addition to the pointing and platform postures. Figure 2.6 demonstrates the ability of the hand to achieve these grasps and postures. As indicated by [12], these grasps span a large portion of the grasp set of the human hand. Figure 2.7 shows some additional grasps and postures representative of the activities of daily living. The postures shown in Figs. 2.6 and 2.7 were achieved in real time by an able-bodied user using a five channel handheld controller in place of a myoelectric interface. This device utilizes force sensitive resistors to send input signals which are proportional to fingertip force for the corresponding degree of freedom. Note also that a video is included with the supplemental material that illustrates several of the grasps represented in Figs. 2.6 and 2.7.

IV. Forearm/Actuation Design

The actuation units were designed to provide the fingers with sufficient force and speed to perform activities of daily living and to be as light weight and efficient as possible. Exact specifications of "sufficient" force and speed are difficult to obtain. Most activities of daily living (ADL's) require prehensile forces under 70 N and are characterized by a frequency content of motion between 0.5 and 5 Hz [17]. As such, the thumb and independent fingers (the forefinger and middle finger) were designed for continuous fingertip forces of approximately 20 N each, while the two smaller fingers were designed for a combined tip force of 20 N. Given the nominal geometry of each finger and the respective tendon paths, a 20 N finger tip force requires a tendon force of approximately 120 N. Assuming grasp forces are primarily reacted against the palm, such design would provide for a maximum continuous grasp force of approximately up to 80 N if the thumb is also contributing. Further, as discussed in [17], the joints of the hand reach angular velocities of approximately 3 to 4 rad/sec (150 to 200 degrees/sec) during most ADL's. Assuming a typical hand joint range of motion is approximately 90 degrees, this would indicate a bandwidth of motion of approximately 1 Hz for a full amplitude finger motion, or a bandwidth of approximately 2 Hz for a half amplitude motion.

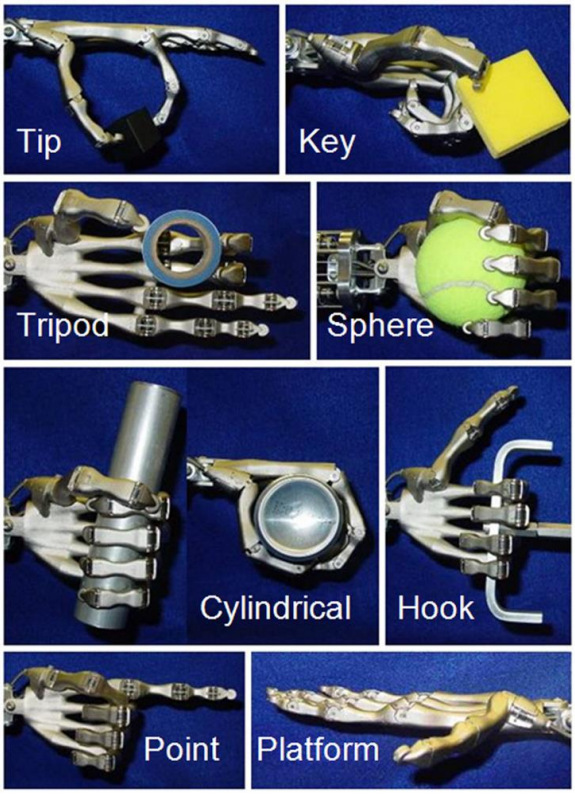

Figure 2.6 - Eight canonical hand postures, which constitute one of the primary design objectives of the hand prototype.

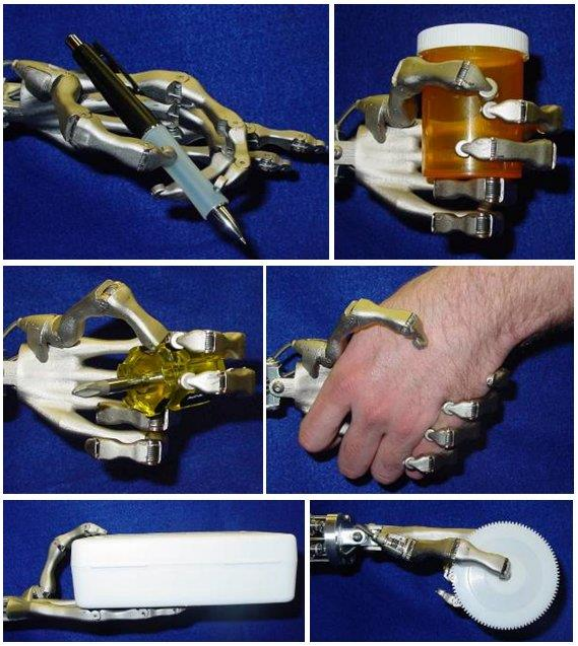

Figure 2.7 - Additional grasps and postures representative of typical activities of daily living.

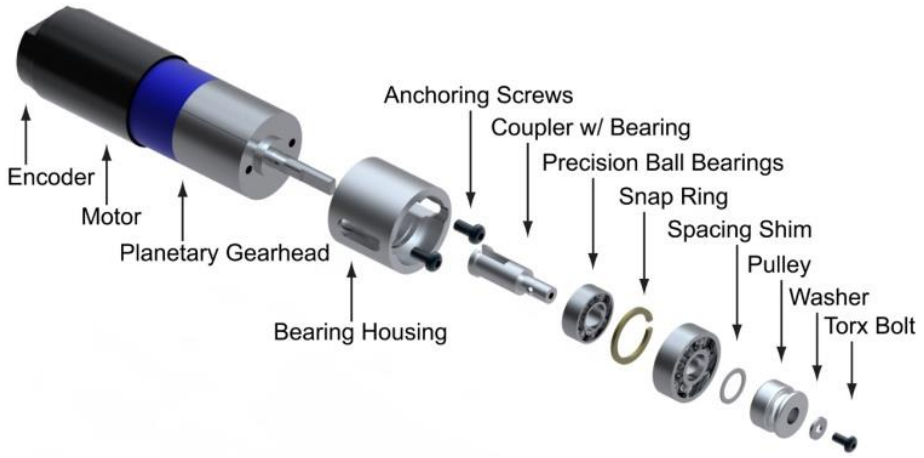

Figure 2.8 - Exploded view of an actuation unit.

In order to achieve a tendon force of 120 N and a half-amplitude motion bandwidth of 2 Hz, the actuation units shown in Fig. 2.8 were developed. Each unit is composed of a brushed DC servomotor (Faulhaber 1724 SR12) with integrated magnetic encoder (Faulhaber 1E2 516) and planetary gearhead (Faulhaber 16/7 43:1), coupled to a bearing housing across the structural plates of the extrinsic actuation housing. Within the bearing housing are two miniature, high precision (ABEC 7) radial bearings (New Hampshire Ball Bearing SSR3 and SSRI614). A coupling shaft cantilevered within the bores of these bearings transmits torque from the motor to the pulleys about which the tendon material is wrapped. Note that each unit is fully backdriveable (the return force being provided by the torsion springs embedded in the joints of the digits, Fig. 2.3) as per the design objectives previously stated. The actuation units transfer force to the digits via braided spectra cable (the “tendon”) which runs from the motor pulleys, around idler pulleys for redirection, and through the distal-most plate of the forearm (see Fig. 2.10). From here, the tendons pass through Bowden cables between the forearm and hand (allowing for positioning of the wrist) and then through routing tunnels in the hand (shown in Figs. 2.4 and 2.5) to terminate in the distal phalanx. These tendon paths are lined with Teflon tubing to reduce friction. Braided spectra cable of 0.75 mm (0.03 in) diameter and 668 N (150 lbf) rated strength was chosen for tendon material due to its high strength, high tensile fatigue resistance, low creep and low stretch characteristics.

Figures 2.9 and 2.10 show the five actuation units situated within the forearm. An open space-frame structure consisting of four plates rigidly connected by stainless steel tubing houses the actuators and is visible in Figs. 2.9. The space-frame is scalable, lightweight and provides easy access to the actuation units; allowing for quick maintenance and modification.

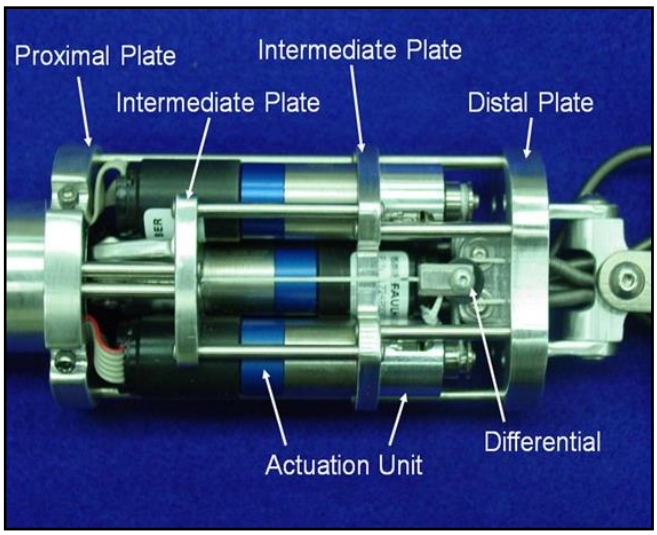

Figure 2.9 - Anterior view of the actuation unit housing showing structural plates, actuation units, and differential mechanisms.

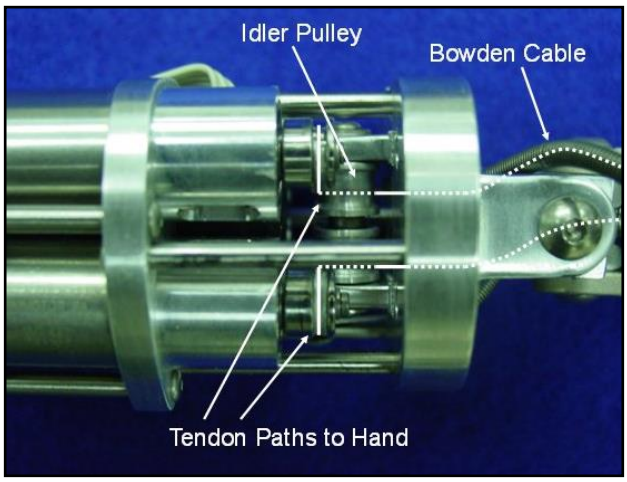

Figure 2.10 - Close-up lateral view of the actuation unit housing showing idler pulleys, Bowden cables, and tendon pathways. The solid lines highlight the observable visible paths for the tendons, while the dotted lines represent the cable paths obscured from view.

V. Performance

The dynamic performance of the hand prosthesis was characterized quantitatively in terms of closed-loop position tracking, open-loop force tracking, and maximum fingertip normal force as a function of position (tendon excursion) for the index finger.

A. Closed-loop position tracking

The position tracking capability of the prosthesis, shown in Fig. 2.11, was investigated by commanding the position of the index finger around the mid-flexion point (corresponding to 50% of total tendon excursion). Specifically, the index finger tracked a sinusoidal position signal which

varied around the mid-flexion point by ±25% of total tendon excursion (i.e., 50% of the total finger motion) for various frequencies. The bandwidth was determined using the integrated encoders to send position information to MATLAB software by way of a Humusoft 624 DAQ card. The results indicate a bandwidth of 4.5 Hz in position tracking. Note that this bandwidth also provides some degree of characterization of the degree of backdriveability, since the extension portion of the movement is driven entirely by the springs backdriving the motors. In comparison with the native hand, recall that joint angular velocities reach approximately 4 rad/sec in typical ADL's (although the hand is capable of up to 40 rad/sec) [17]. The bandwidth shown in Fig. 2.11 represents a joint angular velocity of 7.07 rad/sec, thus indicating joint speeds more than adequate for most ADL's, and in general is representative of human capability [18].

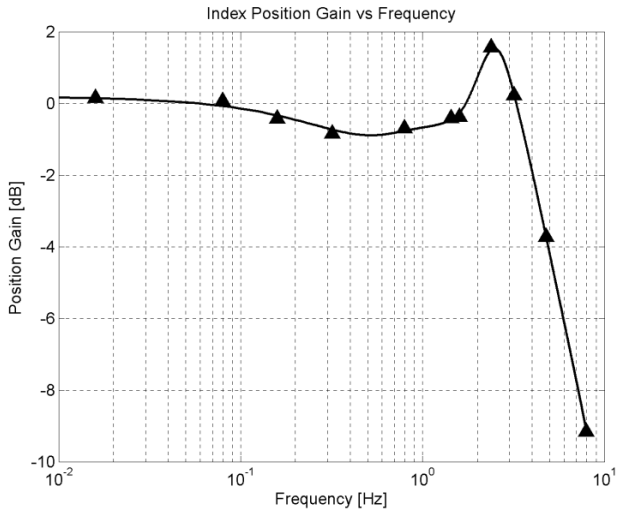

Figure 2.11 - Index position gain vs. frequency for ±25% tendon excursion about mid-flexion point indicating a bandwidth of 4.5 Hz.

B. Open-loop force tracking

Although the closed-loop position tracking provides a characterization of the positional bandwidth of the fingers, the hand was designed to be operated in a force control mode. Since the actuation units are highly backdriveable, such force control simply constitutes current control in the DC motors. The force tracking capability of the prosthesis was characterized by commanding a positive 0.5A peak-to-peak amplitude sinusoidal current (current being linearly related to tendon force by the motor torque constant and pulley diameter) through the motor at various frequencies using open-loop force (i.e., current) control. The experimental setup consisted of a load cell (Measurement Specialties model ELFM-T2E-025L) connected to MATLAB software via an analog signal conditioning circuit and Humusoft 624 DAQ card. Force normal to the index fingertip at the fully open (0% excursion) position was then measured using the calibrated load cell. The results, shown in Fig. 2.12, indicate a force tracking bandwidth of

approximately 36 Hz. These data show the DC force to current gain at the open (0% excursion) position as being 17.5 Newtons/Ampere in dB (7.5 N/A or 1.7 lbf/A). Note that these forces are averaged over several cycles and do not represent peak values.

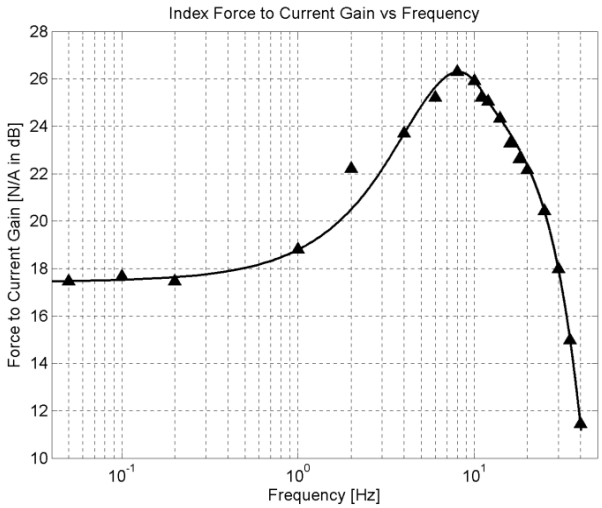

Figure 2.12 - Index Force-to-Current Gain vs. Frequency indicating a bandwidth of 36 Hz and a DC gain of 17.5 Newtons/Amp in dB (7.5 N/A or 1.7 lbf/A).

C. Maximum force as a function of position

The maximum fingertip normal force was measured as a function of percent tendon excursion for the index finger using an Extech Instruments 475044 tension and compression force gauge rigidly mounted in a variety of positions relative to the palm. The index finger was flexed and held in place for each position to be measured. The force gauge was then mounted with its sensing tip placed adjacent and perpendicular to the fingertip face. With the finger in position, a current of 1A (the thermal limit for short term operation) was passed through the motor so that the maximum force could be recorded with a minimum amount of initial travel. This was repeated three times and an average of the forces was taken. These values were then normalized by the initial maximum force at the fully open position, F_o=11.7 N, the results of which are shown in Fig. 2.13.

The curvature in the data points of Fig. 2.13 may be explained as follows. At small tendon excursions there is no considerable counteracting force from the springs in the joints of the finger. As tendon displacement increases, the springs provide a (linearly) increasing opposing force, causing the fingertip force to initially drop. Simultaneously, as the finger traverses its range of motion, the tendons act through increasingly greater moment arms (across the finger joints) and by 20% of tendon excursion the maximum fingertip force begins to increase again. The drop in maximum force due to spring resistance is therefore eventually overcome by greater mechanical advantage as tendon excursion, and finger position, increases.

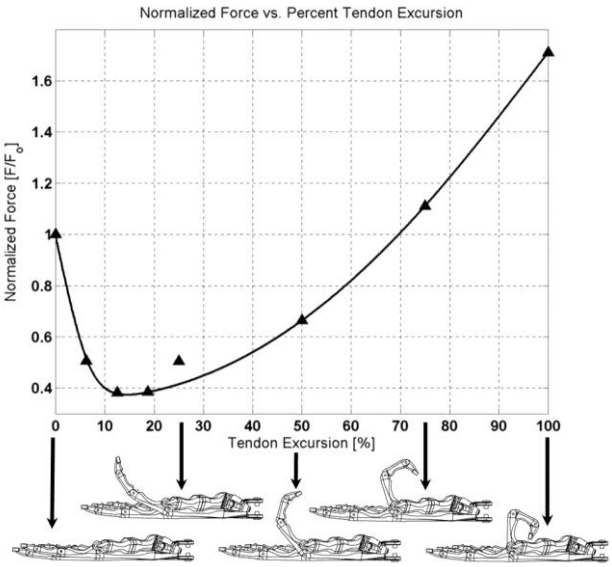

Figure 2.13 - Normalized fingertip normal force vs. percent tendon excursion.

The maximum force is found by multiplying the initial force by the normalized force at full excursion. This results in a maximum force of 19.9N, indicating that the hand can attain the fingertip normal force of 20N (at full flexion) specified in the actuation unit design. A summary of the technical specifications of the hand is given in Table 2.3.

Table 2.3 - Prosthetic Hand Technical Specifications

SPECIFICATION	VU HAND
Number of Actuators	5
Number of Active Digits	5
Number of Joints	16
Weight	580 g
Maximum Force	80N
Grasp Patterns	8
Grasp Speed (Time to Close)	400 ms
Noise (dBA @ 1 meter)	52.1

VI. Conclusion and Future Work

This paper describes a prototype prosthesis designed for use with a multiple channel EMG interface. By utilizing underactuation governed by moment isotropy the hand was shown to achieve a complete grasp taxonomy consisting of eight desired hand postures utilizing five independent actuators. The hand is operated in an open-loop force control configuration and the actuation units are backdriveable. This permits the preservation of some degree of native force sensing in the user's existing musculature rather than providing sensory feedback using

additional instrumentation and hardware.

The hand is capable of providing a 20 N maximum fingertip force at the forefinger which is also representative of the thumb and middle fingers (the other two digits in general are capable of one half of that force, since the tendon force is split between the two with a pulley differential). The continuous force (~80N) is less than the peak capability of a native hand but adequate for most activities of daily living. It was further demonstrated that the hand is capable of tracking forefinger position at 4.5 Hz, which is representative of the native human hand and suitable for the activities of daily living. The prosthesis also features anthropomorphic design, normal kinematic and kinetic hand function, and quiet operation. Furthermore the device can scaled on an individual basis and directly manufactured to facilitate user acceptance.

Current work includes the incorporation of an outer layer designed to mimic the soft tissue properties of the natural hand (i.e., a cosmesis), and inclusion of off-axis compliance to improve physical robustness (i.e., to mitigate the effects of shock loading). Both issues are of critical importance to the functionality of a prosthetic hand. In addition to enhancing cosmetic appearance, the cosmesis will also: enhance grasping by providing compliant, slip reducing surfaces, provide some degree of environmental robustness and acoustically dampen sound from the motors. Finally, the cosmesis will complement the torsional springs in each joint (in providing an extension moment), although the cosmesis stiffness is expected to be a fraction of the torsion spring stiffness currently utilized in the hand.

Future work includes the design of a new version of the hand, wherein the actuation units are located within the hand (i.e., conversion of the current prototype to an intrinsic hand with comparable speed/force performance, in order to make the hand more applicable to a broader set of transradial amputees). Additional future work includes the addition of a two degree-of-freedom wrist, the implementation of embedded power and electronics, and the use of myoelectric signals to control the prosthesis.

Epilogue

Experiments conducted with the prosthetic system described above demonstrated that the extrinsic hand was capable of adopting grasps and postures which span over 85% of the activities of daily living, while producing levels of force and speed biomechanically relevant to those required during such activities. These results provided an encouraging proof of concept for the prosthesis; however, several practical issues remained unaddressed. For instance, to be applicable to the largest demographic, and for commercial viability, greater modularity was required. That is, the extrinsic hand as designed precluded use by persons with amputations below the most proximal transradial level (i.e. the device could not be worn by those with distal transradial or wrist disarticulation amputations). Also, due to backdriveability in actuation, constant effort by the user and persistent power consumption were required to maintain a given

grasp or posture. Furthermore, the user interface was unsuitable for an amputee as it required the use of a native hand to provide user input. Such considerations motivated the next stage in development of the multigrasp prosthesis, and the work presented in the following chapter.

References

[1] L. A. Miller, K. A. Stubblefield, R. D. Lipschutz, B. A. Lock, and T. A. Kuiken, "Improved myoelectric prosthesis control using targeted reinnervation surgery: a case series," *IEEE Trans Neural Syst Rehabil Eng,* vol. 16, pp. 46-50, Feb 2008.

[2] L. Miller, R. Lipschutz, K. Stubblefield, B. Lock, H. Huang, T. Williamsiii, R. Weir, and T. Kuiken, "Control of a Six Degree of Freedom Prosthetic Arm After Targeted Muscle Reinnervation Surgery," *Archives of Physical Medicine and Rehabilitation,* vol. 89, pp. 2057-2065, 2008.

[3] Y. Kamikawa and T. Maeno, "Underactuated five-finger prosthetic hand inspired by grasping force distribution of humans," in *Intelligent Robots and Systems, 2008. IROS 2008. IEEE/RSJ International Conference on*, 2008, pp. 717-722.

[4] P. J. Kyberd and J. L. Pons, "A comparison of the Oxford and Manus intelligent hand prostheses," in *Robotics and Automation, 2003. Proceedings. ICRA '03. IEEE International Conference on*, 2003, pp. 3231-3236 vol.3.

[5] H. Huang, L. Jiang, Y. Liu, L. Hou, H. Cai, and H. Liu, "The Mechanical Design and Experiments of HIT/DLR Prosthetic Hand," in *Robotics and Biomimetics, 2006. ROBIO '06. IEEE International Conference on*, 2006, pp. 896-901.

[6] L. Zollo, S. Roccella, E. Guglielmelli, M. C. Carrozza, and P. Dario, "Biomechatronic design and control of an anthropomorphic artificial hand for prosthetic and robotic applications," *Ieee-Asme Transactions on Mechatronics,* vol. 12, pp. 418-429, Aug 2007.

[7] M. Controzzi, C. Cipriani, and M. C. Carrozza, "Mechatronic design of a transradial cybernetic hand," in *Intelligent Robots and Systems, 2008. IROS 2008. IEEE/RSJ International Conference on*, 2008, pp. 576-581.

[8] A. Kargov, C. Pylatiuk, R. Oberle, H. Klosek, T. Werner, W. Roessler, and S. Schulz, "Development of a multifunctional cosmetic prosthetic hand," in *IEEE International Conference on Rehabilitation Robotics*, 2007, pp. 550-553.

[9] S. Jung and I. Moon, "Grip force modeling of a tendon-driven prosthetic hand," in *International Conference on Control, Automation and Systems*, 2008, pp. 2006-2009.

[10] C. M. Light and P. H. Chappell, "Development of a lightweight and adaptable multiple-axis hand prosthesis," *Medical Engineering & Physics,* vol. 22, pp. 679-684, Dec 2000.

[11] C. L. Taylor and R. J. Schwarz, "The Anatomy and Mechanics of the Human Hand," *Artificial Limbs,* vol. 2, pp. 22-35, May 1955.

[12] M. R. Cutkosky, "On grasp choice, grasp models, and the design of hands for manufacturing tasks," *Robotics and Automation, IEEE Transactions on,* vol. 5, pp. 269-279, 1989.

[13] D. Silcox, M. Rooks, R. Vogel, and L. Fleming, "Myoelectric Prostheses. A Long Term Follow up and a Study of the use of Alternate Prostheses," *Journal of Bone and Joint Surgery-American Volume,* vol. 75A, pp. 1781-1789, 1993.

[14] D. J. Atkins, D. C. Y. Heard, and W. H. Donovan, "Epidemiological Overview of Individuals with Upper-Limb Loss and Their Reported Research Priorities," *Journal of Prosthetics and Orthotics,* vol. 8, pp. 2-10, 1996.

[15] P. J. Kyberd, D. J. Beard, J. J. Davey, and J. D. Morrison, "A Survey of Upper-Limb Prosthesis Users in Oxfordshire," *Journal of Prosthetics and Orthotics,* vol. 10, pp. 85-91, 1998.

[16] J. E. Colgate and N. Hogan, "Robust Control of Dynamically Interacting Systems," *International Journal of Control,* vol. 48, pp. 65-88, 1988.

[17] R. F. Weir, "Design of Artificial Arms and Hands for Prosthetic Applications," in *Standard Handbook of Biomedical Engineering and Design*, M. Kutz, Ed., ed New York: McGraw-Hill, 2003, pp. 32.1-32.61.

[18] L. A. Jones and S. J. Lederman, *Human Hand Function*. New York: Oxford, 2006.

Chapter 3 - Design of a Multigrasp Transradial Prostheses

Tuomas E. Wiste, Skyler A. Dalley, H. Atakan Varol, and Michael Goldfarb

Vanderbilt University

Nashville, TN

From: ASME Journal of Medical Devices, Volume 5, Issue 3

Status: Published August 18, 2011

Prologue

In the following work, the extrinsically actuated prosthesis was redesigned with intrinsic actuation to provide greater modularity. To accomplish this, four (vs. five) actuators were utilized, each of which was smaller in size. To compensate for the loss in torque associated with the use of smaller motors, and to provide tendon forces comparable to the previous design, brushless dc motors (which have superior torque density), a higher planetary gear ratio, and smaller diameter pulleys were utilized. Bidirectional clutches incorporated into the actuation units, in conjunction with series elastic elements, allowed position/force to be maintained in the absence of user input, alleviating cognitive burden and reducing power consumption. The redesigned hand can be seen in Figs. 3.i.

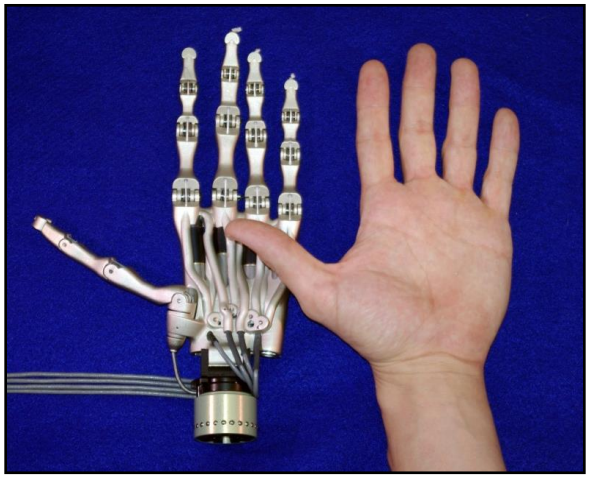

Figure 3.i -The intrinsically actuated multigrasp prosthetic hand.

New drive electronics were developed to accommodate the brushless motors. This involved the design of a custom PCB board with connectors for data acquisition (Humusoft MF624) and sockets for brushless DC servo drives (Advanced Motion Controls AZB6A8C), depicted in Fig. 3.ii. Control was modified to include a PI controller wrapped around the torque control loop of the servo drives, but still depended on FSR or programmed user input.

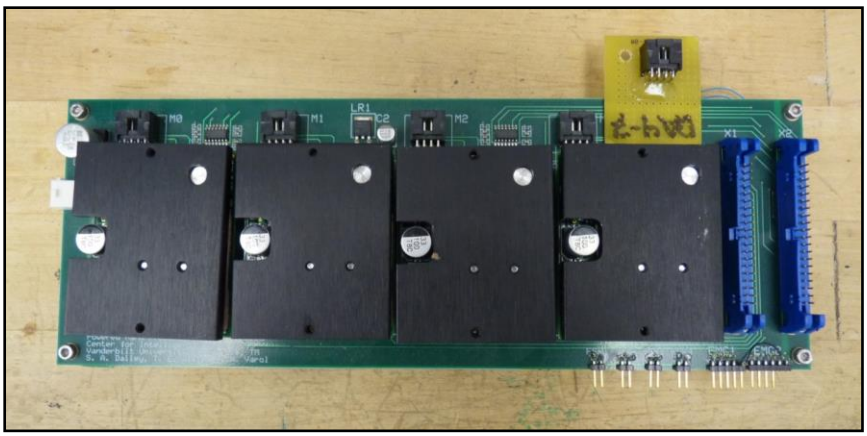

Figure 3.ii - Brushless DC electronics for power and control of the intrinsic hand.

Abstract

This paper describes the design and performance of a new prosthetic hand capable of multiple grasp configurations, and capable of fingertip forces and speeds comparable to those used by healthy subjects in typical activities of daily living. The hand incorporates four motor units within the palm, which together drive sixteen joints through tendon actuation. Each motor unit consists of a brushless motor that drives one or more tendons through a custom two-way clutch and pulley assembly. After presenting the design of the prosthesis, the paper presents a characterization of the hand's performance. This includes its ability to provide eight grasp postures, as well as its ability to provide fingertip forces and finger speeds comparable to those described in the biomechanics literature corresponding to activities of daily living.

I. Introduction

The human hand contains approximately twenty degrees of freedom (DoF). In contrast, a traditional prosthetic hand (either body-powered or myoelectric) contains one. In an effort to provide upper extremity amputees with a more functional approximation of the human hand, several multi-degree-of-freedom prosthetic hands have been developed. Since control inputs from the amputee are limited, and since size and weight are constraining factors, these hands have been designed with fewer degrees of freedom and/or a greater degree of coupling than contained in the native hand. Further, prosthetic hands typically include all actuation within the hand (i.e., they are intrinsically actuated), such that they accommodate a larger population of transradial amputees. Some notable examples of such multi-degree-of-freedom prosthetic hands include those described in [1-9]. Of these devices, the most highly underactuated one is the hand described in [1], which utilizes a single ultrasonic motor to drive fifteen joints (three in each digit) through a fifteen-way differential coupling. The hands described in [2] and [3] each incorporate two independent actuators. The hand described in [2] (disregarding the wrist joint) contains nine powered joints (three in the thumb and three in each of the second and third digits). One actuator

drives the six joints in the second and third digits through a pulley and tendon arrangement that provides kinematic coupling between the joints, while the second actuator controls the three joints in the thumb via a Geneva wheel mechanism that switches control between two thumb movements based on input range. Note that the fourth and fifth digits are not actuated, but rather can be passively positioned in different configurations. The hand described in [3] incorporates sixteen powered joints, wherein the four fingers (twelve joints) are driven by one motor through a compliant coupling mechanism, and the thumb (four joints) is driven by a second motor through a Geneva wheel mechanism in a conceptually similar manner to the hand described in [2]. The prosthetic hand described in [4, 5] contains sixteen powered joints (three in each finger and four in the thumb), which are driven by four independent actuators. Specifically, two motors are utilized to actuate the thumb, one to actuate the index finger, and one to actuate the remaining three fingers through a compliant differential coupling. The prosthetic hand described in [6] incorporates sixteen powered joints (three in each finger and four in the thumb), which are driven by six independent actuators through a linkage-based kinematic coupling mechanism. In particular, each finger is actuated by a separate motor, while the thumb is actuated by two. Like the hand in [6], the hand described in [7] utilizes six motor actuators allotted in a similar fashion, although the hand described in [7] incorporates fused distal-interphalangeal (DIP) joints in each digit, and thus incorporates eleven rather than sixteen powered joints. The underactuation in [7] is accommodated by combined tendon/linkage kinematic mechanisms. Finally, the fluidic hand described by [8, 9] utilizes a single electric motor to drive a miniature hydraulic pump, and incorporates five miniature electrohydraulic valves to control eight powered joints via miniature hydraulic actuators (two valves control the thumb, two control the index finger, and one controls the remaining digits).

In addition to the aforementioned hand prostheses reported in the engineering literature, some multi-grasp hand prostheses have recently been introduced, or are currently emerging on the commercial market. These include the “i-LIMB” hand (Touch Bionics), the “Bebionic” hand (RSL Steeper), and the “Michelangelo” hand (Otto Bock). The i-LIMB and Bebionic hands, both of which have a similar configuration, each contain ten powered joints (two in each finger, two in the thumb) driven by five motors (one for each digit) via belts and linkages, respectively, in addition to one passive joint (palmer abduction/adduction of the thumb), which can be manually manipulated. The Michelangelo hand contains six joints (one in each finger and two in the thumb) which are positioned by two actuators – one that switches the thumb between palmer abduction and adduction, and one that powers a compliantly coupled flexion of all the remaining joints.

This paper presents the design of a new intrinsically actuated prosthetic hand, which was designed to achieve a set of eight grasp postures, to provide proportional movement between these grasp postures, to achieve force and speed characteristics appropriate for most activities of daily living, and to adhere to appropriate size and weight constraints. Following a description of

the prosthesis design, experimental results are presented that characterize the force and speed capabilities of the respective digits. The basic configuration of the hand is similar to the configuration utilized in [4, 5] (i.e., four motors actuate sixteen joints with a similar arrangement of underactuation). Unlike the prosthesis described in [4, 5], however, the hand prosthesis described herein incorporates a significantly different structure; leverages a nickel-coated additive manufacturing process to enhance the compactness of the design; includes a different motor unit design, particularly with respect to a custom integrated two-way clutch and pulley mechanism; incorporates a different tendon routing configuration enabled by the additive manufacturing approach; includes series elastic elements in the tendon paths; and incorporates an approach to tendon force estimation and control enabled by the combination of series elastic elements and motor current measurement. Note that these design elements (with the exception of the nickel-coated additive manufacturing methods), in addition to the fact that all actuation is incorporated inside the hand, also distinguish the hand described herein from an extrinsically actuated hand previously described by the authors [10]. These distinct elements are described subsequently, followed by a performance characterization of each degree of actuation of the hand.

II. Design Objectives

The hand prosthesis described herein was designed to enable amputees to better perform activities of daily living (ADLs), relative to a single-degree-of-freedom prosthesis, primarily by enabling a set of hand grasps and postures which better span the grasp taxonomies commonly used in such activities. As described by [11] and categorized by [12], these grasps include the tip, lateral, tripod, cylindrical, spherical, and hook grasps. In fact, as studied in [13] and reported in [14], this set of grasps constitute approximately 85% of the grasps used in activities of daily living, and as such, constitute a reasonable set of grasp objectives for the design of a multi-degree-of-freedom hand prosthesis. In addition to achieving this set of grasps, two additional postures, a pointing posture and a platform posture, are useful for activities of daily living. Specifically, a pointing posture provides the user with the ability to push buttons or keys (e.g., on telephone or a keyboard), and a platform posture enables a user to reach inside a pocket, or cradle a book or dinner plate. As such, the hand described herein was designed to obtain the aforementioned six grasps (i.e., tip, lateral, tripod, cylindrical, spherical and hook), in addition to two postures (i.e., point and platform). In order to make such grasps useful, the hand prosthesis must provide fingertip forces commensurate with typical activities of daily living. The fingertip forces exerted during activities of daily living (in healthy individuals) have been measured in several studies [15-21].

Pylatiuk et al. [15] conducted a study that measured the hand forces involved in three tasks representative of typical activities of daily living. One task involved (emulated) pouring from a bottle; one involved twisting the lid off of a cylindrical tin; and one involved using a tip grasp to zip

a large zipper (such as would open or close a backpack). In these studies, Pylatiuk et al. measured maximum fingertip forces (excluding impact) of approximately 10 N (which occurred during the zipper task). Kargov et al. [16] conducted a similar study, although in this study they considered only tasks involving the cylindrical grasping of a glass bottle, and found that healthy subjects exerted a maximum contact force of approximately 4 N while grasping the bottle. Smaby et al. [17] measured the lateral pinch (also called key grasp) forces involved in 12 insertion tasks, including inserting a key into a keyhole, a fork into putty, a plug into an electrical outlet, and pressing a button on a remote entry key. Of these tasks, Smaby et al. state that 9 of the 12 required pinch forces of less than 10.5 N. Of the remaining three tasks, zipping close a large horizontal zipper (e.g., on a suitcase) required pinch forces of up to 15 N for an average subject, pulling an electrical plug out of a socket required on average approximately 18 N, and inserting an electrical plug into an outlet approximately 25 N. Radwin et al. [18] conducted a study measuring the fingertip forces exerted when vertically grasping objects of varying size (between 45 and 65 mm span) and varying mass (between 1 and 2 kg). In their study, they report subject averaged maximum index fingertip forces of approximately 8 N, and subject averaged maximum middle, ring, and little fingertip forces of approximately 6 N, 4 N, and 4 N, respectively. In a different study, Fowler and Nicol [19] measured the index fingertip forces exerted during a number of different ADLs, including opening a jar, turning a water tap, turning a key, and pouring a jug. The study reports subject averaged maximum values of index finger (normal force) between 16 N (jug pouring) and 26 N (jar opening), where the maximum forces for the other tasks are bounded by these. Note that Purves and Berme [20] conducted similar studies, although as discussed in [19], their studies are likely less accurate, and thus weren't utilized here. Finally, Redmond et al. [21] conducted a study that measured the forces involved in texting with a typical cellular telephone, and report maximum (fingertip or thumbtip) forces of approximately 10 N.

Data characterizing typical finger speeds during ADLs is sparse. It is estimated in [22] that the joints of the hand reach angular velocities of approximately 3 to 4 rad/s (170 to 230 deg/s) during typical ADLs. Note that these estimates correlate well with the specifications of the Otto Bock Sensorhand Speed prosthetic hand (which is perhaps the fastest commercially available myoelectric prosthetic hand), which according to the manufacturer provides a fingertip speed of 300 mm/s, which assuming a finger length of 100 mm, would correspond to a maximum angular velocity (of the metacarpophalangeal joint) of 3 rad/sec.

For a sinusoidal motion with a peak-to-peak amplitude of 45 deg (i.e., approximately 50% joint range of motion (RoM), assuming typical finger joint range of motion of 90 deg), these angular velocities would correspond to a frequency of movement between 1.2 and 1.6 Hz. Alternatively, assuming a minimum jerk trajectory and a nominal joint range of motion of 90 deg, a maximum joint angular velocity of 4 rad/s would correspond to a "time-to-close" (i.e., the time required from full open to full close) of 740 ms.

Finally, consistent with surveys of upper extremity amputees (e.g., [9, 23-25]), the prosthetic hand must be of a mass that is acceptable to the amputee user. Although a precise specification in this regard is difficult to obtain, the mass of the native limb, along with the mass of other emerging multi-degree-of-freedom prosthetic hands, were used together as a nominal mass target for the hand described herein. According to [26], the mass of the typical human hand is approximately 400 g. According to the respective manufacturer's data sheets, the mass of the i-LIMB (pulse) is 460 g, and the mass of the Bebionic hand with standard wrist is 500 g (both exclude the mass of the cosmesis and battery).

The design objectives described in this section are thus summarized as:

- Achieve six grasp types (tip, lateral, tripod, cylindrical, spherical, and hook)
- Achieve point and platform hand postures
- Provide fingertip forces commensurate with typical ADLs; namely, maximum index fingertip forces of approximately 25 N, similar thumbtip force capability, and maximum combined fingertip forces of approximately 12 N for the remaining digits
- Provide joint angular velocities of at least 4 rad/s, which corresponds to a half-RoM bandwidth of 1.5 Hz
- Total hand mass (excluding cosmesis and battery) less than 500 g

Note that these design objectives are consistent with four of the top five priorities of amputees as presented by [27], where the top five priority not specifically addressed by these design objectives is the user's desire to "feel the grasping force". The remainder of this paper describes the design of the hand prosthesis, and provides experimental measurements characterizing the performance of the prosthesis with respect to each of the aforementioned design criteria.

III. Hand Design

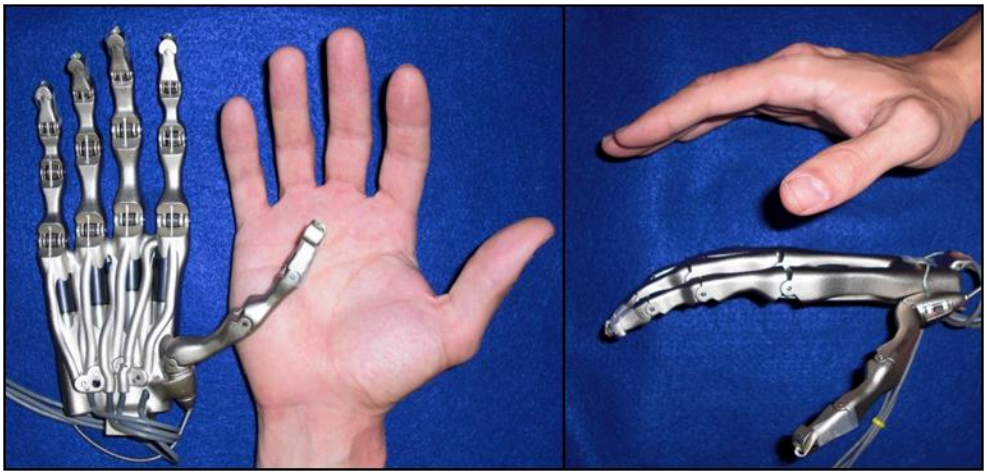

Figure 3.1 - Hand prosthesis prototype (without cosmesis), shown with intact hand for reference.

A. Basic Configuration

The assembled hand prosthesis prototype is shown in Fig. 3.1. The hand prosthesis incorporates sixteen degrees of freedom, which are single-DoF metacarpophalangeal (MCP), proximal interphalangeal (PIP), and distal interphalangeal (DIP) joints in each finger, and a two-DoF carpometacarpal (CMC) and single-DoF MCP and interphalangeal (IP) joints in the thumb. That is, each finger has three DoFs, which enable finger flexion/extension, and the thumb has four DoFs, which enable thumb flexion/extension and palmer abduction/adduction. These sixteen degrees of freedom enable the hand to fully achieve the six grasps and two postures previously described (although it is noted that the significance of the finger DIP and thumb IP joints is arguable). In the absence of hybrid transmissions (which switch the coupling between the motors and joints, as is implemented in designs such as [2] and [3]), independently achieving the aforementioned grasps and postures requires four motors, wherein one actuates thumb (digit I) flexion, one provides for palmer abduction of the thumb, one actuates index finger (digit II) flexion, and one actuates flexion of the remaining fingers (digits III-V). Note that, even with four motors, only six of the aforementioned grasps and postures can be achieved independently of an object being grasped. That is, the distinction between the tripod, cylindrical, and spherical grasps are dependent on the shape and position of an object being grasped, in addition to compliance in the drive couplings. Such a dependency, however, is reasonable, since such grasps are only meaningful (with regard to ADLs) in the context of grasping an object.

In order to minimize mass and enhance the compactness of the prosthesis, tendon-based actuation was utilized to transmit motion between the motors and the joints of the hand. Since the fingertip forces required for typical ADLs are in the direction of finger/thumb flexion (see, for example, [15-19, 21]), a unidirectional tendon configuration was selected, such that the tendon drives provide torques required for finger/thumb flexion, while the hand relies on torsional springs embedded in each joint to provide the torques required for finger/thumb extension. That is, closing of the hand is driven by the tendons, while opening is driven by the torsional springs. Similarly, palmer abduction of the thumb is driven by tendon actuation, while palmer adduction is provided by a torsional spring.

Each tendon is driven by a motor unit, which consists of a brushless motor and gearhead, a two-way clutch that prevents backdriving the motor, and a pulley upon which each tendon is wrapped. The construction of these motor units is described in the following section. The movement associated with each motor unit is referred to as a degree-of-actuation (DoA). The hand prosthesis therefore has four DoAs, which are thumb flexion, thumb abduction, index finger flexion, and digits III-V flexion. The thumb abduction (digit I abduction, or DI-A) motor unit drives only the palmer abduction axis of the CMC joint. The thumb flexion (digit I flexion, or DI-F) motor unit therefore drives three joints (one axis of the CMC joint, the thumb MCP joint, and the thumb IP joint), all via a single tendon. Similarly, the index finger (digit II flexion, or DII-F) motor unit

drives the MCP, PIP, and DIP of the index finger, also via a single tendon. Finally, the digit III-V flexion (DIII-V-F) motor unit drives the MCP, PIP, and DIP joints of the remaining three fingers via three tendons, one for each finger. As such, the DI-A, DI-F, and DII-F motor units each drive a single tendon pulley, while the DIII-V-F motor unit drives three tendon pulleys (stacked in series along the motor unit output shaft), one for each of the DIII-V fingers. All tendons are constructed from polyethylene fiber (Spectra) rated for a load of 580 N (130 lb). Note that, as subsequently discussed, the DIII-V tendons all contain series elastic elements, which enable a compliant differential coupling between these fingers (i.e., they are not strictly kinematically coupled). Figure 3.2 highlights the layout of each of these DoAs, indicating the layout of each motor unit, and the routing of each associated tendon.

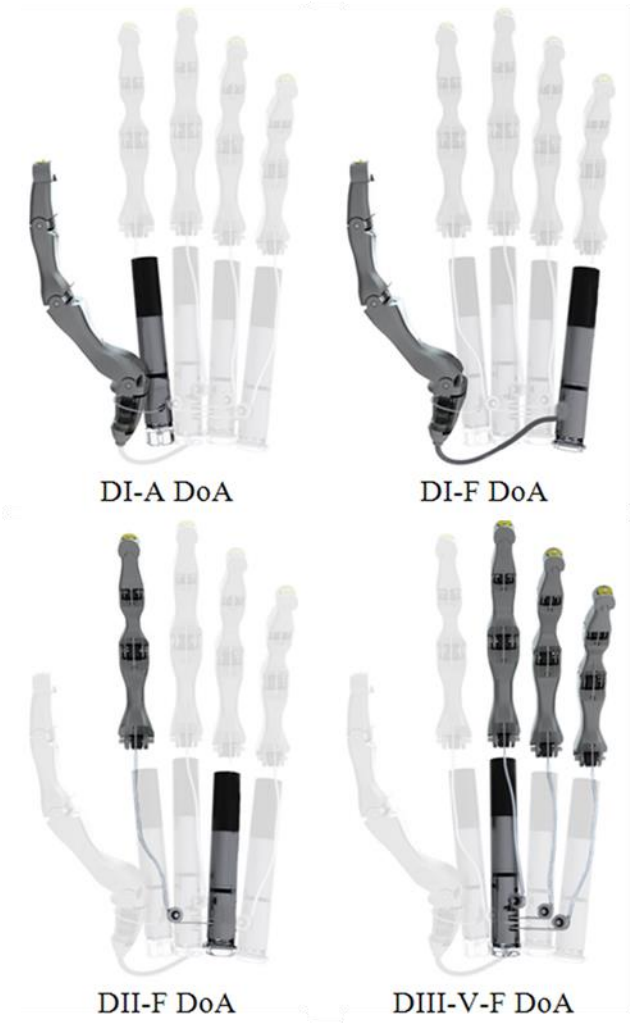

Figure 3.2 - Computer rendering of hand with palm structure removed, illustrating the motor unit layout and tendon routing for each respective degree-of-actuation (DoA). Note that the thumb flexion tendon exits through the dorsal aspect of the hand and is routed through a flexible cable housing (visible in the figure), while all other tendons are routed via pulleys and channels in the palm structure.

Figure 3.3 shows a cross-section through a representative digit (in this case, the thumb). This cross-sectional view highlights the nature of the tendon paths within each digit, the location of the series elastic springs associated with each tendon, and the location of the torsional springs (also referred to as parallel springs) that provide extension torques for each joint. As can be seen in the figure, each fingertip contains a urethane compression spring through which a tendon transmits its actuator force to the finger. The series elastic springs enable improved control of grasping force through the two-way clutches, particularly when grasping a rigid object, and also provide a compliant coupling between the DIII-V fingers. The range of motion of each joint, along with the torsional stiffness of each parallel spring, is given in Table 3.1. Note that all torsional springs have a natural position that is extended 20 degrees relative to the joint range of motion, such that all springs are effectively preloaded by a load corresponding to 20 degrees of deflection. Finally, note that the thumb IP and finger DIP joints have approximately twice the stiffness of the other joints. As such, the IP and DIP joints are not fused, but generally do not flex significantly until relatively high tendon loads are imposed.

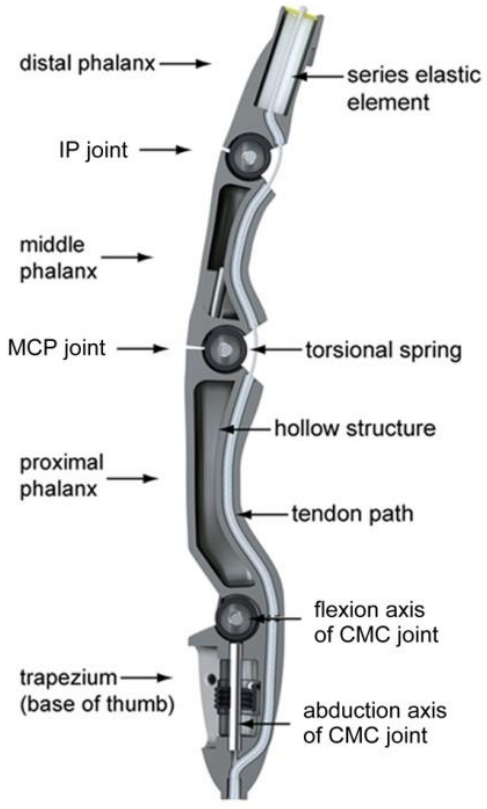

Figure 3.3 - Section view of thumb, showing tendon routing, torsional springs (in each joint), and series elastic elements (in distal phalanx).

Table 3.1 - Range of Motion and Torsional Spring Stiffness in Each Joint.

JOINT	RANGE OF MOTION (Deg)	TORSIONAL SPRING STIFFNESS (N-mm/deg)
Thumb CMC (abduction)	90	0.80
Thumb CMC (flexion) and MCP	105	0.85
Index MCP and PIP	105	0.85
Thumb IP, Index DIP	85	1.50
DIII-V MCP and PIP	105	0.63
DIII-V DIP	85	1.00

B. Motor Units

Each of the four motor units consist of the combination of a brushless motor, planetary gearhead, two-way clutch, and tendon pulley, and additionally includes angular position sensing via Hall effect sensors integrated into the motor. Note that the two-way clutches prevent the load from driving the motor units, without introducing significant friction or loss in the drive train. In this manner, the hand can grasp an object and maintain that grasp, without expending electrical power to do so. Based on the force and speed design objectives previously discussed, each motor unit incorporates a brushless DC servomotor (Faulhaber 1226B), which incorporate integrated Hall effect sensors for measurement of tendon excursion, coupled to a planetary gearhead (Faulhaber 12/4 64:1). The gearhead output drives a 2.5 mm diameter pulley (around which the Spectra tendon is wrapped) through a two-way clutch, which as previously mentioned prevents back-driving without introducing significant loss. The output assembly (consisting of the two-way clutch, tendon pulley, and housing) is shown in an exploded view in Fig. 3.4. The two-way clutch, which is a custom design, is shown in a cross-sectional view in Fig. 3.5. In the forward drive mode, the input shaft drives the pulley through the clutch bearings, without interference from the output assembly housing. In the backward drive mode, the pulley wedges the clutch bearings against the output assembly housing, thus effectively locking the pulley against the housing and preventing the pulley from driving the input shaft. These clutches are characterized in the “Hand Performance” section that follows.

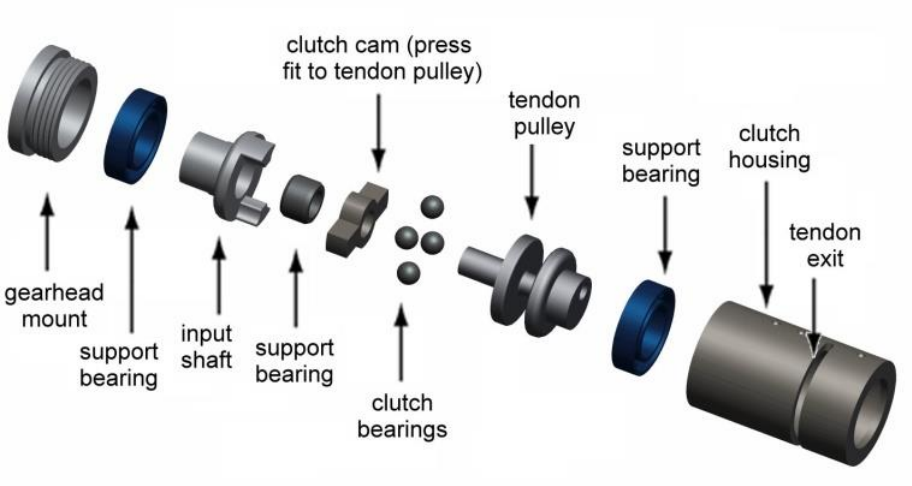

Figure 3.4 - Exploded view of a motor unit output assembly, showing integrated two-way clutch and tendon pulley.

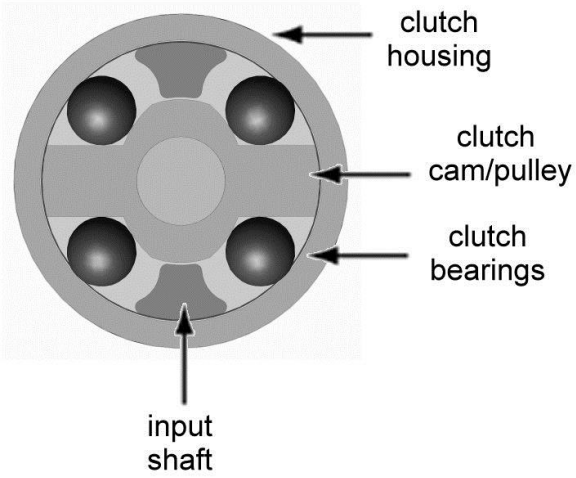

Figure 3.5 - Sectional view through two-way clutch.

C. Structure

A unique aspect of the prosthetic hand described here is the fundamental use of additive manufacturing methods in its conception and design. The entire structure of the hand (i.e., the palm and all digits) is fabricated with a stereolithography (SLA) process from a thermoplastic resin, after which the plastic parts are strengthened with a nickel coating. The additive process enables a realization of hollow, monocoque components with complex features, which are not possible or not practical with conventional fabrication techniques. Some of these features include integrated electrical wire routing in the palm and integrated tendon routing in the palm and all digits. All tendon and wire routing paths incorporate complex curvatures to increase compactness and decrease tendon friction, and which cannot be realized with conventional fabrication techniques.

D. Sensing

As previously mentioned, the implementation of series elasticity provides non-kinematic coupling (i.e., enables conformal grasping) between the DIII-V fingers. Of equal importance, the series elastic elements enable control of grasping force, despite the presence of the two-way clutches, by leveraging the position control loop (enabled by the Hall effect sensors in the motor units) that is already in place around the motor units. The hybrid position/force control aspect of the hand is designed to function as follows. When the fingertip is not in contact with an object, the tendon force is a well known function of the tendon displacement (based on the combination of series and parallel springs). By monitoring this relationship (i.e., via the measured motor displacement and the actuator current), one can ascertain when each finger has come into contact with an object. Once in contact with an object, the measurement and control of the tendon displacement provides measurement and control of the grasping force, where the change in applied force is related to the change in tendon displacement by the stiffness of the series elastic elements. As such, a controller can be constructed to control both displacement of the fingers (when gesturing) and control of grasp force (when grasping), both based on the measurement and control of tendon displacement (which is measured by integrated Hall effect sensing in the brushless motor unit), and by monitoring the commanded motor currents (which requires no additional instrumentation). Further, since the series elastic elements are located between the object load and the two-way clutches, presence of the clutches do not impair the ability of the hand to impose stable, force-controlled grasping. Finally, just as the clutches effectively “lock in” a given finger position under pure position control, the same clutches with the series elastic elements and described hybrid controller provide the dual function of locking in position when gesturing, or locking in force when grasping.

IV. Experimental Characterization of Hand Performance

The following sections provide either an experimental demonstration or characterization, as appropriate, for each of the design objectives discussed in the “Design Objectives” section of this paper.

A. Ability to Provide Grasps and Postures

As previously mentioned, the hand was designed to achieve a set of six grasps and two postures. The ability of the hand to achieve these grasps and postures is demonstrated in Fig. 3.6. A video of the hand prosthesis achieving these grasps and postures in real-time can be viewed at http://research.vuse.vanderbilt.edu/cim/VMGhand.wmv.

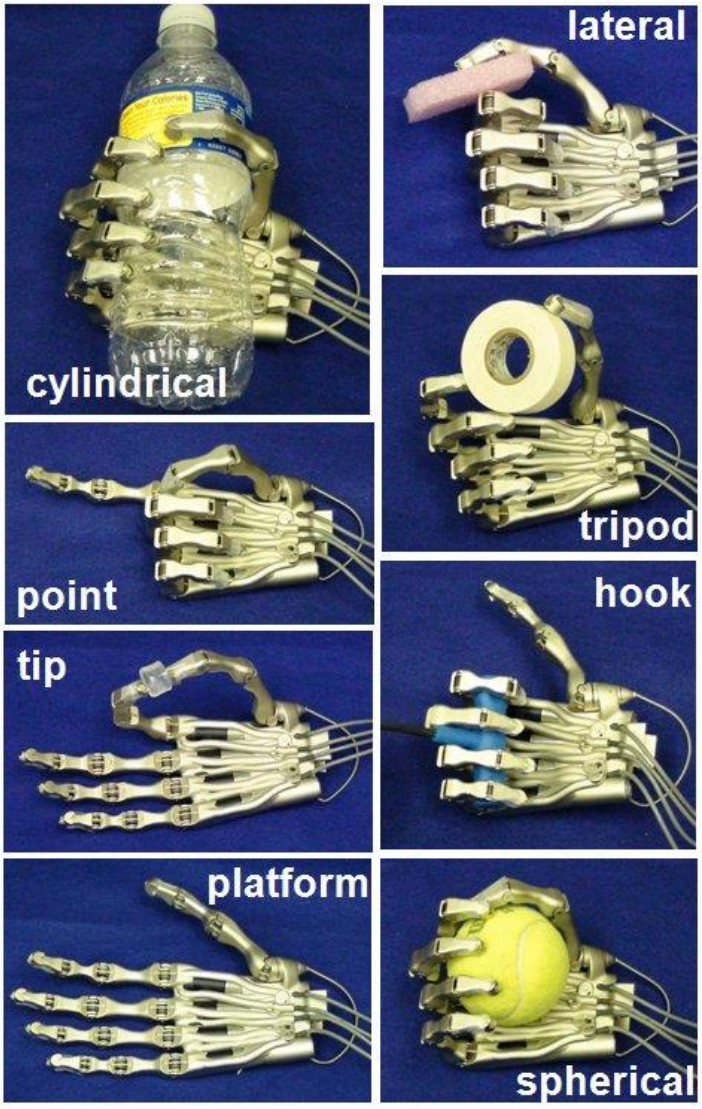

Figure 3.6 - Six hand grasps and two hand postures, which constitute one of the primary design objectives of the hand prototype.

B. Fingertip Forces

The maximum fingertip normal force was measured as a function of percent-tendon-excursion for each DoA (see Fig. 3.2) using a force gauge rigidly mounted orthogonally to the tip of the finger or thumb. In order to measure the combined force of the DIII-V fingers, the three fingers were coupled via extension springs to the same force gage. The maximum force is a function of the maximum allowable current in the motor, which in turn is thermally limited by the maximum allowable winding temperature. Since grasping is typically characterized by a constant force, and since the prosthesis described herein incorporates series elastic elements in the fingers and two-way clutches in the motor units, the motors need only provide a short period of active force in order to grasp an object and deform the series elastic elements, after which that

force will be maintained passively by the two-way clutches (assuming the object does not continue to deform). Based on thermal simulation of the motors, if each motor is initially at room temperature, each can withstand a current of 1.8 A for approximately five sec before reaching its recommended thermal limit. Since the fingers can fully close in approximately 300 ms, a full grasp can be obtained and held (by the clutches) in considerably less time (than five sec). Therefore, based on the same thermal modeling of the motors, each motor can continuously sustain a current of 1.8 A for approximately 800 ms every ten seconds (i.e., a new object can be grasped every ten seconds, with each grasp held continuously). In order to provide a margin of safety, a 400 ms current pulse of 1.8 A was used to characterize the maximum (continuous) force capability of each DoA as a function of percent tendon excursion, the results of which are shown in Fig. 3.7.

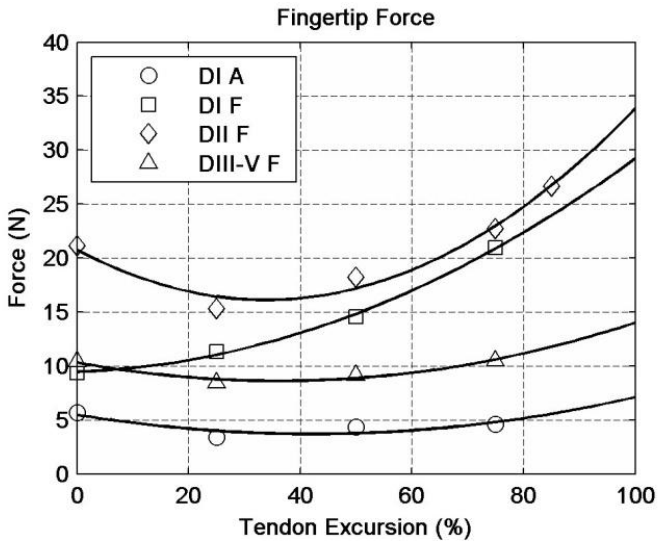

Figure 3.7 - Fingertip normal force vs. percent tendon excursion for each DoA.

As shown in the figure, the index finger is capable of exerting forces between approximately 15 N and 35 N in flexion; the thumb is capable of between 10 N and 30 N in flexion and approximately 5 N in palmer abduction; and the remaining three fingers are collectively capable of exerting between 10 N and 15 N in flexion. Since most grasps are characterized by large tendon excursions (e.g., the spherical grasp shown in Fig. 3.6 is characterized by approximately 70% tendon excursions), maximum usable grasp forces for most ADLs will be approximately 20-25 N for index finger flexion, approximately 18-23 N for thumb flexion, approximately 10-12 N for DIII-V finger flexion, and approximately 5 N for thumb abduction. Recall that the design objectives, based on measured forces during ADLs, were approximately 25 N in index finger and thumb flexion and approximately 12 N for flexion of the remaining digits. Based on the data presented in Fig. 3.7, these objectives were fully achieved in all digits, and largely (although not fully) achieved in the range of motion in which such ADLs are likely to occur.

C. Clutch Holding Capacity

The clutches were tested to verify that their torque holding capacity exceeded the breaking strength of the Spectra tendons. Specifically, their torque holding capacity was measured by loading a test tendon from the clutch output pulley with a lever arm, and measuring the resultant load with a force gage. In these tests, the clutches were loaded to a maximum continuous torque of 790 mNm, which corresponds to a 630 N (140 lb) load in the test tendon. The clutch was not loaded beyond this point, since the actual tendon used in the hand prosthesis is rated at 580 N (130 lb), and thus the failure would most likely occur in the tendon prior to failure of the two-way clutch.

D. Speed Characterization

As previously mentioned, the velocity-based design objective requires a half-RoM bandwidth of 1.5 Hz. As such, the half-RoM position tracking capability of each degree-of-actuation was characterized by commanding the position of the finger (or fingers) around the mid-flexion point (corresponding to 50% of total tendon excursion). In these assessments, each tendon tracked a sinusoidal position signal which varied ±25% of total tendon excursion around the mid-flexion point for various frequencies. The bandwidth was determined using the integrated Hall effect sensors to measure tendon pulley position via a Humusoft 624 DAQ card and the real-time interface provided by MATLAB Real-Time Workshop. Figure 3.8 shows the resulting tracking bandwidth for each DoA, indicating that the index finger flexion, thumb flexion, and DIII-V finger flexion axes each have (-3 dB) position tracking bandwidths of between 4 and 5 Hz, while the thumb abduction axis has a position tracking bandwidth of approximately 11.5 Hz. Further, in terms of full tendon excursion, all fingers were able to fully close (i.e., move from the fully extended position to the fully flexed position) in approximately 280 ms. Thus, the maximum velocity capability of the hand prostheses fully satisfies the design objective for speed of movement.

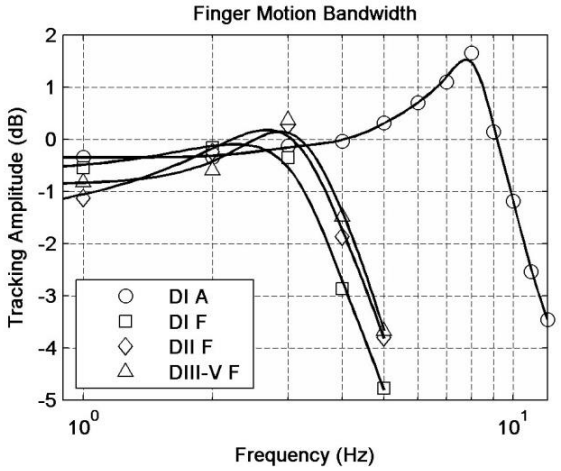

Figure 3.8 -Tendon excursion tracking bandwidth for ±25% tendon excursion about mid-flexion point for each of the degrees of actuation.

E. Mass Projections

The total mass of the hand prosthesis as shown (i.e., without cosmesis, battery, or electronics) is 320 g. As previously mentioned, the design objective is for a mass less than 500 g, excluding cosmesis and battery, but including electronics. Although the current prosthesis prototype does not currently include embedded electronics, it is estimated that such electronics would have a mass less than 100 g. As such, it is estimated that the total mass of the prosthesis prototype, once embedded electronics are included, would be approximately 420 g. A summary of the technical specifications of the hand, including the force and speed characteristics, is given in Table 3.2.

Table 3.2 - Summary of Prosthetic Hand Technical Specifications.

SPECIFICATION	VU HAND
Degrees of freedom	16
Number of actuators	4
Mass (w/o cosmesis, battery, electronics)	320 g
Grasp patterns	8
Grasp speed (time to close)	280 ms
Audible noise (dBA @ 1 meter)	52.1
Max index fingertip force (70% excursion)	22 N
Max index thumb tip flexion force (70% excursion)	19 N
Max DIII-V combined fingertip force (70% excursion)	10 N
Max thumbtip abduction force (70% excursion)	4.5 N
Max index fingertip force (100% excursion)	34 N
Max index thumb tip flexion force (100% excursion)	29 N
Max DIII-V combined fingertip force (100% excursion)	14 N
Max thumbtip abduction force (100% excursion)	7 N

F. Power Projections

Although one cannot fully characterize power consumption without embedded and battery-powered electronics, a characterization of the electrical power required for actuation is useful in understanding the first-order power requirements of the prosthesis. Based on motor current and voltage measurement, approximately 5 J of electrical energy are required at the leads of the brushless motors to fully close the hand prosthesis (recall that, once achieved, the two-way clutches will maintain the grasp without continued power consumption). Assuming 80% efficient servoamplifiers, 6.25 J would be required of a battery for each grasp. As such, a 740 mAh, 11.1 V lithium polymer battery (e.g., Thunderpower TP730-3SJPL2), which has a mass of 57 g, would provide sufficient energy for approximately 4700 grasps. Of course, one cannot project accurately the expected battery life without accurate estimates of the power requirements of the embedded system, including the power required for computation, sensing, communication, and power management. Despite this, the power required at the actuators of the prosthesis prototype appears reasonable.

V. Conclusion and Future Work

This paper describes a hand prosthesis capable of providing six grasps and two postures, which (based on prior studies) collectively constitute over 85% of the grasps and postures used in activities of daily living. The hand prosthesis utilizes additive manufacturing methods and incorporates brushless motors with integrated position sensing to achieve a compact and relatively light weight design with a high power-to-weight ratio. The fingertip forces and movement speeds of the hand were characterized, and shown to be comparable to the respective forces and speeds characteristic of many activities of daily living.

Future work includes the integration of embedded electronics and a cosmesis. Importantly, such a device will not be fully useful to the amputee without a command interface that provides access to the full functionality of the hand in a manner that does not require undue cognition on the part of the amputee. Such an interface is also a topic of future work.

Epilogue

The work described above revealed that the Intrinsic Hand was capable of forces and speeds comparable, if not superior, to those of the extrinsic hand. While the intrinsic hand displayed desirable technical performance, a dependable user interface which would allow an amputee to quickly, reliably and intuitively access the functionality of the multigrasp device was still required. This served to motivate the work in the following chapter.

References

[1] Y. Kamikawa and T. Maeno, "Underactuated five-finger prosthetic hand inspired by grasping force distribution of humans," in *Intelligent Robots and Systems, 2008. IROS 2008. IEEE/RSJ International Conference on*, 2008, pp. 717-722.

[2] J. L. Pons, E. Rocon, R. Ceres, D. Reynaerts, B. Saro, S. Levin, and W. Van Moorleghem, "The MANUS-HAND dextrous robotics upper limb prosthesis: mechanical and manipulation aspects," *Autonomous Robots,* vol. 16, pp. 143-163, Mar 2004.

[3] J. Chu, D. Jung, and Y. Lee, "Design and control of a multifunction myoelectric hand with new adaptive grasping and self-locking mechanisms," in *IEEE International Conference on Robotics and Automation*, 2008, pp. 743-748.

[4] C. Cipriani, M. Controzzi, and M. C. Carrozza, "Progress towards the development of the SmartHand transradial prosthesis," in *IEEE International Conference on Rehabilitation Robotics*, 2009, pp. 682-687.

[5] C. Cipriani, M. Controzzi, and M. C. Carrozza, "Objectives, criteria and methods for the design of the SmartHand transradial prosthesis," *Robotica,* vol. 28, pp. 919-927, 2010.

[6] C. M. Light and P. H. Chappell, "Development of a lightweight and adaptable multiple-axis hand prosthesis," *Medical Engineering & Physics,* vol. 22, pp. 679-684, Dec 2000.

[7] S. Jung and I. Moon, "Grip force modeling of a tendon-driven prosthetic hand," in *International Conference on Control, Automation and Systems*, 2008, pp. 2006-2009.

[8] C. Pylatiuk, S. Mounier, A. Kargov, S. Schulz, and G. Bretthauer, "Progress in the development of a multifunctional hand prosthesis," in *Proceedings of the IEEE Engineering in Medicine and Biology Society*, 2004, pp. 4260-3.

[9] A. Kargov, C. Pylatiuk, R. Oberle, H. Klosek, T. Werner, W. Roessler, and S. Schulz, "Development of a multifunctional cosmetic prosthetic hand," in *IEEE International Conference on Rehabilitation Robotics*, 2007, pp. 550-553.

[10] S. A. Dalley, T. E. Wiste, T. J. Withrow, and M. Goldfarb, "Design of a Multifunctional Anthropomorphic Prosthetic Hand With Extrinsic Actuation," *IEEE/ASME Transactions on Mechatronics,* vol. 14, pp. 699-706, 2009.

[11] C. L. Taylor and R. J. Schwarz, "The Anatomy and Mechanics of the Human Hand," *Artificial Limbs,* vol. 2, pp. 22-35, May 1955.

[12] M. R. Cutkosky, "On grasp choice, grasp models, and the design of hands for manufacturing tasks," *Robotics and Automation, IEEE Transactions on,* vol. 5, pp. 269-279, 1989.

[13] C. Jacobson-Sollerman and L. Sperling, "Grip Function of the Healthy Hand in a Standardised Hand Function Test," *Scandinavian Journal of Rehabilitation Medicine,* vol. 9, pp. 123-129, 1977.

[14] C. Sollerman and A. Ejeskär, "Sollerman Hand Function Test: A Standardised Method and its Use in Tetraplegic Patients," *Scandinavian Journal of Plastic and Reconstructive Surgery and Hand Surgery,* vol. 29, pp. 167-176, 1995.

[15] C. Pylatiuk, A. Kargov, S. Schulz, and L. Doderlein, "Distribution of Grip Force in Three Different Functional Prehension Patterns," *Journal of Medical Engineering & Technology,* vol. 30, pp. 176-182, 2006.

[16] A. Kargov, C. Pylatiuk, J. Martin, S. Schulz, and L. Doderlein, "A Comparison of the Grip Force Distribution in Natural Hands and in Prosthetic hands," *Disability and Rehabilitation,* vol. 25, pp. 705-711, 2004.

[17] N. Smaby, M. E. Johansen, B. Baker, D. E. Kenney, W. M. Murray, and V. R. Hentz, "Identification of Key Pinch Forces Required to Complete Functional Tasks," *Journal of Rehabilitation Research and Development,* vol. 41, pp. 215-224, 2004.

[18] R. G. Radwin and S. Oh, "External Forces in Submaximal Five-Finger Static Pinch Prehension," *Ergonomics,* vol. 35, pp. 275-288, 1992.

[19] N. K. Fowler and A. C. Nical, "Measurement of External Three-Dimensional Interphalangeal Loads Applied During Activities of Daily Living," *Clinical Biomechanics,* vol. 14, pp. 646-652, 1999.

[20] W. K. Purves and N. Berme, "Resultant Finger Joint Loads in Selected Activities," *Journal of Biomedical Engineering,* vol. 2, pp. 285-289, 1980.

[21] B. Redmond, R. Aina, T. Gorti, and B. Hannaford, "Haptic characteristics of some activities of daily living," in *Haptics Symposium, 2010 IEEE*, 2010, pp. 71-76.

[22] R. F. Weir, "Design of Artificial Arms and Hands for Prosthetic Applications," in *Standard Handbook of Biomedical Engineering and Design*, M. Kutz, Ed., ed New York: McGraw-Hill, 2003, pp. 32.1-32.61.

[23] D. Silcox, M. Rooks, R. Vogel, and L. Fleming, "Myoelectric Prostheses. A Long Term Follow up and a Study of the use of Alternate Prostheses," *Journal of Bone and Joint Surgery-American Volume,* vol. 75A, pp. 1781-1789, 1993.

[24] D. J. Atkins, D. C. Y. Heard, and W. H. Donovan, "Epidemiological Overview of Individuals with Upper-Limb Loss and Their Reported Research Priorities," *Journal of Prosthetics and Orthotics,* vol. 8, pp. 2-10, 1996.

[25] P. J. Kyberd, D. J. Beard, J. J. Davey, and J. D. Morrison, "A Survey of Upper-Limb Prosthesis Users in Oxfordshire," *Journal of Prosthetics and Orthotics,* vol. 10, pp. 85-91, 1998.

[26] C. E. Clauser, J. T. McConville, and J. W. Young, "Weight, Volume, and Center of Mass of Segments of the Human Body," Wright Patterson Air Force Base, Dayton, Final Report AMRL-TR-69-70, 1969.

[27] C. Pylatiuk and S. Schulz, "Using the Internet for an Anonymous Survey of Myoelectrical Prosthesis Wearers," presented at the Myoelectric Controls Symposium, Fredericton, New Brunswick, Canada, 2005.

Chapter 4 - A Method for the Control of Multigrasp Myoelectric Prosthetic Hands

Skyler A. Dalley, Huseyin Atakan Varol, and Michael Goldfarb

Vanderbilt University

Nashville, TN

From: IEEE Transactions on Neural Systems and Rehabilitation Engineering,

Volume 20, Issue 1

Status: Published January 19, 2012

Prologue

A standard, two-site, electromyogram (EMG) interface (electrodes placed proximally on the anterior and posterior aspects of the forearm) was chosen to obtain user input for the control of the multigrasp hand prosthesis. This interface was chosen as it is minimally invasive, involves a small number of electrodes, and has a dependable track record as the clinical standard in traditional, single DOF, myoelectric devices. Custom EMG circuitry, shown in Fig. 4.i, was then developed and utilized for signal amplification and filtering.

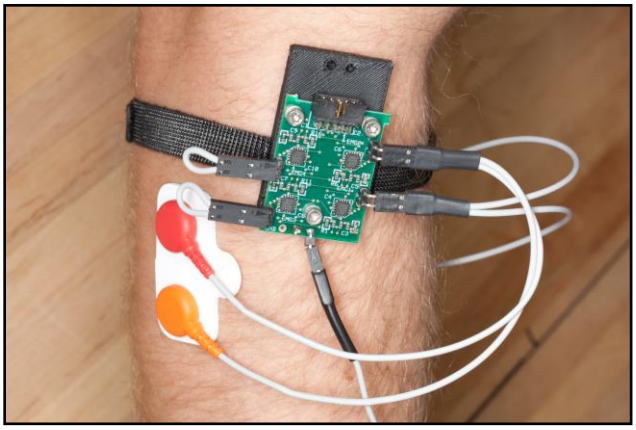

Figure 4.i - Custom EMG circuitry for signal amplification and filtering. The posterior forearm electrode is also visible, where the upper arm is above, and the hand is below.

Abstract

This paper presents the design and preliminary experimental validation of a multigrasp myoelectric controller. The described method enables direct and proportional control of multigrasp prosthetic hand motion among nine characteristic postures using two surface EMG electrodes. To assess the efficacy of the control method, five non-amputee subjects utilized the multigrasp myoelectric controller to command the motion of a virtual prosthesis between random sequences of target hand postures in a series of experimental trials. For comparison, the same subjects also utilized a data glove, worn on their native hand, to command the motion of the virtual prosthesis for similar sequences of target postures during each trial. The time required to transition from posture to posture and the percentage of correctly completed transitions were evaluated to characterize the ability to control the virtual prosthesis using each method. The average overall transition times across all subjects were found to be 1.49 and 0.81 seconds for the multigrasp myoelectric controller and the native hand, respectively. The average transition completion rates for both were found to be the same (99.2%). Supplemental videos demonstrate the virtual prosthesis experiments, as well as a preliminary hardware implementation.

I. Introduction

The human hand is extensively articulated, possessing approximately twenty major degrees of freedom which allow it to execute a wide variety of grasps and postures. Movement of the hand is dictated by the action of an even greater number of muscles, which are concerted by a multitude of efferent and afferent neural signals. This stands in contrast to traditional, commercially available, myoelectric hand prostheses. Until recently, these devices have been restricted to a single degree-of-freedom (DoF), driven by a single actuator and commanded by a single electromyogram (EMG) input (two EMG electrodes placed on antagonistic muscle pairs of the residual forearm). Although such prostheses have far fewer DoFs than the native hand, there are several advantages related to this approach. Primarily, the control of these devices requires little cognitive effort due to the one-to-one mapping between the actuator and EMG input. Also, traditional myoelectric prostheses can provide direct, proportional control of motion. Because they only require a single pair of EMG electrodes the interface is manageable and is easily incorporated into a socket. Furthermore, the control method is not computationally demanding and can occur with minimal delay. A modern version of a single grasp myoelectric prosthesis is the MyoHand VariPlus Speed (Otto Bock, Germany).

Despite these advantages, it has also been noted that single grasp devices have limited grasping capability (because they cannot conform to objects and there is little contact area) and unnatural appearance of motion (mainly due to their low level of articulation) [1]. This is supported by patient surveys which indicate that greater functionality [2] and increased articulation [3] are among their top design priorities. In response to these limitations, and facilitated greatly by recent technological advances (such as improved batteries, actuators, and microelectronics), several multigrasp prosthetic hands have been developed [4-13]. These multigrasp hands are highly articulated (containing 8 to 16 joints), are driven by a plurality of actuators (ranging from 2 to 6), and hold the potential for improved grasping, manipulation, and fidelity of motion. However, the full realization of this potential requires the development of an effective multigrasp control interface, as noted in [14].

An effective multigrasp interface must enable the user to access the multifunctional capability of the prosthetic hand accurately and dependably. The control approach should be direct and intuitive, offering continuous and proportional control of motion with negligible latency. This remains a challenging area in upper extremity prosthetics research, although several significant strides have been made. Prevalent approaches to multigrasp control thus far include pattern recognition [14-19] and event driven finite-state control [20-27]. Pattern recognition for multigrasp hands involves determining user intent (i.e., selecting postures and grasps) based on the observation (of typically a plurality) of EMG inputs, which are observed in a series of moving windows in time (frames). In this approach, a classifier is trained which associates EMG input patterns with intended postures and grasps. During operation, the classifier examines each frame

of EMG data and makes a decision (or classification) about which movement is being commanded.

In event driven finite-state (EDFS) approaches, the controller consists of a series of interconnected states. For each state the control action is uniquely defined. Transitions among the respective states are based on predefined events or conditions which depend on sensory inputs. The overall behavior of an EDFS controller is therefore a function of the structure and interconnectedness of the states, the device behavior within each state, and the events and conditions required to transition among states (all of which are interdependent). This approach was initially developed and applied to myoelectric prosthetic hand control in the 1960's ([20, 21]), followed by the more recent work described in [22-27]. In [22-24], EDFS control approaches were used to modulate grasp within a preselected hand posture based on measured EMG amplitudes. In these works, posture preselection depended on the activation of contact switches located on the prosthesis. Later in [25-26], a control approach was proposed which also utilized EDFS for grasp modulation, but where EMG pattern recognition, rather than contact switches, was utilized for posture preselection. Alternatively, in [27], an EDFS control approach was described in which an EMG-amplitude-based algorithm was used to preselect a given posture, but where the grasping process was automated by the controller to differing degrees. Specifically, after posture preselection, an automated grasping action was initiated by the controller or by the user (depending on controller variation). Grasping was then either terminated automatically, based on measured grasp force, or manually via a subsequent EMG command (depending again on controller variation).

This paper presents the design and preliminary experimental validation of a myoelectric control methodology for multigrasp transradial hand prostheses. Like the approaches presented in [22-27], the control approach involves event-driven finite-state methods. Unlike these approaches, however, the controller allows for selection of a given posture based on continuous movement through the finite-state control structure. This provides access to any one of nine possible hand postures, in addition to the continuum of configurations between them. In this way, posture selection and grasp modulation within that posture may occur simultaneously.

This approach to multigrasp myoelectric control is described in detail in Section II. To assess the efficacy of the proposed method in obtaining the nine different hand postures, relative to the ability to obtain the same set of postures with the native hand, the control approach was implemented on a virtual multigrasp prosthesis and experiments were conducted with non-amputee subjects. These experiments are described in Section III of the paper, and the results are discussed in Section IV. A video is included in the supplemental material that depicts the virtual prosthesis experiments and demonstrates preliminary use of the multigrasp myoelectric controller with hardware.

II. Description of Multigrasp Myoelectric Control Structure

Theoretically, a multigrasp prosthesis should enable amputees to better perform the activities of daily living, primarily by providing a set of hand postures and grasps which better span the prehensile forms employed during them. As studied in [28] and reported in [29], there are six grasps (i.e., tip, lateral, tripod, cylindrical, spherical and hook) which constitute approximately 85% of those used in the activities of daily living. In addition to this set of grasps, two postures, a pointing posture and a platform (open-palm) posture, are also useful for interaction with the environment. The Multigrasp Myoelectric Controller (MMC) was therefore designed to enable the attainment of these grasps and postures utilizing a standard, two-electrode EMG interface as user input.

To allow for this, it was assumed that the hardware (the hand prosthesis) to be controlled could at minimum provide digit I (thumb) flexion and extension, digit I opposition and reposition, digit II (index) flexion and extension, and simultaneous flexion and extension of digits III through V (middle, ring, and little finger). It was also assumed that the respective digit displacement (i.e., position) and digit grasping forces are measureable or known. The proposed method is applicable to any multigrasp prosthesis with the aforementioned minimum requirements. Examples of multigrasp prostheses that meet these criteria are those described in [6-13].

To coordinate the motion of the digits, the MMC incorporates an event driven finite-state control structure. The topography of this structure is depicted in Fig. 4.1. The states of the MMC consist of the postures and grasps which multigrasp hands, such as those mentioned above, are capable of providing. These include the thumb reposition (platform), point, hook, lateral pinch, thumb opposition, tip, and combined cylindrical/spherical/tripod postures. Note that the latter state includes three postures, as the determination of posture in this state depends also on the shape of the object being grasped. There are thus seven states, and nine possible grasps/postures. The future state of the prosthesis is determined as a function of the current state and the inputs to the finite-state controller, which include EMG signals, hand configuration information, and grasp force information. It is important to note that the topography of the state chart, where the states have been arranged progressively according to the degree of hand closure and where postures and grasps have been grouped specifically based on the position of the thumb, is unique to the work presented here. This arrangement is intended to provide streamlined access to the enhanced functionality of a multigrasp hand and lends itself to navigation of multiple postures using a traditional myoelectric interface.

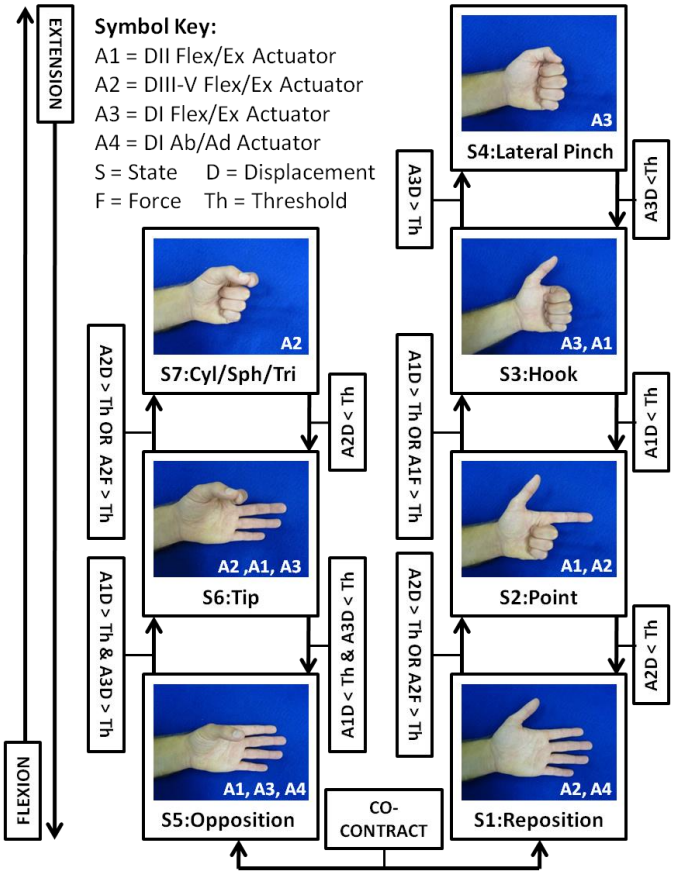

Figure 4.1 - The structure of the MMC finite-state machine. The states are comprised of different hand postures. The active actuators are indicated for each state. Transitions from state to state depend on actuator displacement, actuator forces, and co-contraction detection logic. In general, the actuator displacement and force thresholds for each transition are unique. Contraction of the forearm flexors is associated with upward movement in the state chart. Contraction of the forearm extensors is associated with downward movement in the state chart. Co-contraction initiates an automated toggling motion between the opposition and reposition states.

The user navigates the state chart by four essential inputs which are standard in current clinical devices and are indicated by measured EMG at two electrode sites: flexion, extension, co-contraction, and rest. Flexion involves the contraction of the anterior musculature of the forearm and is associated with closing of the prosthesis (upward movement through the state chart in Fig. 4.1). Extension involves the contraction of the posterior musculature of the forearm and is associated with opening of the prosthesis (downward movement through the state chart in Fig. 4.1). Note that the speed with which the prosthesis closes or opens is proportional to the strength of muscular contraction. Co-contraction involves simultaneous contraction of the antagonistic flexion/extension muscle groups and occurs when both EMG channels concurrently exceed their respective thresholds (the determination of these thresholds is described below). Co-contraction toggles between the opposition and reposition states, causing automated positioning of the

thumb. Because the state chart has been arranged such that all states in which the thumb are opposed stem from the opposition state (the left side of the state chart) and all states in which the thumb are reposed stem from the reposition state (the right side of the state chart) co-contraction effectively selects which branch of the state chart the user may navigate by virtue of flexion or extension. The position of the thumb therefore provides an important visual indication to the user regarding which portion of the state chart the prosthesis is operating in. Note that the opposition and reposition states are the only states in which co-contraction has effect. Co-contraction in any other state will not elicit toggling of the thumb or additional control action. Because the effects of co-contraction are restricted to the opposition and reposition postures in which grasping and manipulation generally do not occur, an unintended co-contraction should not have an effect on grasping capability or robustness. Finally, relaxation of the forearm musculature (resting) halts movement within the state chart (i.e. the prosthesis remains stationary).

Transitions within the state chart are based on logical conditions that operate on measured digit displacements (e.g., joint angles), measured digit forces, and/or measured EMG levels (i.e. detection of co-contractions). The behavior of the hand within each state is determined by a coordination controller that governs which subset of actuators is active in the hand at any given time. If a transition occurs, the current state of the hand changes, and a new subset of actuators become activated by the coordination controller. The actuators which are active are always those associated with transitions to adjacent states.

For example, and with reference to Fig. 4.1, assume the hand is in the platform posture (State 1). In this posture, the actuator(s) responsible for the flexion and extension of the third, fourth and fifth digits, is (are) active (A2). Contraction of the forearm flexors (Electrode 1) generates a velocity level signal which is integrated and *added* to the current position reference for the active actuator(s). Consequently, the third, fourth and fifth digits begin to flex. If the digit flexion or force exceeds a certain threshold (i.e. if these digits either nearly close or come into contact with an object) a state transition will occur, and the hand will transition to the point posture (State 2). In the point posture the actuator(s) responsible for the movement of the second digit (A2), as well as the actuator(s) responsible for flexion of digits three through five, are active. If flexion continues, the position references for these digits will increase. Because digits three through five are almost fully closed upon entering the point posture, their position reference will quickly saturate. However, the position reference for digit II will continue to increase until its displacement or force exceeds a certain threshold, at which point the hand will transition to the hook posture (State 3). Alternatively, if contraction of the forearm extensors (Electrode 2) had occurred after entering the point posture (State 2), a velocity level signal would have been generated, integrated and *subtracted* from the current position references for the active actuators corresponding to digits two and three through five. In this scenario, since the second digit is almost fully open upon entering the point posture, its position reference will quickly saturate.

However, the position reference for digits three through five will continue to diminish until the third, fourth and fifth digits are fully extended, at which point the hand will be in the reposition posture (State 1) once again. The user may toggle from the reposition posture (State 1) to the opposition posture (State 5) by co-contraction. When a desired posture or grasp is obtained, the user relaxes the flexors and extensors of the forearm. This causes the velocity-level references to fall to zero. As these signals are then integrated, the position references for all actuators remain constant (i.e., the digits remains stationary). The user may relax at any time during transitions, and therefore has access to all of the intermediate positions between the idealized states.

In summary the MMC consists primarily of a uniquely structured finite-state machine and a coordination controller. The output of the finite-state machine, the current hand state (posture), dictates which subset of actuators is active in the hand at any given time. The position references for these actuators are driven by proportional signals arising from a standard two-channel EMG interface. Changes in digit position or digit grasping force trigger transitions in the state chart based on pre-established position and force thresholds. Co-contraction commands cause transitions between the reposition (platform) and opposition postures. When a state transition occurs, a new subset of motors becomes activated by the coordination controller. The active motors are always those associated with transitions to adjacent states. This, in conjunction with the controller structure, provides access to any one of nine possible hand postures, in addition to a continuum of configurations among adjacent postures. In this way, posture selection and grasp modulation within a posture may occur simultaneously.

III. Experimental Methods

A. Subject Information and Testing Overview

Experiments were conducted to assess the ability of the MMC to control hand posture. Five healthy, non-amputee subjects aged 22-44 participated in the experiments. Of these subjects, four were right-handed and one was left-handed. Each subject participated in six trials. Each trial involved tasks with both the data glove and MMC, and each of the five subjects attempted each transition type three times during each experimental task. This resulted in 45 data points for each transition type for both the data glove and the MMC. The time between trials ranged from one day to three weeks and all subjects completed the six experimental trials within a time frame of approximately one month. All experiments were conducted on the right hand and forearm. The experimental protocol for this study was approved by the Vanderbilt University Institutional Review Board.

B. Data Acquisition with Data Glove

Figure 4.2 -The data glove used to capture motion of the native hand. Four sensors are used to capture flexion and extension of digits I-III, as well as abduction and adduction of the thumb. An individual flex sensor is also shown.

A custom data glove was constructed to track the movement of the native hand (See Fig. 4.2). This was accomplished using variable resistance flex sensors (Spectra Symbol) attached to a lightweight, highly flexible, slip-on glove (Fox Head, Inc.). The flex sensors were inserted into elastic sleeves which had been stitched onto the glove. The sensors were allowed to translate within the sleeve to accommodate for stretching of the glove over the joints. Four flex sensors were used to capture the flexion and extension of digits I-III (digits IV and V of the virtual prosthesis tracked digit III) as well as abduction and adduction of digit I. This allowed for the detection of the postures attainable with the configuration of the MMC described in this paper. The variable resistance flex sensors were incorporated into a voltage divider circuit whose output was amplified, adjusted, and buffered before being acquired using an MF624 data acquisition card (Humusoft) and accessed at a sampling rate of 1 kHz using Simulink Real Time Windows Target (The Mathworks). These signals were then low-pass filtered at 2 Hz and normalized in Simulink to be used as position references for control of the virtual prosthesis. Each subject was allowed to manipulate the virtual prosthesis using the data glove to gain familiarity with the interface before starting the experimental trials.

C. Data Acquisition with EMG

Two self-adhesive, Ag/AgCl snap bipolar electrodes with a spacing of 22 mm (Myotronics, Inc.) were used for EMG data acquisition. The electrodes were placed on the anterior and posterior surfaces of each subject's forearm in the approximate vicinity of the flexor carpi radialis (Electrode 1) and extensor carpi radialis muscles (Electrode 2). These muscles were chosen due to their proximity to the skin, proximal location on the forearm, and because of their role in flexion and extension of the hand at the wrist. Additionally, because these muscles are located in close proximity to the flexor digitorum superficialis and extensor digitorum muscles respectively, flexion

or extension of the digits, along with the hand about the wrist, was seen to produce strong EMG signals. An alcohol pad was used to clean the electrode sites before electrode placement. The analog EMG signals detected by the electrodes were differentially preamplified with a gain of 100 and low pass filtered at a cutoff frequency of 500 Hz using custom analog circuitry at the electrode site. This information was sampled at 1 kHz using the MF624 data acquisition card and accessed using Simulink Real Time Windows Target. The signals were then digitally high-pass filtered at 50 Hz, rectified, and low pass filtered again at 2 Hz for use as velocity references.

The EMG signals of each subject were calibrated by establishing normalization parameters and co-contraction threshold levels before the experimental trials. The mean EMG values during Flex and Rest (Electrode 1) and Extend and Rest (Electrode 2) were established as upper and lower bounds for each signal, respectively. A dead band of 10% of full range was utilized for both channels to avoid spurious motion. To enable real-time co-contraction detection, thresholds were established for each EMG channel based on an exhaustive search. The thresholds which maximized the number of correctly detected co-contractions, and minimized the number of incorrectly detected co-contractions during the calibration session were selected. As noted above, a co-contraction was assumed to have occurred if both signals concurrently exceeded their respective thresholds. This process transformed the two EMG signals into two normalized, proportional signals which were used to provide velocity references and co-contraction events for multigrasp prosthesis control. *Once established, this calibration was not repeated for the remainder of all experiments* (for a given subject). The resulting normalization parameters and co-contraction thresholds were maintained for the duration of the multi-week experimental sessions. Subjects were allowed to operate the virtual prosthesis using EMG signals until they were familiar with the structure and operation of the multigrasp myoelectric control scheme before starting the experimental trials.

D. Virtual Prosthesis

To create the virtual prosthesis (See Fig. 4.3), solid model part and assembly files of the hand prosthesis described in [12] were exported from Pro/Engineer (PTC) to a virtual reality modeling language (.vrml) file. The virtual reality model was then animated using signals generated in Simulink (The Mathworks). The virtual ghost was created by inserting another, darkly shaded copy of the virtual prosthesis into the virtual environment. The virtual prosthesis was controlled by the user via signals emanating from either the data glove or MMC. The virtual ghost was controlled automatically by the computer and served as a postural reference for the user. For the experiments described here, the MMC was modified to control the virtual prosthesis. Because the virtual environment did not allow for interaction with objects, force dependent transitions were not invoked in the state chart. Instead, state chart transitions were strictly position dependent. The velocity gains in the MMC were set so that the virtual prosthesis moved

with speeds reflective of the capabilities of a multigrasp prosthetic hand (i.e., the maximum speeds as described in [12]).

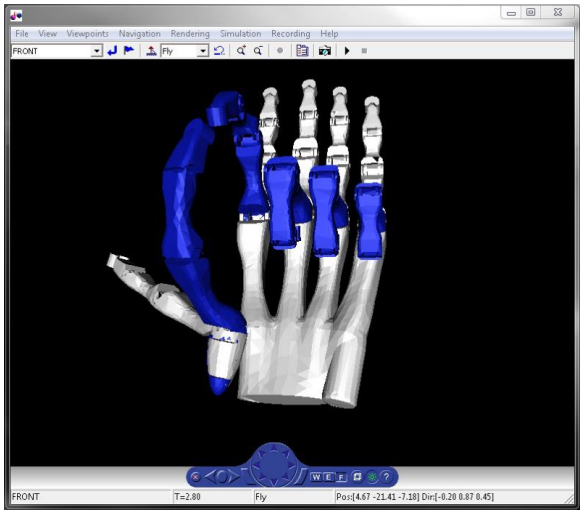

Figure 4.3 - The virtual prosthesis (light) and virtual ghost (dark). The virtual ghost is controlled automatically by the computer, and serves as a postural reference for the user. When the user brings the virtual prosthesis sufficiently close to the virtual ghost, the ghost is no longer displayed, indicating to the user that they have acquired the desired target posture.

E. Experimental Procedure

Each trial consisted of two experimental tasks which involved the acquisition of target postures. In the first task, the data glove was used to control the movement of the virtual prosthesis with the native hand. In the second task, EMG signals were used to control the movement of the virtual prosthesis with the MMC. Note that the first task (data glove) was intended to characterize the performance of the native hand and thereby establish a performance benchmark for the MMC. In both tasks, seven target postures (e.g. the reposition, point, hook, lateral pinch, opposition, tip, and cylindrical postures displayed in Fig. 4.1) were presented randomly. Because differentiation of the cylindrical, spherical, and tripod grasps is dependent upon the grasped object, and as grasping was not involved in the virtual environment, the cylindrical/spherical/tripod grasp was reduced to only the cylindrical grasp in the virtual experiments. Thus, there were seven unique postures to be obtained with the virtual prosthesis in the experiments, and from these, 42 unique transitions, each of which was presented three times per task. This resulted in 126 movements per task, with each of the seven postures being presented 18 times.

Each target posture was displayed visually on a computer monitor by the virtual ghost. When a subject brought the virtual prosthesis to the target posture the virtual ghost was no longer displayed, indicating that the user had sufficiently achieved the desired pose. For a movement to be considered successful, and before a new target posture was displayed, it was required that the target posture be held for three seconds without excessive deviation (within 25% of the total

range of motion for each digit). This was done both to deter overshoot and to allow subjects to rest between subsequent postures. If a transition was not acquired within 5 seconds, it was considered unsuccessful and a new target posture was presented.

The operation of the data glove and MMC were explained before the trials to prepare subjects for the above procedure. In addition, each subject was allowed to use the data glove and the MMC interface to control the virtual prosthesis until they were comfortable with each. In either case, and for all subjects, these familiarization periods required less than 5 minutes. A video which includes footage of an experimental trial is available in the supplemental material.

F. Performance Metrics

The time required for each transition, starting at the instant when the target posture was initially displayed and ending when the target posture was successfully acquired, was recorded. This was defined as the *transition time.* The number of successfully completed transitions (those completed within 5 seconds) over the total number of attempted transitions was defined as the *transition completion rate*. These metrics are similar to the real-time performance metrics used in [19] to quantify pattern recognition based myoelectric control. Note, however, that the transition time as defined in this study includes visual, cognitive, neural, and muscular delay, in addition to joint angular velocity limits (representative of a physical prosthesis), which were imposed on the virtual prosthesis.

IV. Experimental Results & Discussion

A. Performance Trends

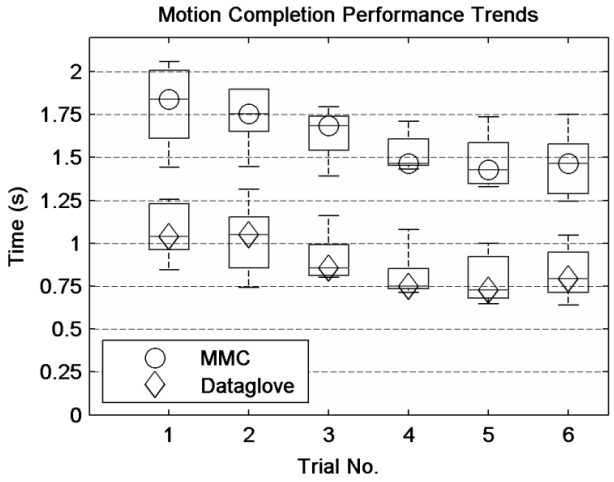

Figure 4.4 - Plot of average motion completion times for each subject for each of six trials. The central mark for each box denotes the median motion completion time and each box encompasses the 25th to 75th percentiles for that trial and control methodology.

The median overall transition times for both the data glove and MMC decreased with essentially every subsequent trial (See Fig. 4.4). (The second data glove trial was an exception to this decreasing trend.) After the third trial, the median transition times for both the data glove and MMC fell within 10% of their collective means. Specifically, the median times for data glove trials 4, 5 and 6 were within 6% of their mean, and the median times for MMC trials 4, 5 and 6 were within 2% of their mean. This was considered to be indicative of a performance plateau and the final three trials were utilized to obtain the results reported here. These trends also imply that the MMC approach is intuitive, as both data glove and MMC transition times displayed similar trends and reached a plateau during the same trial. Additionally, in all cases familiarization periods were brief (< 5 minutes). It is also important to note that only a single calibration was used over the one month trial period. In contrast, it has been noted that pattern recognition approaches can require retraining on a more frequent basis due to various sensitivities [30, 31]. Because inter-trial variation existed in electrode placement over the course of these experiments, the MMC approach appears to be robust with respect to some degree of spatial and temporal variation in EMG measurement. This is similar to single DoF commercial myoelectric hand prostheses, in which two-site, direct, EMG velocity control is known to provide a degree of robustness relative to variations in electrode placement. This is due in part to the significant degree of physical separation between electrodes, the significant degree of muscular decoupling between the anterior and posterior forearm musculature, and due to the fact that velocity control integrates the EMG, which decreases sensitivity to noise and gain in the EMG measurement. In this way, the MMC approach leverages the benefits of traditional methods (e.g. direct mapping of input, simplified interface, robustness), while enabling the control of a multigrasp hand.

B. Transition Times

The average transition times for each transition type are given for the native hand and the MMC in Tables 4.1 and 4.2, respectively. The same information is displayed graphically in Fig. 4.5. As can be seen in Tables 4.1, 4.2 and Fig. 4.5, transition times for the native hand are relatively uniform (standard deviation of 0.10 seconds) when compared to the MMC (standard deviation of 0.58 seconds). The distribution of transition times for the MMC may be attributed to the distance between the original and target postures on the state chart as depicted in Fig. 4.5. That is, transition times between adjacent postures are relatively short (average of 0.87 seconds), whereas transition times between states which lie at the far ends of the state chart (e.g. the lateral pinch and cylinder/sphere/tripod grasps) are longer (average of 2.55 seconds). The structure of the state machine imposes this distribution.

To provide a measure of overall performance, the *overall* transition times were calculated for the native hand and MMC. This is the average time required to get to *any* given posture from *any other*. The overall transition time for each subject, and the average overall transition time over all

subjects are given in Table 4.3. For the native hand, the average overall transition time was 0.81 seconds with a standard deviation of 0.14 seconds. For the MMC the average overall transition time was 1.49 seconds with a standard deviation of 0.15 seconds. These data suggest that the MMC performs similarly to the native hand when transitioning between adjacent states, but is slower when transitioning among states that are non-adjacent.

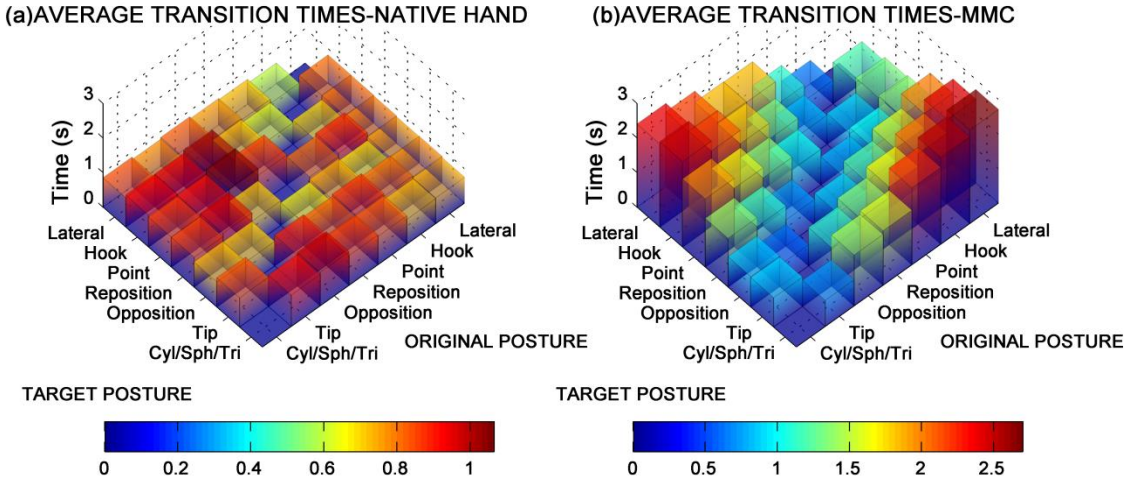

Figure 4.5 - Average transition times for: (a) the native hand (using the data glove) and (b) multigrasp myoelectric control (using electrodes). Note that the grayscale duration bars are scaled differently for (a) and (b). It can be seen that the transition times are relatively uniform for the native hand while for MMC they are dependent on distance between the original and target posture in the state chart. Note that transition times for adjacent postures with MMC are similar to the average transition time for the native hand.

Table 4.1 - Average Transition Times Of All Subjects Between Different Grasps and Postures for the Native Hand*

		Target Posture						
		Lateral	**Hook**	**Point**	**Reposition**	**Opposition**	**Tip**	**Cyl/Sph/Tri**
Original Posture	**Lateral**		0.81 (0.36)	0.81 (0.36)	0.79 (0.36)	0.76 (0.50)	0.78 (0.25)	0.74 (0.21)
	Hook	0.59 (0.12)		0.69 (0.25)	0.90 (0.65)	0.67 (0.19)	0.80 (0.28)	0.72 (0.19)
	Point	0.72 (0.31)	0.62 (0.15)		0.81 (0.60)	0.73 (0.19)	0.88 (0.26)	0.82 (0.28)
	Reposition	0.76 (0.25)	0.72 (0.18)	0.86 (0.48)		0.65 (0.28)	0.82 (0.50)	0.86 (0.22)
	Opposition	0.82 (0.30)	1.02 (0.48)	1.06 (0.53)	0.71 (0.19)		0.89 (0.30)	0.97 (0.38)
	Tip	0.77 (0.12)	0.94 (0.47)	0.90 (0.33)	0.96 (0.33)	0.71 (0.23)		0.91 (0.39)
	Cyl/Sph/Tri	0.85 (0.42)	0.92 (0.33)	0.86 (0.31)	0.86 (0.27)	0.72 (0.15)	0.84 (0.24)	

*Standard deviations are displayed in parenthesis.

Table 4.2 - Average Transition Times of All Subjects Between Different Grasps and Postures for Multigrasp Myoelectric Control*

		Target Posture						
		Lateral	**Hook**	**Point**	**Reposition**	**Opposition**	**Tip**	**Cyl/Sph/Tri**
Original Posture	**Lateral**		1.20 (0.63)	1.32 (0.53)	1.37 (0.21)	2.02 (0.70)	2.43 (0.68)	2.70 (0.69)
	Hook	0.67 (0.14)		0.89 (0.29)	1.05 (0.14)	1.60 (0.39)	2.03 (0.51)	2.50 (0.95)
	Point	1.12 (0.35)	0.84 (0.22)		0.81 (0.43)	1.25 (0.36)	1.67 (0.32)	2.21 (0.50)
	Reposition	1.82 (0.96)	1.34 (0.36)	1.02 (0.31)		0.92 (0.51)	1.36 (0.51)	1.57 (0.56)
	Opposition	1.84 (0.44)	1.79 (0.56)	1.38 (0.43)	0.75 (0.26)		1.11 (0.43)	1.47 (0.88)
	Tip	2.16 (0.44)	2.18 (0.56)	1.68 (0.38)	1.15 (0.44)	0.61 (0.13)		0.75 (0.10)
	Cyl/Sph/Tri	2.40 (0.40)	2.46 (0.61)	1.97 (0.55)	1.40 (0.37)	0.88 (0.17)	0.85 (0.22)	

*Standard deviations are displayed in parenthesis.

C. Transition Completion Rate

Transition completion rates for each subject, as well as the average transition completion rates for both the data glove and MMC, are given in Table 4.3. The average transition completion rate for the data glove was 99.2% with a standard deviation of 0.00% (coincidentally, all subjects had exactly 3 failed attempts when using the data glove). The average transition completion rate for the MMC was also 99.2%, but with a standard deviation of 0.67% (subjects had from one to seven failed attempts using the MMC). Qualitative feedback from subjects indicated that causes for missed transitions were misinterpretation of reference postures (data glove and MMC), accidental excessive deviation from the target posture (data glove and MMC), and the inability to switch between thumb opposition and reposition as a result of an insufficient co-contraction effort (MMC). The latter could have likely been mitigated by retraining the controller, but as previously stated, the authors chose instead to train the controller a single time at the outset, and not retrain during the course of these experiments.

These data indicate that transitions were completed as often with the MMC as with the native hand and that, in either case, transitions were completed (in under 5 seconds) nearly 100% of the time. Because of this, the average transition times reported in the previous section are representative of typical performance, whether or not the 5 second time limit is considered. These results indicate that the experimental subjects were able to reliably adopt target postures using the MMC.

Table 4.3 - Overall Transition Times and Transition Rates*

Subject	Criteria	Data glove	MMC
HS1 (RH)	Transition Time	0.74	1.48
	Transition Rate	99.2	99.7
HS2 (LH)	Transition Time	1.04	1.73
	Transition Rate	99.2	98.1
HS3 (RH)	Transition Time	0.84	1.50
	Transition Rate	99.2	99.7
HS4 (RH)	Transition Time	0.75	1.33
	Transition Rate	99.2	99.2
HS5 (RH)	Transition Time	0.68	1.40
	Transition Rate	99.2	99.5
Average	Transition Time	0.81 (0.14)	1.49 (0.15)
	Transition Rate	99.2 (0.00)	99.2 (0.67)

*RH and LH are abbreviations for right-handed and left-handed, respectively. The standard deviations are given in parentheses.

D. Real-Time Control

In order to demonstrate real-time control commands, the minimal hardware configuration (for the MMC) was assumed, in which one actuator (A3) provides digit I flexion and extension, a second actuator (A4) provides digit I opposition and reposition, a third actuator (A1) provides digit

II flexion, and a fourth actuator (A2) provides coupled flexion for digits III through V. Given such a hardware configuration (implemented virtually), Fig. 4.6 shows the EMG inputs, hand state, and normalized digit displacement (where unity corresponds to the fully flexed position and zero corresponds to the fully extended position) for a 55 second session using MMC. During this session the user was sequentially prompted through the full range of hand postures. The figure demonstrates several important characteristics of MMC. First, the same EMG input can affect positional references for different actuators based on the current state of the hand. For instance, EMG input coming from the forearm flexors (Electrode 1) generates references for A2 around the point state, and generates references for A1 around hook state (between t=0 and t=10 seconds). Second, a single EMG input may govern multiple actuators, such as Electrode 1 simultaneously controlling actuators A1 and A3 between transitions from opposition to tip states around t=33 and t=46 seconds. Third, a high intensity co-contraction of flexor and extensor muscles results in a co-contraction event at t=28 and t=50 seconds. The co-contraction event causes automated opposition and reposition of the thumb. As can also be seen in Fig. 4.6, response to user intent is immediate. That is, movement occurs as soon as elevated EMG signal levels are detected.

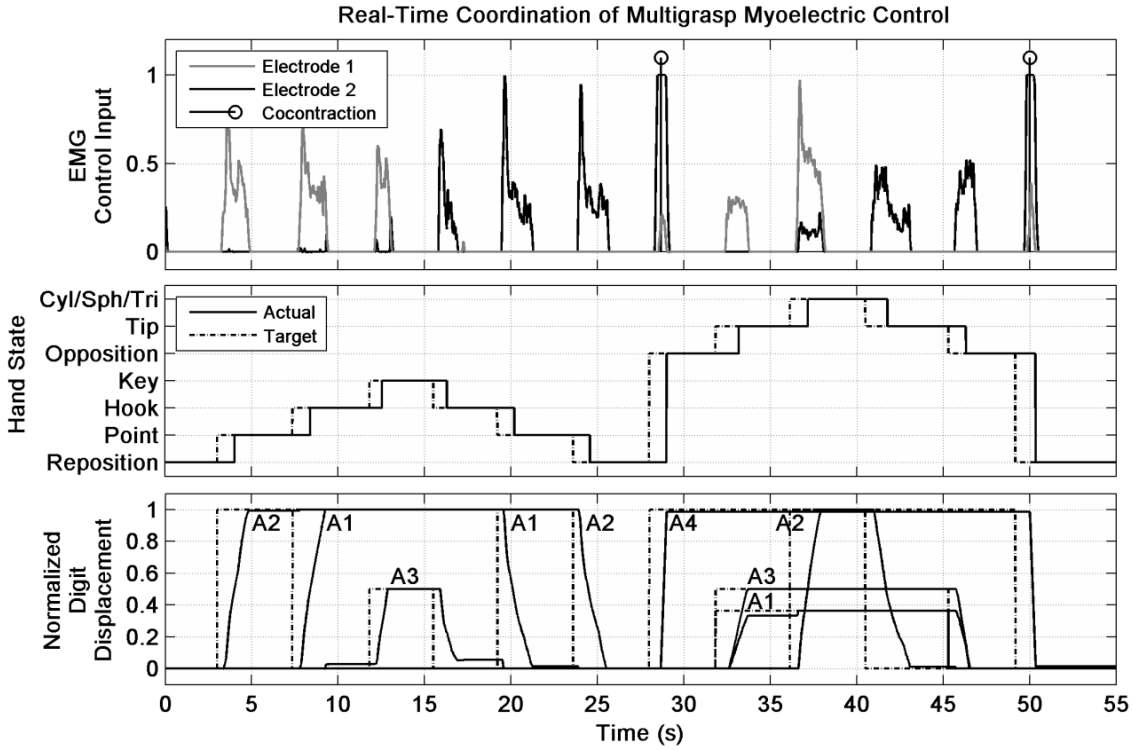

Figure 4.6 - Plot of EMG input, hand state, and normalized digit displacement as a user is prompted through a series of target postures. Here, actuator A1 provides digit II flexion and extension, actuator A2 provides coupled flexion and extension of digits III through V, actuator A3 provides digit I flexion and extension, and actuator A4 provides digit I abduction and adduction.

E. Continuous and Proportional Motion

The continuous and proportional motion allowed by the MMC is illustrated in Fig. 4.7 and shown in the accompanying video. This was done using the second digit in the point state. After displacing the second digit to approximately half of its full range, high frequency motion was produced by rapid alternating contractions of the forearm flexors and extensors (t=7-11 seconds). This was followed by periods of intermittent flexion and extension, punctuated by brief periods of rest, causing graded, step-like motion (t = 11-32 seconds). Next, slow, low frequency motion was produced with low-level EMG input (t=32-44 seconds). Finally, the virtual prosthesis was taken through all of the states to show that continuous motion amongst the idealized states was possible within the state chart (t=44-54 seconds). The demonstration ended with the second digit back in its middle position.

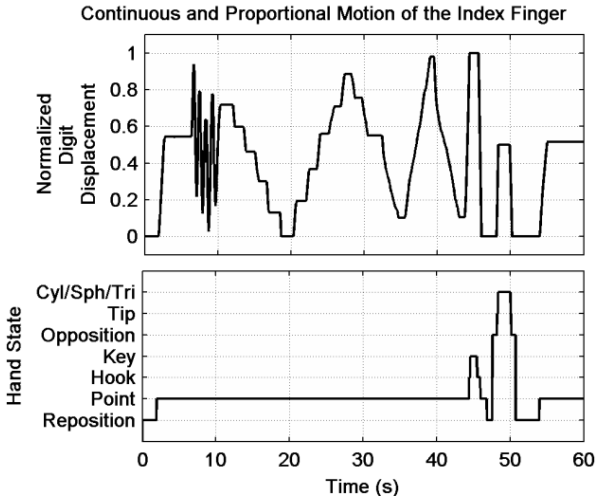

Figure 4.7 - Plot of normalized digit displacement and hand state during continuous and graded motion of the index finger. High frequency motion, graded motion, low frequency motion, and motion of the index finger during transitions through the state chart are displayed.

F. Physical Interaction

The virtual experimental paradigm utilized in this paper enables characterization of the ability of several subjects to transition from a given posture to all other (randomly presented) given postures (within a desired set of hand postures). Despite this, in many activities of daily living, the use of a hand prosthesis fundamentally entails interaction with the environment, which introduces physical forces on the prosthesis and limb, and can correspondingly modify EMG patterns. As indicated elsewhere in this paper, the standard, two-site EMG approach was incorporated into the MMC structure because of its proven history of efficacy in the control of myoelectric prostheses. Since the EMG interface with single-grasp myoelectric hands is not substantially altered by interaction with the environment, and since the nature of the traditional EMG interface is essentially intact in the MMC method, the authors expect that physical interaction with the

environment will not significantly alter the ability of the user to obtain hand postures and grasps. This assertion, however, cannot be confirmed without performing a set of appropriate experiments incorporating the controller described herein with an appropriate multigrasp hand prosthesis, and assessing the ability of the user to obtain a set of desired grasps, or perform a set of desired tasks. The investigators hope to conduct such experiments in future work. As a preliminary step toward this goal, and to demonstrate the efficacy of the controller in physical hardware, the MMC has been implemented on the multigrasp prosthesis prototype described in [12]. A video demonstrating the implementation of the multigrasp controller on this prosthesis prototype is included in the accompanying supplemental material.

V. Conclusion

This paper presents a multigrasp myoelectric control interface that enables coordinated control of a multigrasp hand prosthesis using a standard EMG electrode interface. Specifically, the use of two EMG electrodes (on the anterior and posterior aspects of the forearm), along with position and force information from sensors in the hand, enables a user to navigate through a finite state control structure, and in doing so, to achieve one of nine possible hand postures, in addition to a continuum of configurations between adjacent postures. Experiments were conducted on five non-amputee subjects, in which the subjects utilized the myoelectric controller to command the motion of a virtual prosthesis between random sequences of target hand postures to assess the efficacy of the controller with respect to controlling hand posture. The results of these experiments were compared to the same subjects' ability to achieve similar random sequences of target postures with their native hand, as measured by a data glove. The average time (across all subjects) to transition from one posture to another was 1.49 seconds for the myoelectric controller, and 0.81 seconds for the native hand, while the average completion rates were the same for both (99.2%). As such, the experimental results presented here indicate that the multigrasp myoelectric control approach enables (non-amputee) subjects to effectively obtain target postures within a virtual environment.

Epilogue

The results of this study indicated that, in terms of the speed and reliability of posture adoption, the performance of a prosthesis controlled by MMC would be comparable to that of the native hand, particularly when moving among adjacent states (i.e. grasping). These results also compared favorably to other multigrasp control approaches such as pattern recognition, where transition times of 1.61 seconds (where transition time has been taken as the sum of the motion selection and motion completion times reported in [24] for the sake of comparison) and completion rates of 69.4% (in under 5 sec) have been reported for the classification of 6 hand postures using 12 electrodes placed on the intact arm [24].

References

[1] M. Zecca, S. Micera, M. C. Carrozza, and P. Dario, "Control of multifunctional prosthetic hands by processing the electromyographic signal," *Critical Reviews in Biomedical Engineering,* vol. 30, pp. 459-85, 2002.

[2] E. Biddiss, D. Beaton, and T. Chau, "Consumer design priorities for upper limb prosthetics," *Disability & Rehabilitation: Assistive Technology,* vol. 2, pp. 346-357, 2007.

[3] D. J. Atkins, D. C. Y. Heard, and W. H. Donovan, "Epidemiological Overview of Individuals with Upper-Limb Loss and Their Reported Research Priorities," *Journal of Prosthetics and Orthotics,* vol. 8, pp. 2-10, 1996.

[4] J. L. Pons, E. Rocon, R. Ceres, D. Reynaerts, B. Saro, S. Levin, and W. Van Moorleghem, "The MANUS-HAND dextrous robotics upper limb prosthesis: mechanical and manipulation aspects," *Autonomous Robots,* vol. 16, pp. 143-163, Mar 2004.

[5] J. Chu, D. Jung, and Y. Lee, "Design and control of a multifunction myoelectric hand with new adaptive grasping and self-locking mechanisms," in *IEEE International Conference on Robotics and Automation*, 2008, pp. 743-748.

[6] C. Cipriani, M. Controzzi, and M. C. Carrozza, "Progress towards the development of the SmartHand transradial prosthesis," in *IEEE International Conference on Rehabilitation Robotics*, 2009, pp. 682-687.

[7] C. Cipriani, M. Controzzi, and M. C. Carrozza, "Objectives, criteria and methods for the design of the SmartHand transradial prosthesis," *Robotica,* vol. 28, pp. 919-927, 2010.

[8] C. M. Light and P. H. Chappell, "Development of a lightweight and adaptable multiple-axis hand prosthesis," *Medical Engineering & Physics,* vol. 22, pp. 679-684, Dec 2000.

[9] S. Jung and I. Moon, "Grip force modeling of a tendon-driven prosthetic hand," in *International Conference on Control, Automation and Systems*, 2008, pp. 2006-2009.

[10] A. Kargov, C. Pylatiuk, R. Oberle, H. Klosek, T. Werner, W. Roessler, and S. Schulz, "Development of a multifunctional cosmetic prosthetic hand," in *IEEE International Conference on Rehabilitation Robotics*, 2007, pp. 550-553.

[11] C. Pylatiuk, S. Mounier, A. Kargov, S. Schulz, and G. Bretthauer, "Progress in the development of a multifunctional hand prosthesis," in *Proceedings of the IEEE Engineering in Medicine and Biology Society*, 2004, pp. 4260-3.

[12] T. E. Wiste, S. A. Dalley, H. A. Varol, and M. Goldfarb, "Design of a Multigrasp Transradial Prosthesis," *ASME Journal of Medical Devices,* vol. 5, pp. 1-7, 2011.

[13] S. A. Dalley, T. E. Wiste, T. J. Withrow, and M. Goldfarb, "Design of a Multifunctional Anthropomorphic Prosthetic Hand With Extrinsic Actuation," *IEEE/ASME Transactions on Mechatronics,* vol. 14, pp. 699-706, 2009.

[14] F. C. P. Sebelius, B. N. Rosén, and G. N. Lundborg, "Refined myoelectric control in below-elbow amputees using artificial neural networks and a data glove," *The Journal of Hand Surgery,* vol. 30, pp. 780-789, 2005.

[15] M. Vuskovic and D. Sijiang, "Classification of prehensile EMG patterns with simplified fuzzy ARTMAP networks," in *Proceedings of the 2002 International Joint Conference on Neural Networks*, 2002, pp. 2539-2544.

[16] J. Zhao, Z. Xie, L. Jiang, H. Cai, H. Liu, and G. Hirzinger, "EMG control for a five-fingered underactuated prosthetic hand based on wavelet transform and sample entropy," in *IEEE/RSJ International Conference on Intelligent Robots and Systems*, 2006, pp. 3215-3220.

[17] L. H. Smith, L. J. Hargrove, B. A. Lock, and T. A. Kuiken, "Determining the Optimal Window Length for Pattern Recognition-Based Myoelectric Control: Balancing the Competing Effects of Classification Error and Controller Delay," *IEEE Transactions on Neural Systems and Rehabilitation Engineering,* vol. 19, pp. 186-192, 2011.

[18] L. Hargrove, Y. Losier, B. Lock, K. Englehart, and B. Hudgins, "A real-time pattern recognition based myoelectric control usability study implemented in a virtual environment," in *IEEE International Conference of the Engineering in Medicine and Biology Society*, 2007, pp. 4842-4845.

[19] G. Li, A. E. Schultz, and T. A. Kuiken, "Quantifying pattern recognition-based myoelectric control of multifunctional transradial prostheses," *IEEE Transactions on Neural Systems and Rehabilitation Engineering,* vol. 18, pp. 185-192, 2010.

[20] J. C. Baits, R. W. Todd, and J. M. Nightingale, "The feasibility of an adaptive control scheme for artificial prehension," *Proceedings of the Institution of Mechanical Engineers,* vol. 183, pp. 54-59, 1968.

[21] M. Rakic, "The 'Belgrade Hand Prosthesis'," *Proceedings of the Institution of Mechanical Engineers,* vol. 183, pp. 60-67, 1968.

[22] J. M. Nightingale, "Microprocessor control of an artificial arm," *Journal of Microcomputer Applications,* vol. 8, pp. 167-73, 1985.

[23] P. H. Chappell and P. J. Kyberd, "Prehensile control of a hand prosthesis by a microcontroller," *Journal of Biomedical Engineering,* vol. 13, pp. 363-369, 1991.

[24] P. J. Kyberd, O. E. Holland, P. H. Chappell, S. Smith, R. Tregidgo, P. J. Bagwell, and M. Snaith, "MARCUS: a two degree of freedom hand prosthesis with hierarchical grip control," *IEEE Transactions on Rehabilitation Engineering,* vol. 3, pp. 70-76, 1995.

[25] C. M. Light, P. H. Chappell, B. Hudgins, and K. Englehart, "Intelligent multifunction

myoelectric control of hand prostheses," *Journal of Medical Engineering & Technology,* vol. 26, pp. 139-146, 2002.

[26] D. P. J. Cotton, A. Cranny, P. H. Chappell, N. M. White, and S. P. Beeby, "Control strategies for a multiple degree of freedom prosthetic hand," *Measurement & Control,* vol. 40, pp. 24-27, Feb 2007.

[27] C. Cipriani, F. Zaccone, S. Micera, and M. C. Carrozza, "On the shared control of an EMG-controlled prosthetic hand: analysis of user-prosthesis interaction," *IEEE Transactions on Robotics,* vol. 24, pp. 170-184, 2008.

[28] C. Jacobson-Sollerman and L. Sperling, "Grip Function of the Healthy Hand in a Standardised Hand Function Test," *Scandinavian Journal of Rehabilitation Medicine,* vol. 9, pp. 123-129, 1977.

[29] C. Sollerman and A. Ejeskär, "Sollerman Hand Function Test: A Standardised Method and its Use in Tetraplegic Patients," *Scandinavian Journal of Plastic and Reconstructive Surgery and Hand Surgery,* vol. 29, pp. 167-176, 1995.

[30] E. Scheme, A. Fougner, O. Stavdahl, A. D. C. Chan, and K. Englehart, "Examining the adverse effects of limb position on pattern recognition based myoelectric control," in *IEEE International Conference of the Engineering in Medicine and Biology Society*, 2010, pp. 6337-6340.

[31] L. Hargrove, K. Englehart, and B. Hudgins, "A training strategy to reduce classification degradation due to electrode displacements in pattern recognition based myoelectric control," *Biomedical Signal Processing and Control,* vol. 3, pp. 175-180, 2008.

Chapter 5 – Comparative Functional Assessment of Single and Multigrasp Prosthetic Terminal Devices

Skyler A. Dalley, Daniel A. Bennett, and Michael Goldfarb

Vanderbilt University

Nashville, TN

Status: To Be Submitted

Prologue

Although the previous study demonstrated that the MMC controller, as used by able-bodied participants, was capable of providing rapid and reliable transitions in a virtual environment, testing in a physical setting with an amputee participant was still required. In addition, it was desired that the functional capabilities of the physical system be compared to those of other contemporary devices. As such, the following case study was conducted, wherein a transradial amputee performed a clinically validated functional assessment using a variety of prosthetic terminal devices.

I. Abstract

This work presents a case study involving the functional assessment of a variety of prosthetic terminal devices. In particular, a transradial amputee subject performed the Southampton Hand Assessment Procedure (SHAP) using five different terminal device types, including a Hosmer-Dorrance Corp. 5XA body-powered split hook, a Motion Control Inc. Electric Terminal Device, an Otto Bock MyoHand VariPlus Speed, a Touch Bionics Inc. i-Limb Revolution multigrasp hand, and the Vanderbilt Multigrasp Hand. While the highest Index of Function (IoF) was obtained with the two split-hook terminal devices (92 out of 100 points), the IoF scores for the other devices differed by no more than eight percent. However, the similarity of these results was not consistent with the functional differences experienced by the participant when using the various devices in the activities of daily living. In order to address the disparity between the quantitative results obtained here and the experience of the subject in daily living, the authors offer considerations for future assessment instruments, which, if implemented, may better characterize some aspects of terminal device functionality of importance to upper extremity amputees.

II. Introduction

The human hand is extensively articulated, possessing approximately twenty major degrees-of-freedom that allow it to perform a multitude of grasps and postures. In contrast, the body-powered and myoelectric terminal devices traditionally used to replace the hand after amputation possess only one degree-of-freedom (DoF), and are therefore only capable of a single grasp (i.e., they may be opened and closed). While this reduction to a single DoF is a significant physical abstraction of the native hand, single grasp devices greatly simplify the control interface required for their use (in both the body-powered and myoelectric cases), and the consistency of a single grasp may facilitate manipulation in the absence of proprioception and haptic sensation. Nevertheless, surveys concerning single grasp devices indicate that increased articulation [1] and greater functionality [2] are among the top design priorities for the individuals who use them.

Enabled by recent technological advances, several multigrasp prosthetic hands have begun to emerge in both academic research and commercial trade (see, for example [3-8]). These prosthetic hands have increased articulation and fidelity of motion relative to single DOF terminal devices and, as such, are intended to provide greater functionality during the activities of daily living (ADLs). Despite this, very few functional assessments have been conducted to formally examine the capability of multigrasp hands, particularly as compared to single grasp devices. In [9] and [10] the performance of a single grasp Otto Bock DMC Plus is compared to a multigrasp Touch Bionics i-Limb representing, to the authors knowledge, the extent of such comparative investigations. As noted in [11], this type of information is critical to the prescription and continued development of upper extremity terminal devices. This is particularly true in regard to multigrasp hands, and the need to utilize validated, objective measures to generate a body of knowledge regarding functional outcomes has been made evident [11, 12].

In this paper, the authors aim to contribute to this body of knowledge through the presentation of a case study in which the functionality of five different upper-extremity terminal devices is assessed using the Southampton Hand Assessment Procedure. Specifically, this study compares the ability of an individual with transradial amputation to conduct the ADLs using a myoelectric multigrasp hand developed by the authors, in addition to several commercially-available terminal devices, including: a body-powered split hook, a myoelectric split hook, a myoelectric single-grasp hand, and a myoelectric multigrasp hand. To the authors' knowledge, this is the first study comparing prosthetic function across such a wide breadth of terminal device types, as it spans single-grasp and multigrasp articulation; body-powered and myoelectric control; split hook and hand style end effectors; and commercial products and research prototypes.

III. Devices

A. Body-Powered Systems

In body-powered systems, an end effector, typically some form of split hook, is operated via a harness worn on the shoulders. Relative motion of the shoulders, such as that achieved through scapular abduction, is then used to pull on a Bowden cable attached to the harness. The cable then works against an elastic element to voluntarily open or close the split hook. In the absence of user input, the prosthesis is either held closed by elastic bands (voluntary open), or held open by elastic elements (voluntary close). Relative to the myoelectric systems described below, advantages of body-powered systems often include [13]: lower cost, lower weight, greater ruggedness, and the ability to transmit, to some extent, kinesthetic information to the user. Common disadvantages of body-powered systems (relative to myoelectric) include: relatively low anthropomorphic/cosmetic fidelity (particularly in the case of the split hook, although some body-powered hands are available, such as the Becker Mechanical Hand Co. Imperial Hand), a limited

functional envelope (depending on the position of the upper limb, it may be difficult to perform movements required for opening/closing of the device), strength and range of motion requirements which may be prohibitive to some users (such as individuals with high-level amputations, the elderly, or the young), and potential discomfort associated with the harness system. A body-powered system assessed in this work is the Hosmer-Dorrance Corp. 5XA split-hook.

The Hosmer-Dorrance Corp. 5XA Split-Hook

The 5XA is a single joint, single degree of freedom body-powered split-hook (pictured with passive wrist in Fig. 1). It is capable of a single grasp and is operated by way of a shoulder harness and cable system. The harness and cable translate shoulder abduction into opening of the device, which is normally closed by elastic bands. The grasp force for the 5XA depends on the number and type of elastic bands utilized. The 5XA is made from aluminum forgings, with nitrile rubber gripping surfaces and weighs 113 grams without socket or harness.

Figure 5.1 - The Hosmer-Dorrance Corp. 5XA split-hook.

B. Single Grasp Myoelectric Systems

In myoelectric systems the bioelectric potential generated upon muscle contraction is detected using electrodes on the surface of the skin. This signal, called the *electromyogram* or *EMG*, is then amplified and conditioned to direct the behavior of an electromechanical prosthesis. Typically, this is a single degree of freedom device, where opening and closing of the prosthesis is controlled by the activity of antagonistic muscle groups. For example, the flexors and extensors of the forearm, which in the intact arm are associated with flexion and extension of the wrist and closing and opening of the fingers, respectively, are typically utilized in the transradial amputee. Reasonably intuitive, bidirectional control may then be achieved by mapping contraction of the forearm flexors and extensors to the closing and opening of the prosthetic device, respectively. Because the amplitude of the EMG signal increases with the degree of muscular contraction, proportional control of the speed and/or force exerted by a myoelectric prosthesis is also possible. Relative to the body-powered systems described above, typical advantages of

myoelectric systems include [13]: enhanced anthropomorphic/cosmetic fidelity, an expanded functional envelope, reduced strength and motion requirements, and the elimination or simplification of the body harness. Typical disadvantages include: greater cost, higher weight, and reduced ruggedness. Two single grasp myoelectric systems assessed in this work are the Motion Control, Inc. Electric Terminal Device, and the Otto Bock MyoHand VariPlus Speed.

The Motion Control Inc. Electric Terminal Device

The Electric Terminal Device (ETD) is a single joint, single degree of freedom myoelectric split-hook driven by a single motor (pictured with passive wrist in Fig. 2). It is capable of a single grasp and is operated (in this study) using proportional, 2-site control, where EMG signals emanating from the forearm extensors and flexors are mapped to velocity of opening and closing of the split hook, respectively. The ETD is capable of grasp forces of up to 110 N. It is housed in plastic with aluminum split hooks and weighs 408 grams.

Figure 5.2 - The Motion Control Inc. Electric Terminal Device.

The Otto Bock MyoHand Variplus Speed

The MyoHand VariPlus Speed (MVS) is a 2 joint, single degree of freedom myoelectric hand driven by a single motor (pictured in Fig. 2). It is capable of a single (tripod) grasp and is operated (in this study) using proportional, 2-site control, where EMG signals emanating from the forearm extensors and flexors are mapped to velocity of opening and closing of the hand, respectively. The MVS is capable of grasp forces up to 100 N. It is made primarily of aluminum and covered in a PVC-based cosmesis which includes passive ring and little fingers. The MVS weighs approximately 460 grams without cosmesis.

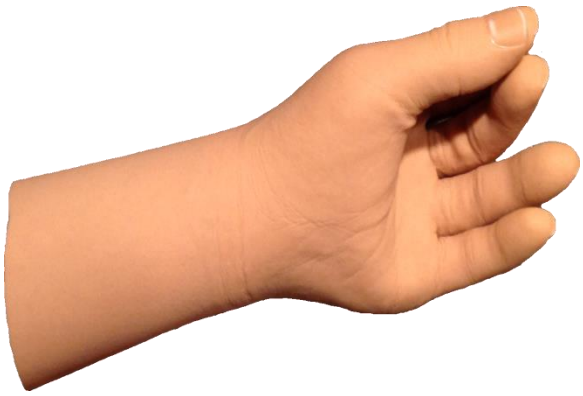

Figure 5.3 - The Otto Bock MyoHand Variplus Speed

C. Multigrasp Myoelectric Systems

Multigrasp myoelectric hand prostheses operate on the same principles as single grasp myoelectrics, but have a plurality of actuators and multiple DoFs that allow them to perform a variety of grasps and postures. With increased articulation and fidelity of motion, multigrasp hands are intended to provide enhanced biomechanical function and capability; however, functional assessment of these devices remains limited. Two multigrasp myoelectric prostheses assessed in this work are the Touch Bionics Inc. i-Limb Revolution, and the Vanderbilt Multigrasp Hand.

The Touch Bionics i-Limb Revolution

The Touch Bionics i-Limb (ILM) is an 11 joint, 6 degree of freedom myoelectric hand driven by 5 electric motors (pictured in Fig. 4). Each of the 5 digits has 2 joints and is driven by a single motor to provide flexion/extension. In the original i-Limb, an additional passive joint allows for thumb opposition/reposition to be set manually. In the i-Limb Revolution, this joint is actuated by an additional motor to provide active thumb opposition/reposition. The ILM Revolution weighs 515 grams without cosmesis. The ILM is capable of a wide variety of grasps and postures, but must be preprogrammed to select which subset of postures the user can directly access (i.e. those postures which can be selected via EMG signals). The grasps typically used by the participant in this study were the power grasp, tripod grasp, tip grasp (where the thumb remains stationary), and lateral pinch.

Figure 5.4 - The Touch Bionics i-Limb Revolution

The Vanderbilt Multigrasp Hand

The Vanderbilt Multigrasp (VMG) Hand is a 9 joint, 9 degree of freedom myoelectric hand driven by 4 brushless DC motors (pictured in Fig. 5). Movement of the fingers is caused by the action of polyethylene tendons, which spool onto pulleys affixed to the shafts of Brushless DC motors that are housed in the palm. The thumb has one DoF in flexion/extension and another in opposition/reposition, each driven bidirectionally by a single motor; the index finger has a single DoF in flexion/extension driven bidirectionally by a single motor, and the middle, ring, and little fingers each have two DoF that are driven in flexion by a single motor with extension being provided by passive torsion springs. This actuation scheme was designed to explicitly provide both precision and conformal grasp capability, where the configuration of the thumb and index finger are determined uniquely as commanded by the motor units, while the configuration of the remaining digits is determined by a combination of the motor unit command and the nature (i.e., shape) of the object being grasped through compliant coupling. The VMG Hand weighs 540 grams with partial cosmesis. A detailed description of the VMG hand is provided in [5].

Figure 5.5 - The Vanderbilt Multigrasp Hand

The VMG hand is controlled by a multigrasp myoelecric controller (MMC). The MMC is an event-driven, finite-state controller which interprets high-level commands issued by the user to coordinate the motion of a multigrasp prosthesis (see Fig. 3) using a standard, two-site myoelectric interface (i.e., utilizes the same electrode sites as the other myoelectric devices assessed here). Specifically, by contraction of the forearm flexors and extensors (located on the anterior and posterior aspects of the forearm, respectively), the user may determine whether the hand closes or opens. Depending on the initial position of the thumb, closing of the hand (caused by flexion) proceeds continuously through either the Reposition (Platform), Point, Hook, and Lateral Pinch postures (states) or the Opposition, Tip, and combined Cylindrical, Spherical, and Tripod postures (states). Opening of the hand (caused by extension) reverses these sequences. State transitions occur based on predefined tendon displacement or force thresholds. To switch between the opposition and reposition states (and thereby determine the position of the thumb), the user may either co-contract the forearm musculature or perform extension after the hand has fully opened in either the opposition and reposition states. Grasping occurs by virtue of movement among the states. The magnitude of the contraction dictates either the speed of movement (if moving in space) or magnitude of force (if grasping an object). A detailed description of the MMC may be found in [6].

For the study described here, a quick-connect myoelectric adapter (Texas Assistive Devices QDMEWA01-0N2) was used to attach the VMG hand to the participant's left forearm socket. Disposable Ag/AgCl electrodes (Norotrode N120-1) were then used for EMG signal acquisition. This allowed the socket to be used for structural support of the VMG hand, while ensuring that no electrical interference occurred between the two. The temporary electrodes were placed adjacent to the fixed electrode sites within the participant's socket.

IV. Methods

A. Hand Functionality Assessment

To generate information about the effectiveness of the above devices, a validated measure of hand function was required. In a recent publication by the Upper Limb Prosthetic Outcome Measures (ULPOM) working group, five outcome measures specific to hand function were identified for this purpose [11]. These tests were: the Purdue Pegboard [14], Box and Blocks Test [15], Jebsen Standardized Test of Hand Function [16], Sollerman Hand Function Test [17], and the Southampton Hand Assessment Procedure (SHAP) [18]. While each assessment instrument possesses desirable characteristics, the SHAP was ultimately selected for the present work, primarily because the SHAP evaluates multiple grasps and postures (unlike the Purdue Pegboard and Box and Blocks tests) and is an objective measure (unlike the Sollerman test). The SHAP bears several similarities to the Jebsen test, although the former more explicitly considers various grasp types, while the latter has not yet been validated for use by amputees [11]. Finally,

the SHAP has been used recently in the assessment of two myoelectric terminal devices [9, 10], thus allowing for comparison among studies, and the addition of information to an established body of knowledge. As such, the SHAP was selected for use in the assessment here.

The SHAP is comprised of a series of tasks which require the manipulation of 12 abstract objects and the performance of 14 exercises representative of the activities of daily living (ADLs). The exercises specifically require use of the spherical, tripod, power, lateral, tip and extension grasps. The ADLs utilized in the SHAP consist of: picking up coins, undoing buttons, simulated food cutting, turning pages, removing a jar lid, pouring from a glass measuring cup, pouring from a carton, lifting a heavy jar, lifting a light can, lifting a tray, rotating a key, opening/closing a zipper, rotating a screw, and using a door handle. Each of these tasks is self-timed (i.e. recorded by the participant). In this study, each task was repeated three times, with the best time recorded. A set of composite performance scores are calculated from the individual recorded times for each task, resulting in an Index of Function (IoF), which provides an overall indication of function, and a Functionality Profile (FP), which provides scores specific to the six prehensile forms above. SHAP IoF scores indicative of typical healthy function range from 95-100, with lesser scores indicating some degree of impairment and greater scores indicating exceptional performance. For a detailed description of the SHAP assessment, including how scores are determined, the reader is referred to [18]. In this study, SHAP assessments were conducted with each of the five devices until the respective IoF scores had essentially plateaued (i.e., until the subject had completed the learning curve for each device, as defined by the subsequent increment in score falling below the increment considered significant in the SHAP [18]). Testing of all five terminal devices through the learning curve of all devices occurred over a period of 322 days. Once the learning curve was completed, the fourth and final assessment of each respective device occurred within a period of 18 days. The protocol utilized in this study was approved by the Vanderbilt University IRB.

B. Participant Details

The participant in this study was a 33 year old male having bilateral transradial amputation as the result of traumatic injury sustained in 2008. The participant's right and left residual forearms are 15.2 cm and 17.8 cm in length as measured from the medial epicondyle. Prior to injury the participant was right hand dominant. However, as the injury sustained to the right arm was more severe, and required longer recovery and rehabilitation, the participant now favors the left arm, and as such functional of the left arm and terminal device was assessed in this study. The participant is an active individual, and uses both body-powered and myoelectric prostheses in daily activities. All terminal devices used in this study were owned by the participant, and had been prescribed for him. The prosthetic configuration most often worn by the participant (approximately 90% of the time) consists of two myoelectric devices: a Motion Control ETD worn

on the left hand, and a Touch Bionics ILM Revolution on the right. The participant generally utilizes a pair of body-powered split hooks for the remainder of the time, and specifically when engaged in activities involving heavy physical work, or when the terminal devices (TDs) might become dirtied or wet.

V. Results

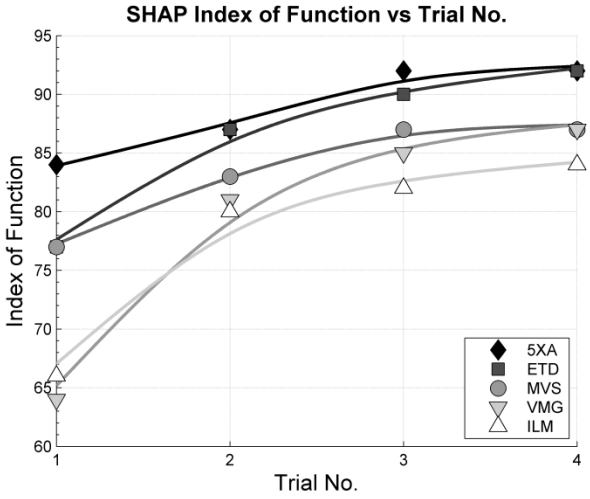

Figure 5.6 – SHAP Index of function vs. trial number, indicating improvement over the course of the study, and relative performance of the assessed devices.

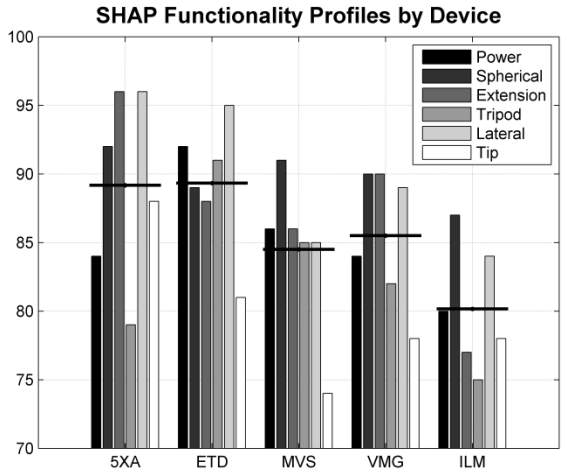

Figure 5.7 – SHAP Functionality profiles by device type, indicating grasp proficiency and profile means (horizontal lines) for each device for the fourth and final trial.

The Index of Functionality for each device across the four trials of each is depicted in Fig. 6. After the third trial improvement was minimal, with each device gaining two IoF points or less (where, as indicated in [19], an IoF score less than 2 is considered insignificant). The study was

therefore concluded after the fourth trial, after which functional performance was considered to have converged. As indicated in the figure, significant improvement occurred over the course of the study for all devices measured. This is especially true for the multigrasp hands, which improved by 20 IoF points on average and with which the participant had the least experience prior to the start of the study. At the beginning of the trials, the SHAP IoF scores were ordered from highest to lowest by body powered device (5XA), single grasp myoelectric devices (ETD and MVS), and multigrasp myoelectric devices (ILM and VMG). By the end of the trials, the score of the myoelectric split hook (ETD) matched that of the body-powered split hook (5XA), and the score of the Vanderbilt multigrasp myoelectric hand (VMG) matched that of the single grasp myoelectric hand (MVS). The final IoF scores, indicating overall functionality, were as follows: 5XA 92, ETD 92, OBH 87, VMG 87, and ILM 84, with each device showing an overall improvement of 8, 15, 10, 23 and 18 points, respectively. The fourth trial functionality profiles and functionality profile means for each device are presented in Fig. 7. The mean and standard deviation of the fourth trial functionality profiles are as follows: 5XA 89±6.8, ETD 89±4.8, MVS 84±5.6, VMG 86±4.9, and ILM 80±4.5. Based on a multiple comparison, one-way analysis of variance with a 90% confidence interval, there was no significant difference between the functionality profile means of the 5XA and ETD split hooks (89 and 89, respectively) and the MVS and VMG hands (84 and 86, respectively). Similarly, there was no significant difference between the functionality profile means of the MVS and VMG hands (84 and 86, respectively) and the ILM (80). The only significant difference in the functionality profile means were between those of the single grasp 5XA and ETD split hooks (89 and 89) and that of the multigrasp ILM hand (80). Note that, due to lack of weighting, the mean of the functionality profile is not necessarily the same as the overall Index of Function. The above data is tabulated in Table 1.

Table 5.1 – Functional Results of the Southampton Hand Assessment Procedure

Device	Index of Function (IoF)	Functionality Profile (FP)						FP Mean	FP Std Dev
		Power	Spherical	Extension	Tripod	Lateral	Tip		
5XA	92	84	92	96	79	96	88	89	6.8
ETD	92	92	89	88	91	95	81	89	4.8
MVS	87	86	91	86	85	85	74	84	5.6
VMG	87	85	90	90	82	89	78	86	4.9
ILM	84	80	87	77	75	84	78	80	4.5

VI. Discussion

Given these results, one might expect the participant to expressly favor single grasp split hooks (either body powered or myoelectric). However, *this is not the case*. As stated above, the

configuration most often worn by the participant is a single-grasp myoelectric ETD on his left arm, and a multigrasp myoelectric i-Limb Revolution on his right. As described by the participant, this configuration is worn approximately 90% of the time, and is used because the single grasp split hook (ETD) and multigrasp hand (ILM) excel in different functional areas. (Note that, as the participant owns a pair of ETDs and a pair of i-Limbs, a matched set of either could be worn if so desired.) The split hook was stated to be particularly useful in situations that require either large amounts of force or the manipulation of small objects; as in retrieving an object such as a set of keys or a phone from a pants pocket. The multigrasp hand was stated to be useful in situations where stability or delicacy is required; such as picking up and drinking from a disposable cup without crushing or dropping it, eating a sandwich without destroying it, or holding a child's hand without pinching it. Based on the assessment scores alone, however, there is no indication that the ETD and i-Limb would provide these respective functional advantages, and in fact no indication that the i-Limb would provide any functional advantages relative to the ETD.

There is therefore a notable discrepancy between the functionality of the multigrasp devices as measured by the assessment utilized in this study, and the functionality of the multigrasp devices as reported and utilized by the participant, particularly with regard to single grasp split hooks. In the opinion of the authors, this discrepancy may be due to functional considerations which lie outside of the scope of the present assessment method. In this case, the following functional considerations were specifically mentioned by the participant:

1) *The relative stability of grasp* - In the ADLs, the ability to grasp an object securely in the presence of perturbations or disturbances is clearly an important objective, particularly if the object might spill or break if dropped. Although this consideration motivates the use of a multigrasp hand by the participant in this study, this aspect of function is not directly assessed in the SHAP. For instance, while it may be possible to complete a task quickly and without dropping an object, the grasp used to manipulate the object may only be marginally stable. This would result in a good Functionality Profile sub-score, despite the grasp being less desirable during extended practical use. This was noted during manipulation of the tip object for example, which would in some cases rotate during manipulation with the body-powered split hook, but could be placed quickly nevertheless.

2) *The ability to handle delicate objects* - Over the course of the study, it was noted that the split hook style devices were particularly damaging to the assessment materials. Specifically, the lightweight objects in the SHAP kit, which are made of balsa wood, were substantially deformed in some cases, while the carton was often crushed when grasped for pouring, and the jar lid was repeatedly dented when unscrewed. Had this been taken into account, the participant's preference for multigrasp hands when manipulating delicate objects may have been more evident in the assessment results. To some extent, this issue is coupled to the first (stability of grasp) as, in the absence of conformal grasping, split-hooks tend to provide stability through concentrated

grasp force (relative to biomechanical norms). To this extent, measuring the ability to modulate grasp force with a given device, as in [20], may be particularly useful.

In addition to these functional issues (mentioned specifically by the participant above), the authors believe that, based on the experience with this assessment, the following issues should also be considered in the assessment and design of terminal devices:

3) *The ability to utilize modern technology* – To better represent the instrumental ADL's, particularly those regarding the ability to communicate and utilize technology, tasks involving keyboards, cell phones, and/or touch screen devices should be included. This is particularly important as some recent devices, such as the i-Limb, require the use of touch screen for grasp selection. Such tasks are likely to favor terminal devices capable of a pointing posture.

4) *The body as a workspace* - To better represent the basic ADL's, particularly those regarding dressing and eating, buttons and zippers should be worn on the body when manipulated to better represent how these items are encountered in daily life. Similarly, (simulated) food items should be grasped and brought to the face to better represent eating.

5) *The ability to perform compound tasks* - In many ADLs, grasp type may be changed several times over the course of a given task. For example, food preparation might require that a person perform a series of grasp types in order to achieve one goal. In the SHAP, only a single grasp type is considered within a given sub-score, and the time to transition between grasp types (or the time required to orient the device appropriately) is not directly measured. As such, an assessment that measures the ability to transition between grasp types during compound tasks would be a useful measure, reflective of a number of ADLs.

6) *Compensatory movements* – A useful consideration is the extent to which compensatory movements are required to perform a given task, as in [20]. For instance, while a task can be completed with several different grasps, some grasps may require considerably more compensatory movement with the arm and/or upper body than other grasps. Such compensatory movement may be less desirable to the patient, either biomechanically (as it may involve joint stress), aesthetically, or when operating in a confined space (such as a theatre or passenger seat).

VII. Conclusion

In this study, functional assessments were performed by a transradial amputee participant using a wide variety of prosthetic terminal devices. While the differences between device types were small, the highest scores were obtained with body-powered and myoelectric split hooks (IoF scores of 92). This result, however, does not reflect the functional preferences of the participant, who in daily life predominantly wears one myoelectric split hook (IoF scores of 92) and one multigrasp myoelectric hand (IoF score of 84), despite having two of each. The participant noted that, while single-grasp split hooks can exert greater force and excel at manipulating small

objects, the multigrasp device was better able to provide greater grasp stability, and was better able to manipulate soft or fragile objects. Since the SHAP scores did not indicate these distinctions and were not reflective of the participant's preferred configuration, and based on the authors experience over the course of the study, recommendations are made herein to further expand the scope of objective assessment instruments to capture such function, and thus inform continued upper extremity prosthetic use and development.

Epilogue

The work above indicates that, for this particular individual and assessment, the Vanderbilt Multigrasp Hand and Multigrasp Myoelectric Control system have performance comparable to their commercial counterparts, and likely offer enhanced functionality when performing the Activities of Daily Living (particularly in regard to stability and delicacy of grasp). Several considerations were put forth to better characterize these aspects of function for prosthetic end effectors in general, and multigrasp hands in particular.

References

[1] D. J. Atkins, D. C. Y. Heard, and W. H. Donovan, "Epidemiological overview of individuals with upper-limb loss and their reported research priorities," *Journal of Prosthetics and Orthotics,* vol. 8, pp. 2-10, 1996.

[2] E. Biddiss, D. Beaton, and T. Chau, "Consumer design priorities for upper limb prosthetics," *Disability & Rehabilitation: Assistive Technology,* vol. 2, pp. 346-357, 2007.

[3] C. Cipriani, M. Controzzi, and M. C. Carrozza, "Objectives, criteria and methods for the design of the SmartHand transradial prosthesis," *Robotica,* vol. 28, pp. 919-927, 2010.

[4] Y. Losier, A. Clawson, A. Wilson, E. Scheme, K. Englehart, P. Kyberd, and B. Hudgins, "An Overview of the UNB Hand System," in *Myoelectric Controls/Powered Prosthetics Symposium*, Fredericton, New Brunswick, Canada, 2011, pp. 251-254.

[5] D. A. Bennett, S. A. Dalley, and M. Goldfarb, "Design of a hand prosthesis with precision and conformal grasp capability," in *IEEE International Conference of the Engineering in Medicine and Biology Society*, 2012, pp. 3044-3047.

[6] S. A. Dalley, H. A. Varol, and M. Goldfarb, "A method for the control of multigrasp myoelectric prosthetic hands," *IEEE Transactions on Neural Systems and Rehabilitation Engineering,* vol. 20, pp. 58-67, 2012.

[7] C. Medynski and B. Rattray, "Bebionic Prosthetic Design," in *Myoelectric Controls/Powered Prosthetics Symposium (MEC)*, Fredericton, Canada, 2011.

[8] S. Schulz, "First Experiences with the Vincent Hand," in *Myoelectric Controls/Powered Prosthetics Symposium (MEC)*, Fredericton, Canada, 2011.

[9] O. Van Der Niet Otr, H. A. Reinders-Messelink, R. M. Bongers, H. Bouwsema, and C. K. Van Der Sluis, "The i-Limb hand and the DMC Plus hand compared: A case report," *Prosthetics and Orthotics International,* vol. 34, pp. 216-220, 2010.

[10] O. Van Der Niet Otr, H. A. Reinders-Messelink, H. Bouwsema, R. M. Bongers, and C. K. Van Der Sluis, "The i-Limb Pulse hand compared to the i-Limb and DMC Plus hand," in *Myoelectric Controls/Powered Prosthetics Symposium (MEC)*, Fredericton, Canada, 2011, pp. 260-261.

[11] W. Hill, P. Kyberd, L. N. Hermansson, S. Hubbard, O. Stavdahl, and S. Swanson, "Upper Limb Prosthetic Outcome Measures (ULPOM): A working group and their findings," *Journal of Prosthetics and Orthotics,* vol. 21, pp. 69-82, 2009.

[12] F. V. Wright, "Measurement of functional outcome with individuals who use upper extremity prosthetic devices: current and future directions," *Journal of Prosthetics and Orthotics,* vol. 18, pp. 46-56, 2006.

[13] S. G. Millstein, H. Heger, and G. A. Hunter, "Prosthetic use in adult upper limb amputees: a comparison of the body powered and electrically powered prostheses," *Prosthetics and Orthotics International,* vol. 10, pp. 27-34, 1986.

[14] J. Tiffin and E. J. Asher, "The Purdue Pegboard: Norms and Studies of Reliability and Validity," *Journal of Applied Psychology,* vol. 32, pp. 221-233, 1948.

[15] V. Mathiowetz, G. Volland, N. Kashman, and K. Wever, "Adult norms for the Box and Blocks Test of Manual Dexterity," *American Journal of Occupational Therapy,* vol. 39, pp. 386-391, 1985.

[16] R. Jebsen, N. Taylor, and R. Trieschmann, "An objective and standardized test of hand function," *Archives of Physical Medicine and Rehabilitation,* vol. 9, pp. 311-319, 1969.

[17] C. Sollerman and A. Ejeskär, "Sollerman Hand Function Test: A Standardised Method and its Use in Tetraplegic Patients," *Scandinavian Journal of Plastic and Reconstructive Surgery and Hand Surgery,* vol. 29, pp. 167-176, 1995.

[18] C. M. Light, C. Chappell, and P. J. Kyberd, "Establishing a standardized clinical assessment tool of pathologic and prosthetic hand function: Normative data, reliability, and validity," *Archives of Physical Medicine and Rehabilitation,* vol. 83, pp. 776-783, 2002.

[19] P. Kyberd, A. Murgia, M. Gasson, T. Tjerks, C. Metcalf, P. Chappell, K. Warwick, S. E. Lawson, and T. Barnhill, "Case studies to demonstrate the range of applications of the Southampton Hand Assessment Procedure," *British Journal of Occupational Therapy,* vol. 72, pp. 212-218, 2009.

[20] H. Bouwsema, P. Keyberd, W. Hill, C. K. Van der Sluis, and R. M. Bongers, "Determining skill level in myoelectric prosthesis use with multiple outcome measures," *Journal of Rehabilitation Research and Development,* vol. 49, pp. 1331-13-47, 2012.

Chapter 6 – Conclusion

Skyler A. Dalley

Vanderbilt University

Nashville, TN

Summary

Externally powered transradial prostheses have traditionally been limited to devices that are broad abstractions of the native hand, possessing a single degree of freedom and having limited grasping capability. Enabled by recent technological advances, multigrasp prosthetic hands with greater anthropomorphic fidelity have now begun to emerge, although the ability to communicate with and control such devices remains limited. In light of these facts, the goal of the work described herein was to develop an effective control interface to provide full access to the capability of a multigrasp myoelectric hand, and thereby enhance the ability of an amputee to perform the activities of daily living. To achieve this, a multigrasp hand prosthesis was first constructed which can execute a wide variety of grasps and postures with biomechanically relevant levels of force and speed. A state based multigrasp myoelectric controller was then developed to provide direct access to these grasps and postures using a standard, two site EMG interface. The efficacy of the MMC control method was initially demonstrated by non-amputee participants in a virtual environment so that the performance of a virtual prosthesis, as controlled by the multigrasp myoelectric controller, could be compared to the performance of the native hand, as measured by a custom-built dataglove. Functional assessments were then performed by an individual with transradial amputation in a laboratory environment to investigate the effectiveness of the physical system as a whole.

Contribution

As summarized above, this work describes the development, control, and assessment of a multigrasp myoelectric hand prosthesis. The key results of this work, as presented in the four manuscripts above, are as follows:

Manuscript 1 (Chapter 2): *Design of a Multifunctional Anthropomorphic Prosthetic Hand with Extrinsic Actuation*, Skyler A. Dalley, Tuomas E. Wiste, Thomas J. Withrow, and Michael Goldfarb

- Presentation of the first generation design of the Vanderbilt Multigrasp (VMG) Hand
  - 16 degrees of freedom, 5 degrees of extrinsic actuation
  - Brushed DC Motors with full differential between digits IV and V
  - Active flexion of the digits and opposition of the thumb (via motors)
  - Passive extension of the digits and reposition of the thumb (via torsional springs)
  - Fully backdriveable
- The provision of grasps and postures which span over 85% of the activities of daily living
- Experimental characterization demonstrating biomechanically relevant force and speed

Manuscript 2 (Chapter 3): *Design of a Multigrasp Transradial Prostheses*, Tuomas E. Wiste, Skyler A. Dalley, H. Atakan Varol, and Michael Goldfarb

- Presentation of the second generation design of the Vanderbilt Multigrasp (VMG) Hand
  - 16 degrees of freedom, 4 degrees of intrinsic actuation
  - Brushless Motors with compliant coupling of digits III through V
  - Active flexion of the digits and opposition of the thumb (via motors)
  - Passive extension of the digits and reposition of the thumb (via torsional springs)
  - Incorporation of two-way clutch and series elastic elements
  - Non-backdriveable actuation for reduced power consumption/user fatigue
- The provision of grasps and postures which span over 85% of the activities of daily living
- Experimental characterization demonstrating biomechanically relevant force and speed

Manuscript 3 (Chapter 4): *A Method for the Control of Multigrasp Myoelectric Prosthetic Hands,* Skyler A. Dalley, Huseyin Atakan Varol, and Michael Goldfarb

- Description of the Multigrasp Myoelectric Control (MMC) method which allows for direct and proportional control of a multigrasp prosthetic hand among several grasps and postures (in this case, the 8 listed above as well as opposition) using a standard, two site EMG interface.
- Preliminary experimental validation of the MMC method in a virtual environment demonstrating the ability to transition rapidly and reliably among several target postures.

Manuscript 4 (Chapter 5): *Comparative Functional Assessment of Single and Multigrasp Prosthetic Terminal Devices,* Skyler A. Dalley, Daniel A. Bennett, and Michael Goldfarb

- The functional assessment of the Vanderbilt Multigrasp Hand and Multigrasp Myoelectric Control method, as well as a wide variety of prosthetic terminal devices.
- A discussion of considerations for future assessment instruments, which, if implemented, may better characterize terminal device function, particularly in regard to multigrasp devices.

It is the author's hope that the research reported herein will enhance the ability of upper extremity amputees to perform the activities of daily living by providing a method which allows for intuitive and reliable access to the expanded functionality of multigrasp prosthetic hands.

Appendix A - An Early History of Upper Extremity Prostheses

Skyler Ashton Dalley

Vanderbilt University

Nashville, TN

Written: April, 2012

The first recorded use of an artificial hand precedes the Common Era, dating back to the Second Punic War (218-201 BCE) when the Roman General Marcus Sergius rode into battle during the siege of Cremona with an iron hand to brace his shield (as reported in the seventh book of Gaius Plinius Secundus' *Natural History*, CE 73) [1]. Much later, in the twilight of the Middle Ages, articulated prosthetic hands appeared which were similar in appearance to gauntlets and crafted by the same skilled artisans. The spring-loaded mechanical hand made for the Imperial Knight and mercenary Gotz von Berlichingen in 1504 (Fig. 1) is an exemplar of this era in prosthetic design, and could be passively adjusted to grasp a sword and other various objects [1]. Active upper extremity replacements, however, would not come into play for another 300 years.

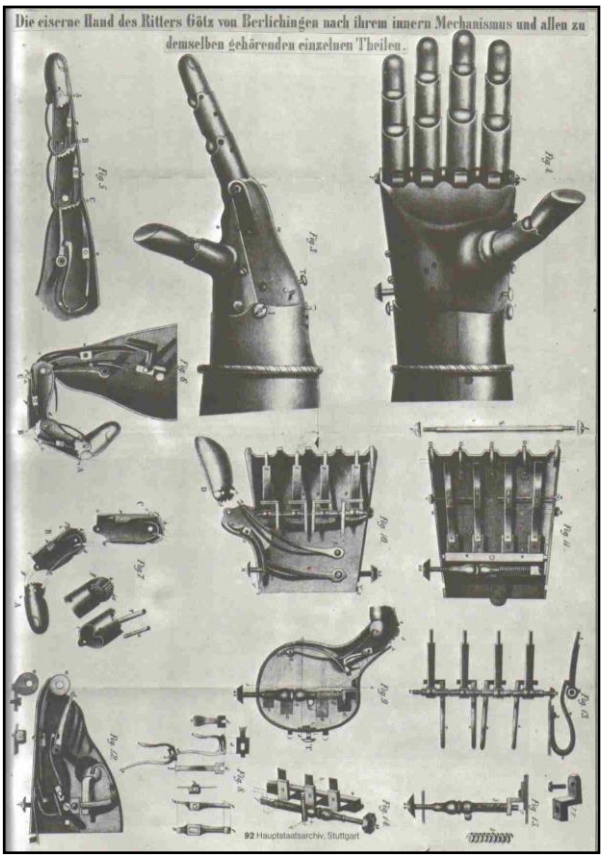

Figure A.1 - The Mechanical hand of Gotz von Berlichingen

In the 1800's the notion of active, body-powered prostheses began to emerge, stemming from the work of a Berlin Dentist named Peter Ballif in 1812 (alt. 1818). Ballif's system utilized a

leather harness attached to the ipsilateral shoulder and trunk to actuate a mechanical hand [2]. This allowed an amputee to extend the fingers (which were spring-biased in the closed position) of a prosthesis using relative motion of the arm and body [1]. In 1844, the Dutch sculptor van Peeterson expanded on Ballif's work to provide for the needs of the above elbow amputee. This was done using a contralateral shoulder harness to provide elbow flexion through an external chord running across the back (a configuration for body-powered prostheses which persists to this day), where a separate series of chords controlled extension of the fingers by way of arm extension or abduction [3]. Several prosthetic variants based on body-powered principles would appear in the years to follow.

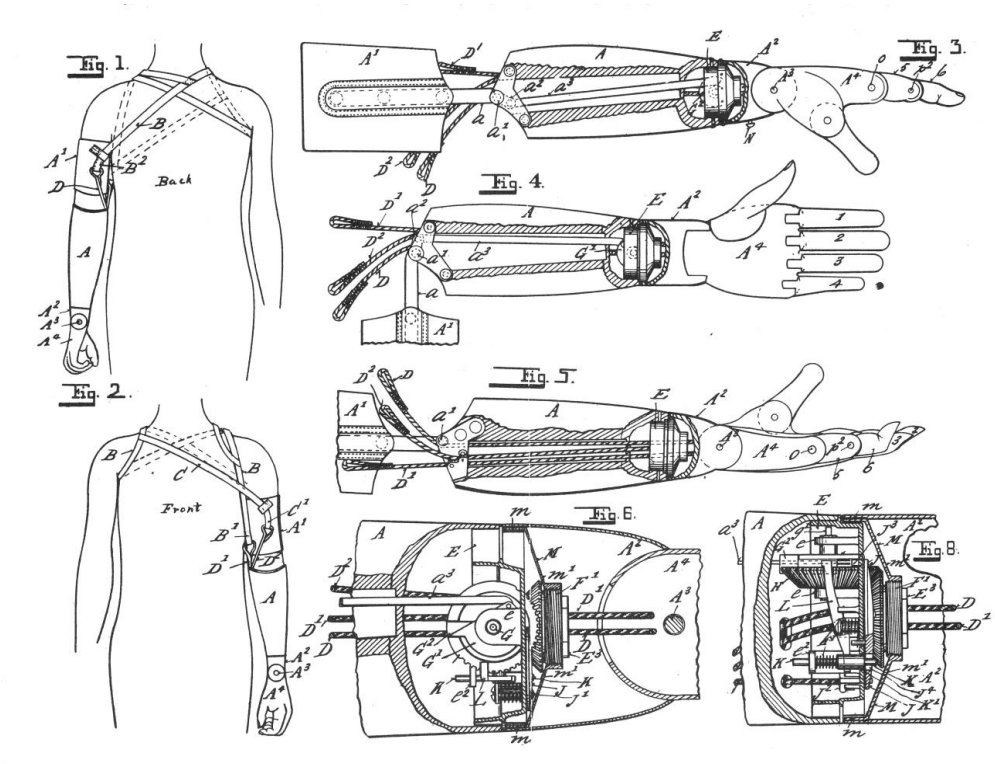

Figure A.2 - The Carnes Artificial Arm, a highly advanced device for its time (Circa 1912).

In 1904 and 1912 patents for a body-powered, anthropomorphic prosthetic arm were awarded to William T. Carnes, founder of the Carnes Artificial Limb Corporation [3]. The Carnes Arm (Fig. 2) represented a conglomeration of prosthetic technology to date, and had several advanced features. These included elbow flexion which was coupled to wrist supination, allowing an amputee to easily bring the hand to the face for feeding or self-care, and digits which locked in

place when closed. The device was regarded as a technological breakthrough and was produced after the First World War in relatively large quantities, either for or by countries struggling to meet the needs of their returning war-wounded. And yet, despite the attention received by the Carnes Arm at the time, the most prominent embodiment of the body-powered prosthesis to this day is probably that of David W. Dorrance, which featured the iconic split-hook terminal device and was also patented in 1912, leading to the formation of the Hosmer-Dorrance Company in the same year. The Dorrance split-hook prosthesis was a model of lightweight, rugged, and simplistic utility. In contrast, the Carnes Arm was a delicate mechanical masterpiece which, in comparison to its more pragmatic counterpart, was relatively costly (being referred to as the “Officers Arm”, as the rank-and-file returning from the First World War could not afford it), heavy, and difficult to maintain. The Carnes Artificial Limb Company eventually folded during the 1930s, a period of time over which upper extremity prosthetic development, like the economy, would also be depressed. It was only in 1945, at the conclusion of the Second World War, that focused research and development would be brought to bear on the field of prosthetics in the United States. The impetus for progress was provided by dissatisfied amputees in military hospitals who, having seen remarkable destructive technology exercised during the war, found their replacement limbs lacking in similar ingenuity and potential performance. Approached by the army Surgeon General Norman T. Kirk, the National Academy of Sciences established what would become known as the Artificial Limb Program, which was administrated by various Committees and Boards from 1945 to 1976 [4]. (The Committee on Artificial Limbs 1945-1947, the Advisory Committee on Artificial Limbs 1947-1955, The Prosthetics Research Board 1955-1959, The Committee on Prosthetics Research and Development and the Committee on Prosthetics Education and Information aka the Committee on Prosthetics and Orthotics 1959-1976.) The Artificial Limb Program mobilized scientific and engineering resources under the purview of the military, private industry, and academia, and provided advances in: the understanding of biomechanical principles, the design of prosthetic devices, sockets and suspension, materials and fabrication methods, surgical techniques, and rehabilitation practices. (For an in-depth review of developments made during this time, the reader is referred to [4], [5].)

Notable among the developments for the upper limb were: the introduction of thermoset plastic resins for socket fabrication, the use of Bowden cables for efficient power transmission, and the harness-operated, alternating-lock elbow mechanism for transhumeral amputees.

External power in upper extremity prosthetics also began to receive increased attention during this time. The use of external power held the promise of reducing the physical burden incumbent upon the amputee relative to body-powered prostheses, for which prosthetic action requires sufficient force and excursion (i.e. power) to be generated by musculature at the control site for prosthetic action. From 1946-1952 S.W. Alderson, supported by International Business Machines and the Veterans Administration, produced several externally-powered electrical arms [6]. (Note that electric prostheses had been in existence since at least 1919, but were impractical until the development of modern, compact electric motors [7].) The Alderson/IBM arms represented an engineering tour de force, and produced impressive demonstrations; yet, evaluations at NYU and UCLA in 1953 concluded that they were difficult to operate, placing excessive cognitive burden on the user. For instance, the model described in the August 7, 1950 edition of LIFE magazine required differential pressure applied to three pneumatic bulbs under the foot to elicit twelve distinct signals for sequential control of the elbow, wrist, and hand. A large part of this complexity undoubtedly arose as a consequence of the unprecedented degree of articulation in the Alderson/IBM devices. However, it is also true that the status quo for upper extremity prosthesis control at this time depended on the action of functionally disparate muscle groups, causing an inherent physiological disconnect between native control pathways and those required for the operation of an artificial replacement. This would change with the introduction of myoelectric control.

Reinhold Reiter, a German physicist working with the Bavarian Red Cross, developed myoelectric control for externally powered upper extremity prostheses in the early forties. The technique allowed for the transduction of control signals via isometric contraction of the residual musculature, and had some notable advantages. For instance, significant power generation and gross movement of the body were not required, enabling control by adolescents and the severely disabled. Also, physiologically appropriate muscle sites could be used, allowing for a direct

mapping of native control pathways to prosthetic function. Reiter's work was published in 1948 [8], but was obscured in the aftermath of war. In the same year, however, MIT professor Norbert Wiener published *Cybernetics* [9], which explored control and communication in the animal and machine. This work examined feedback regulated systems in which man and machine served as reciprocating principal components, a concept which would naturally extend to myoelectric prostheses and control systems. Several groups would build upon these conceptual foundations and advance myoelectric control in the years to follow.

In 1952, Berger and Huppert of NYU investigated the possible use of EMG as a method for controlling an electric arm prosthesis [10] and their findings were used by the Prosthetic Research Division of IBM in an attempt to achieve that goal. The first practical (bench top) demonstration of a myoelectric system (outside of Germany), however, would be that of Battye, Nightingale, and Whillis at Guy's Hospital Medical School in London, 1955 [11]. Soviet scientist would then leverage the newly patented transistor (patented in 1948, the same year as Reiter's publication) to provide a portable, externally powered, myoelectric system in 1960 [12]. Inspired by the so called "Russian Hand", an Austrian by the name of Dr. Zemann contacted the Otto Bock company in 1966, which led to the development of a new electric hand intended for myoelectric control, the Model Z1. The Z1 would then continue to evolve with the electronic expertise of an Austrian hearing aid company, Viennatone (Otto Bock later released its own hand system, the Z6, for clinical use in 1967). The Viennatone Hand was adopted by the Veterans Administration and in 1967 was the first commercially available myoelectric hand system in the United States.

The maturation of myoelectric prosthetic devices was also accompanied by developments in myoelectric control. These developments include: proportional hand control developed by A. H. Bottomley in the United Kingdom, three-state myoelectric control developed by R. N. Scott at the University of New Brunswick, and synergistic prehension (high speed prehension, low speed grasping) developed by Dudley Childress at Northwestern University [13].

The design and control principles established during the 1960's form the cornerstone of myoelectric upper extremity prosthetic systems. However, it is only in the past decade that this foundation has been significantly built upon (this is especially true regarding prosthetic hardware,

in which recent development of multigrasp hands has spawned a new crop of control issues). Now, as in the days of Marcus Sergius, military conflict has served as the impetus for prosthetic development, with technological advancement serving again as both saber and salve. Modern munitions are capable of unprecedented levels of tissue destruction, while modern body armor, field medicine, and medical evacuation methods have increased the number of surviving combat wounded [14]. At the same time, advances in consumer electronics (e.g. powerful microcontrollers, low-profile surface mount electronics, advanced actuation technology, and high energy density batteries) have made the design of anthropomorphic, multifunction, multigrasp prosthetic devices possible. It is the design and control of these devices which will form the next chapter in the storied history of upper extremity prosthetics.

References

[1] R. H. Meier, "History of Arm Amputation, Prosthetic Restoration, and Arm Amputation Rehabilitation," in *Functional Restoration of Adults and Children with Upper Extremity Amputation*, R. H. Meier and D. J. Atkins, Eds., ed New York: Demos Medical Publishing, 2004, pp. 1-7.

[2] S. N. E. Banerjee, *Rehabilitation Management of Amputees*. Baltimore: Williams & Wilkins, 1982.

[3] G. Phillips, *Best Foot Forward: Chas. A. Blatchford & Sons Ltd. (Artificial Limb Specialists) 1890 -1990*. Cambridge: Granta editions, 1990.

[4] H. K. Bowker and J. W. Michael, Eds., *Atlas of Limb Prosthetics: Surgical, Prosthetic, and Rehabilitation Principles*. St. Louis: American Academy of Orthopedic Surgeons, 1992.

[5] B. Furman, *Progress in Prosthetics: A summary under sponsorship of the Prosthetics Research Board of the National Academy of Sciences-National Research Council*. Washington: U.S. Dept. of Health, Education, and Welfare Office of Vocational Rehabilitation, 1962.

[6] D. S. Childress, "Historical Aspects of Powered Limb Prostheses," *Clinical Prosthetics and Orthotics,* vol. 9, pp. 2-12, 1985.

[7] R. Alter, "Bioelectric Control of Prostheses," Massachusetts Institute of Technology, Cambridge, Technical Report, 1966.

[8] R. Reiter, "Eine neue Elektrokunsthand," *Grenzgebiete der Medizin,* vol. 1, pp. 133-135, 1948.

[9] N. Wiener, *Cybernetics: or Control and Communication in the Animal and the Machine*. Cambridge: The MIT Press, 1948.

[10] N. Berger and C. R. Huppert, "The Use of Electrical and Mechanical Muscular Forces for the Control of an Electrical Prosthesis," *American Journal of Occupational Therapy,* vol. 6, pp. 110-114, 1952.

[11] C. K. Battye, A. Nightingale, and J. Whillis, "The Use of Myo-Electric Currents in the Operation of Prostheses," *The Journal of Bone and Joint Surgery,* vol. 37B, pp. 506-510, 1955.

[12] A. E. Kobrinski, S. V. Bolkhovitin, L. M. Voskoboinikova, D. M. Ioffe, E. P. Polyan, B. P. Popov, Y. L. Slavutski, A. Y. Sysin, and Y. S. Yakobson, "Problems of Bioelectric Control," in *Proceedings of the First International Congress of the International Federation of Automatic Control*, Moscow, 1960, pp. 619-622.

[13] A. Muzumdar, *Powered Upper Limb Prostheses-Control, Implementation and Clinical Application*. Berlin: Springer-Verlag, 2004.

[14] R. Bowers. (2008), U.S. Military Builds on Rich History of Amputee Care. *Military in-Step*. Available: http://www.amputee-coalition.org/military-instep/rich-history.html